Assessing the acetylcholinesterase inhibitory potential of novel pharmacophores for potential treatment of Alzheimer's disease

by

Lerato Mamabote Maboko

Thesis submitted in fulfilment of the requirements for the degree

Philosphiae Doctor

in the Department of

Pharmacology

in the

Faculty of Health Sciences

at the

University of Pretoria

Supervisor: Prof Vanessa Steenkamp[1]
Co-supervisors: Dr Anjo Theron[2]
Dr Jenny-Lee Panayides[3]
Prof Werner Cordier[1]

[1]Department of Pharmacology, School of Medicine, Faculty of Health Sciences, University of Pretoria, Pretoria, South Africa

[2]Next Generation Health and [3]Future Production: Chemicals, Council for Scientific and Industrial Research, Pretoria, South Africa

August 2023

Declaration of originality

I, Lerato Mamabote Maboko

Student number: 15357814

Subject of work: Assessing the acetylcholinesterase inhibitory potential of novel pharmacophores for potential treatment of Alzheimer's disease

Declaration

1. I understand what plagiarism entails and am aware of the University's policy in this regard.
2. I declare that this project (thesis) is my own, original work. Where someone else's work was used (whether from a printed source, the internet or any other source) due acknowledgement was given and reference was made according to departmental requirements.
3. I did not submit this work previously (except for published original articles which have resulted from findings in this study before the submission of this completed thesis), nor has it been submitted to any other university for any degree of examination, either by myself or any other party.
4. I did not make use of another student's previous work and submitted it as my own.
5. I did not allow and will not allow anyone to copy my work with the intention of presenting it as his or her own work.

Signature of student: 

Date: 15 August 2023

Abstract

Alzheimer's disease (AD) is the predominant form of dementia which primarily affects the elderly. To date the aetiology of AD has not been fully elucidated, though may include: loss of cholinergic transmission; excessive accumulation of amyloid-beta (Aβ) aggregates extracellularly in the brain; accumulation of tau protein intracellularly; glutamate excitotoxicity and oxidative stress. Current AD therapeutic approaches rely on the administration of acetylcholinesterase inhibitors (AChEIs), memantine and monoclonal antibodies. However, these drugs provide only symptomatic relief and do not prevent progressive neurodegeneration.

Among the above-mentioned approved drugs, AChEIs are suggested to have the ability to inhibit the synthesis, deposition and aggregation of toxic Aβ proteins and tau-protein phosphorylation. For these reasons, AChE has received much attention as the prime target in drug discovery and development for the treatment of AD. However, an overall attrition rate of more than 95% has been noted for novel drugs targeting neurodegenerative diseases, and this is mainly due to a lack of efficacy, blood-brain barrier (BBB) permeability, multifactorial nature and/or toxicity. This reinforces the rationale for assessing a broad spectrum of effects of pharmacophores that show potential for therapeutic use at a preclinical level to reduce the high attrition rate. The aim of the study was to identify novel pharmacophores with the potential to be developed further as treatments for AD.

An in-house miniaturised AChE assay was used to assess the AChEI activity of 1,453 synthetic compounds from a commercial library (Charles River Laboratory/BioFocus, UK) housed at the Council for Scientific and Industrial Research (CSIR). The selected compounds had been previously identified through *in silico* screening of the compound library within the active site of the electric eel and human AChE enzyme. The Swiss Institute for Bioinformatics pharmacokinetic prediction tool, SwissADME, was used to assess the compound's BBB permeability and pharmacokinetics. Combinational AChEI effects of active pharmacophores and donepezil were assessed using a checkerboard assay. The sulforhodamine B assay was employed to determine the active compounds and synergistic combinations cytotoxic potential after 72 h in SH-SY5Y neuroblastoma and brain endothelial (bEnd.5) cells. Michaelis-Menten kinetics of active *in silico* BBB-permeable compounds were determined using the miniaturised AChE assay to elucidate its inhibitory mechanism. Ultra-performance liquid chromatography (UPLC) coupled to a mass spectrometry (MS) was used for quality control analysis to ensure the chemical integrity of compounds. Cellular AChEI activity of active *in silico* BBB-

permeable predicted compounds was determined using an SH-SY5Y AChE-based assay. An *in vitro* BBB model was used to assess the effect of compounds on the integrity of the bEnd.5 monolayer, as well as the permeation of compounds using UPLC-MS.

The miniaturised assay's validation parameters were within acceptable ranges (coefficient of variation ≤ 20%, Z'-factor ≥ 0.5 but < 1, and signal window ≥ 2). Only six compounds (**A8**, **A51**, **A73**, **A136**, **A175** and **A176**) from the primary screen of subset **A** (n = 400) were regarded as possessing AChEI activity (≥ 60% inhibition at 5 µM). For the secondary screen, two subsets of structurally similar compounds, subset **B** (n = 508) and subset **C** (n = 545) were selected and evaluated. The AChEI activity for a further six compounds (**C33**, **C43**, **C53**, **C82**, **C129** and **C189**) were regarded as positive and ranged between 62 and 72%. Of the 12 active compounds, compound **A51** had the lowest half maximal inhibitory concentration (IC_{50}) of 0.20 µM, albeit less potent than donepezil (IC_{50} = 0.03 µM).

The SwissADME pharmacokinetic tool predicted that compounds **A8**, **A73**, **A136**, **C53** and **C129** were BBB-permeable. Synergism (combination index [CI] < 1) was observed between: ¼IC_{50} donepezil and ½IC_{50} **A136** (CI = 0.61); ¼IC_{50} donepezil and IC_{50} **A136** (CI = 0.81); ½IC_{50} donepezil and ½IC_{50} **A136** (CI = 0.81); ½IC_{50} donepezil and IC_{50} **A136** (CI = 0.69); ¼IC_{50} donepezil and ¼IC_{50} **C53** (CI = 0.82). Compounds **A8** and **A73** were not cytotoxic (IC_{50} >100 µM), whereas **A136** (IC_{50} = 4.99 µM) and **C129** (IC_{50} = 13.64 µM) possessed greater cytotoxicity than donepezil and **C53** (IC_{50} = 43.00 and 40.45 µM, respectively). The combination of **A136** and donepezil eradicated all cell growth, while moderate cytotoxicity (20% cell density reduction) was observed for the combination of **C53** and donepezil. Furthermore, no compounds were found to induce cytotoxicity in the bEnd.5 cells (IC_{50} >100 µM).

Donepezil displayed mixed competitive and non-competitive inhibition, while **A8** indicated uncompetitive inhibition, and **A73** and **C53** mixed inhibition. No decomposition was observed for the active *in silico* BBB-permeable non-cytotoxic compounds. Compound **A73** exhibited dose-dependent AChEI activity in SH-SY5Y neuroblastoma cells, whereas **A8** and **C53** did not. At the IC_{50}, 61% AChEI activity was observed for **C53,** with the combination of **C53** and donepezil indicating 69% AChEI activity. The latter possessed the highest *in situ* activity. All compounds, including donepezil, increased transendothelial electrical resistance (TEER) over 48 h exposure, suggesting decreased BBB-permeability of the bEnd.5 monolayer. Furthermore, all compounds were detected in both the apical and basolateral chambers of the *in vitro* BBB

model. This suggests *in vitro* BBB permeation of the compounds and further supporting the *in silico* BBB permeability predictions.

Factors such as efficacy, BBB permeability, and/or toxicity contribute to the high attrition rate noted for central nervous system targeting drugs. In this study 1,453 synthetic compounds were assessed for these aspects in search for potential treatment for AD. Among the 12 compounds that displayed AChEI activity, compound **A51** had the greatest AChEI activity. However, **A51** was predicted *in silico* to be impermeable to the BBB and would most likely not be further developed as it may not cross the BBB. Compound **A136** was cytotoxic as monotherapy and in combination with donepezil, indicating its capability to kill neuronal cells. Due to the low *in situ* AChEI activity displayed by compounds **A8**, **A73** and **C53**, these compounds might not inhibit AChE efficiently *in vivo*. Therefore, compound **C53** alone (at the IC_{50} concentration) and combined with donepezil indicated the potential for further investigation as AChEIs given their promising acellular and cellular AChEI activity, *in silico* BBB-permeability, absence of cytotoxicity, and ability to penetrate the *in vitro* BBB monolayer.

Keywords: acetylcholinesterase, acetylcholinesterase inhibitors, Alzheimer's disease, blood-brain barrier, cytotoxicity.

Dedicated to:

My late father, Mokatakati Aron Maboko, a great father and role model. May your precious soul continue resting in peace.

and

My mother Topisa Mthavini Maboko, the greatest mother ever. Even though you don't have that much education background, thank you for the greatest support.

Acknowledgements

During the course of my master's degree, I vividly remember vowing to myself that I would never, ever do a Doctoral degree. In 2016, I received an email directed to me as "Dr Lerato Maboko" and that was a sign from God.

First and foremost, I would like to thank the Almighty Lord for granting me the opportunity, strength, and wisdom to do what I thought was impossible….

I have an endless list of people to acknowledge and thank for helping me to arrive at this point.

Thank you to my amazing supervisor and co-supervisors; Prof Vanessa Steenkamp, Prof Werner Cordier, Dr Jenny-Lee Panayides, and Dr Anjo Theron.

Thank you, Prof Steenkamp, for starting this journey with me, for your encouragement, guidance, support, and patience. Dr Panayides, thank you for having faith in me since my Council for Scientific and Industrial Research (CSIR) days, for your guidance and support. To Prof Cordier, thank you for your willingness to join this project and your patience when answering my endless questions throughout my laboratory work. Supervising is your gift. Thank you, Dr Theron, for your assistance and valuable laboratory skills I have learnt from you thus far.

This project would not have been possible without the computational and docking skills provided by Dr Johan van der Westhuizen. Thank you so much.

To Prof PJ Becker, thank you for your statistical assistance.

Thank you to Prof Fisher from University of Western Cape for your assistance and allowing us to use your laboratory to conduct the *in vitro* blood-brain barrier permeability model.

To Prof Paul Steenkamp from the CSIR for the chemical analysis of the compounds, thank you.

Special thanks also go out to the Department of Pharmacology, Ms Margo Nell, Ms Petunia Degashu, Mr Solly Mmatli and Mr Amos Kekana for your support and willingness to assist.

I want to express my gratitude to all my colleagues I met during the last five years. Zelie, Bongekile, Keith, Lonwabo, Shamiso, William, Niel and Nicolette, thank you for your advice personally, as well as scientifically. Thank you, guys, for the celebratory braais, they helped me to get a break from science and to replenish my energies. Bongi, thank you for always listening

and being there throughout. To Keith for helping me with my cell work, you are one of the most intelligent people I have ever met.

To the Neurobiology group at the University of the Western Cape, especially Faith, Sivuyile, Thabo and Sisipho, thank you for the warm welcome and allowing me to use some of your laboratory consumables. To Faith and Dr Mentor, thank you for your warmth, love and the sisterhood we built throughout my stay.

To Dr Nzaliseko Mashiya, thank you for your support and always calming me down when the science wasn't sciencing.

I was able to do the research presented here and thanks to the University of Pretoria's (Department of Research and Innovation Support) and CSIR/Department of Science and Innovation Inter-bursary scholarship for the valuable financial support. So, my heartfelt thanks to those of you who pay their taxes.

To my wonderful friends, Bongi, Dikeledi, Kedisaletse, Remoratile, Malefa, Nicolette, Lerato and Oneaho. It is impossible to point out every single aspect you have contributed throughout this journey. You guys always believed more in me than I believed in myself, and I thank you for that and so much more!

To my family, my sisters, Dimakatso and her husband, Morris, and Keya, thank you for being there for me, whenever I needed you. I know, you cannot choose your family, but even if I could, I would not choose another one.

My greatest appreciation goes to my parents, for their encouragement, unconditional love, sacrifices and I could not have asked for a better upbringing, and I owe them an immeasurable debt.

Study outputs

Presentations

Oral presentations:

Maboko LM*, Theron A, Panayides J-L, Cordier W, Steenkamp V. Acetylcholinesterase inhibitory potential of novel pharmacophores for the potential treatment of Alzheimer's disease. 7th All Africa Congress of Pharmacology, Nairobi, Kenya, 17-18 September 2021.

Maboko LM*, Theron A, Panayides J-L, Cordier W, Steenkamp V. Acetylcholinesterase inhibitory potential of novel pharmacophores for the potential treatment of Alzheimer's disease. Department of Medical Biosciences Journal Club, University of Western Cape, South Africa, 6 May 2022.

Maboko LM*, Theron A, Panayides J-L, Cordier W, Steenkamp V. Acetylcholinesterase inhibitory potential of novel pharmacophores for the potential treatment of Alzheimer's disease. South African Society of Basic and Clinical Pharmacology Conference, North-West University, South Africa, 12-13 October 2022.

Maboko LM*, Theron A, Panayides J-L, Cordier W, Steenkamp V. Assessing the acetylcholinesterase inhibitory potential of novel pharmacophores for potential treatment of Alzheimer's disease. Department of Medical Microbiology Journal Club, Stellenbosch University / Tygerberg Hospital, South Africa, 19 September 2023.

Poster presentations:

Maboko LM*, Theron A, Panayides J-L, Cordier W, Steenkamp V. Novel acetylcholinesterase inhibitors: Identifying non-cytotoxic, centrally available pharmacophores. Emerging Researcher Symposium, Council for Scientific and Industrial Research, South Africa, 12 July 2022.

Maboko LM*, Theron A, Panayides J-L, Cordier W, Steenkamp V. Acetylcholinesterase inhibitory potential of novel pharmacophores for the potential treatment of Alzheimer's disease. Health Sciences Faculty Day, University of Pretoria, South Africa, 23 August 2022.

Maboko LM*, Theron A, Panayides J-L, Cordier W, Steenkamp V. Novel pharmacophores with acetylcholinesterase inhibitory activity as potential treatment of Alzheimer's disease.

South African Society of Basic and Clinical Pharmacology Conference, Rhodes University, South Africa, 24-27 August 2023.

List of abbreviations

α-Sec	Alpha-secretase
α-sAPP	Alpha-soluble amyloid precursor protein
A_b	Absorbance of the background
A_s	Absorbance of the AChE activity signal
ACh	Acetylcholine
AChE	Acetylcholinesterase
AChEI	Acetylcholinesterase inhibitor
AICD	Amyloid precursor protein intracellular domain
AD	Alzheimer's disease
ADME	Administration, distribution, metabolism and excretion
APP	Amyloid precursor protein
ARE	Antioxidant response element
ATCI	Acetylthiocholine iodide
ATCC	American Type Culture Collection
Aβ	Amyloid-beta
β-Sec	Beta-secretase
BBB	Blood-brain barrier
BChE	Butyrylcholinesterase
BECs	Brain endothelial cells
BOILED-Egg	Brain or intestinal estimated permeation
BSA	Bovine serum albumin
Ca	Calcium
CAS	Catalytic anionic site
CI	Combination index
ChAT	Choline acetyltransferase
CNS	Central nervous system
CoA	Coenzyme A
CSF	Cerebrospinal fluid
CSIR	Council for Scientific and Industrial Research

CTFα	Alpha-carboxy-terminal fragments
βCTF	Beta-carboxy-terminal fragments
CV	Coefficient of variation
dH_2O	Distilled water
DMEM	Dulbecco's Modified Eagle's Medium
DMSO	Dimethyl sulfoxide
DSI	Department of Science and Innovation
DTNB	5,5-Dithiobis-2-nitrobenzoic acid
eeAChE	Electric eel acetylcholinesterase
EMA	European Medicines Agency
ESI	Electrospray ionisation
fa	Fraction affected
FCS	Foetal calf serum
FDA	Food and Drug Administration
HTS	High throughput screening
HBD	Hydrogen bonding donors
IC_{50}	Half-maximal inhibitory concentration
IgG1	Human immunoglobulin G1
IND	Investigational new drugs
K_m	Substrate concentration
LogP	Logarithmic of the partition coefficient
MaxV	Maximum velocity
$MaxV_s$	Maximum velocity of the sample
$MaxV_c$	Maximum velocity of the negative control
MTT	3-(4,5-dimethylthiazol-2-yl)-2-5- diphenyltetrazolium bromide
NC	Negative control
NCEs	New chemical entities
NFTs	Neurofibrillary tangles
NMDA	*N*-methyl-D-aspartate
NRF2	Nuclear factor-erythroid 2p45 (NF-E2)-related factor
OD	Optical density

OD_{sample}	Optical density of the sample
$OD_{negative}$	Optical density of the negative control
PAS	Peripheral anionic site
PBS	Phosphate-buffered saline
PC	Positive control
Pen-strep	Penicillin/streptomycin
P-gp	P-glycoprotein
PHF	Paired helical filaments
PSEN	Presenilin
P3	Soluble N-terminal peptide fragment
R&D	Research and development
RFT	Random Tree Forest
sAPPα	Alpha-soluble amyloid precursor protein
sAPPβ	Beta-soluble amyloid precursor protein
SA	South Africa
[S]	Substrate concentration
SD	Standard deviation
SD_s	Standard deviation of the signal
SD_b	Standard deviation of the background
SEM	Standard error of mean
SAPHRA	South African Health Products Regulatory Authority
SMILES	Simplified molecular input line entry system
SRB	Sulforhodamine B
SSA	Sub-Saharan Africa
SW	Signal window
TCA	Trichloroacetic acid
TEER	Transendothelial electrical resistance
TIA	Technology Innovation Agency
TJ	Tight junctions
TNB	Thio-2-nitrobenzoate
TPSA	Topological polar surface area

tcAChE	*Torpedo californica* acetylcholinesterase
USA	United States of America
UK	United Kingdom
UPLC	Ultra-performance liquid chromatography
V_{max}	Maximum velocity
w/v	Weight per volume
WLogP	Wildman-Crippen based lipophilicity
Xs	Average of the signal
X_b	Average of the background
ϒ-Sec	Gamma-secretase
Z’	Z-factor

List of symbols and chemical formulae

°C	Degree Celsius
%	Percentage
µL	Microliter
µM	Micromolar
CO_2	Carbon dioxide
g	Gravitational force
h	Hour(s)
M	Molar
min	Minute(s)
$MgCl_2.6H_2O$	Magnesium chloride hexahydrate
mM	Millimolar
NaCl	Sodium chloride
NaOH	Sodium hydroxide
pH	Power of hydrogen
pM	Picomolar
s	Second(s)
Tris-HCl	Tris-hydrochloride

List of Figures

Figure 1: Schematic representation of the beta-amyloid pathway that leads to Alzheimer's disease pathology 2
Figure 2: Progression of events leading to cell death and neurodegeneration 3
Figure 3: Tangle hypothesis of Alzheimer's disease progression 4
Figure 4: Synthesis of acetylcholine in the axon and its hydrolytic pathway 5
Figure 5: Schematic representation of the drug discovery and development process 11
Figure 6: Structure of the blood-brain barrier 14
Figure 7: Chemical principle of Ellman's method. 19
Figure 8: The SwissADME results presented as brain or intestinal estimated permeation plot..... 22
Figure 9: Plate layout used to determine the combinatorial effect of donepezil and the active compound 23
Figure 10: A bicameral system..... 27
Figure 11: Dose-dependent inhibition of acetylcholinesterase by donepezil and galantamine..... 30
Figure 12: Dose-dependent inhibition of acetylcholinesterase by dimethyl sulfoxide..... 31
Figure 13: The acetylcholinesterase inhibitory activity of active compounds from subsets **A** and **C** . 34
Figure 14: Unique structure of compound **A8**..... 35
Figure 15: Chemical structures of the active compounds. 38
Figure 16: A brain or intestinal predicted permeation plot of the 12 compounds with acetylcholinesterase inhibitory activity 42
Figure 17: The effect of compounds with acetylcholinesterase inhibitory activity and donepezil on SH-SY5Y cell density after 72 h exposure..... 48
Figure 18: Cytotoxicity of the combinations which indicated synergistic effect 49
Figure 19: The effect of compounds and donepezil on bEnd.5 cell density after 72 h exposure..... 50
Figure 20: Cytotoxicity of the combinations which indicated a synergistic effect 51
Figure 21: Lineweaver-Burk plot for enzyme inhibition 52
Figure 22: A) Michaelis-Menten graph and B) Lineweaver-Burk plot for compounds with acetylcholinesterase inhibitory activity and predicted blood-brain barrier permeability 53
Figure 23: Lineweaver-Burk plots of compounds with acetylcholinesterase inhibitory activity and predicted blood-brain barrier..... 55
Figure 24: Cellular acetylcholinesterase inhibitory activity of compounds with potential acellular acetylcholinesterase inhibitory activity 57
Figure 25: Cellular acetylcholinesterase inhibitory activity of individual compounds and the synergistic combination..... 58

Figure 26: A graphical representation of the effect of acetylcholinesterase inhibitors, *in silico* blood-brain barrier predicted and non-cytotoxic compounds on bEnd5 permeability upon 12 h, 24 h, and 48 h treatment..... 60
Figure 27: The positive electrospray ionisation chromatograms for the combination of donepezil and **C53**..... 62
Figure 28: The positive electrospray ionisation chromatograms for donepezil, **A8**, **A73**, and **C53**.. 137
Figure 29: The positive electrospray ionisation chromatograms for **A8** at half maximal inhibitory concentration and 1.5 × half maximal inhibitory concentration..... 138
Figure 30: The positive electrospray ionisation chromatograms for **A73** at half maximal inhibitory concentration and 1.5 × half maximal inhibitory concentration..... 143
Figure 31: The positive electrospray ionisation chromatograms for **C53** at half maximal inhibitory concentration and 1.5 × half maximal inhibitory concentration..... 140
Figure 32: The positive electrospray ionisation chromatograms for donepezil at half maximal inhibitory concentration and 1.5 × half maximal inhibitory concentration..... 141

List of Tables

Table 1: Current FDA-approved drugs for the treatment of patients with Alzheimer's disease 9

Table 2: Statistical parameters (intra- and inter-assay) for the miniaturised acetylcholinesterase assay. 32

Table 3: Compounds in subset **A** that inhibited acetylcholinesterase activity by ≥ 60%. 33

Table 4: Compounds in subset **C** that inhibited acetylcholinesterase activity by ≥ 60%. 36

Table 5: Half maximal inhibitory concentration values and coefficient correlation of active compounds. 39

Table 6: Analogues of active compounds reported in literature. 40

Table 7: Physiochemical descriptors for the compounds containing acetylcholinesterase inhibitory activity. 42

Table 8: The concentrations of the compounds and donepezil used to determine the combination index 44

Table 9: Combination index values obtained when combining the compounds with donepezil 44

Table 10: Acetylcholinesterase inhibitory activity of subset **A** compounds 103

Table 11: Acetylcholinesterase inhibitory activity of subset **B** compounds 112

Table 12: Acetylcholinesterase inhibitory activity of subset **C** compounds 124

Table of Contents

Declaration of originality ... **ii**
Abstract ... **iii**
Dedication ... **vi**
Acknowledgements ... **vii**
Study outputs ... **ix**
List of abbreviations ... **xi**
List of Figures ... **xv**
List of Tables ... **xvii**
CHAPTER 1: LITERATURE REVIEW ... **1**
1.1 Alzheimer's disease ... **1**
1.2 Pathophysiology of Alzheimer's disease ... **2**
1.2.1 Amyloid hypothesis ... 2
1.2.2 Tangle hypothesis ... 4
1.2.3 Cholinergic hypothesis ... 5
1.2.4 Glutamatergic hypothesis ... 6
1.2.5 Risk factors associated with types of Alzheimer's disease ... 6
1.3 Progression of Alzheimer's disease ... **7**
1.3.1 Mild stage ... 7
1.3.2 Moderate stage ... 7
1.3.3 Severe stage ... 7
1.4 Treatment of Alzheimer's disease ... **7**
1.4.1 Acetylcholinesterase inhibitors ... 8
1.4.2 *N*-methyl-D-aspartate receptor antagonist ... 8
1.4.3 Monoclonal antibodies ... 9
1.5 Drug discovery and development ... **10**
1.6 Drug discovery and development for neurodegenerative diseases ... **11**
1.6.1 Efficacy ... 12
1.6.2 Cytotoxicity ... 12
1.6.3 Blood-brain barrier permeability ... 13
1.7 Aims and objectives ... **17**
CHAPTER 2: MATERIALS AND METHODS ... **18**
2.1 Compound selection and collection ... **18**
2.2 Acetylcholinesterase inhibitory activity ... **19**
2.2.1 Micro-plate assay miniaturisation and optimisation ... 19
2.2.2 Assay validation ... 20

2.2.3 Single-point and dose-response screening of compounds 21
2.3 Pharmacokinetics prediction 21
2.4 Combinational inhibitory effects of compounds with donepezil 22
2.5 Cytotoxicity screening of biologically active compounds 23
2.5.1 Cell culture and maintenance 23
2.5.2 Cell seeding and exposure 24
2.5.3 Sulforhodamine B colorimetric assay 24
2.6 Michaelis-Menten kinetics assay 25
2.7 Chemical stability analysis 25
2.8 *In situ* acetylcholinesterase inhibitory activity of compounds 26
2.9 Blood-brain barrier permeability assessment 27
2.9.1 The *in vitro* bicameral system 27
2.10 Statistical analysis 28
CHAPTER 3: RESULTS AND DISCUSSION 29
3.1 Acetylcholinesterase inhibitory activity 29
3.1.1 Assay miniaturisation and optimisation 29
3.1.2 Assay validation 32
3.1.3 Acetylcholinesterase inhibitory activity screening of the compounds 32
3.2 Pharmacokinetics prediction 40
3.3 Combinational treatment effects 43
3.4 Cytotoxicity screening 47
3.5 Inhibition kinetics of acetylcholinesterase enzyme 51
3.6 *In situ* acetylcholinesterase inhibitory activity of compounds 56
3.7 *In vitro* blood-brain barrier permeability assessment 59
CHAPTER 4: CONCLUSION 65
CHAPTER 5: LIMITATIONS AND FUTURE RECOMMENDATIONS 67
References 69
Appendix I: Research Ethics approval 98
Appendix II: Reagents preparation 99
Appendix III: Acetylcholinesterase inhibitory activity of the screened compounds 103
Appendix IV: Chromatograms of screened compounds indicating that no degradation took place… 137
Appendix V: Chromatograms of the apical and basal medium indicating that compounds penetrated the blood-brain barrier 138

Chapter 1: Literature review

Dementia is a grouping of pathological traits characterised by impairment of at least two cognitive functions, such as memory loss and judgement.[1,2] The most common underlying pathologies include Alzheimer's disease (AD), Creutzfeldt-Jakob disease, dementia with Lewy bodies, frontotemporal lobar degeneration, mixed dementia, normal pressure hydrocephalus, Parkinson's disease and vascular dementia.[3,4] Among the above-mentioned, AD is accountable for more than 80% of dementia cases, making it the most prominent form of dementia.[5–7]

1.1 Alzheimer's disease

Alzheimer's disease is a progressive irreversible neurodegenerative disorder affecting individuals older than 65 years.[8] This form of dementia was first identified by and named after a German psychiatrist, Alois Alzheimer, in 1906.[9] Since its first diagnosis until the year 2022, the global number of people living with AD has been estimated at more than 55 million people and this number is expected to triple to 152 million by the year 2050.[10,11] The prevalence is expected to increase in future in both developed and developing countries.[5]

In the United States of America (USA) alone, about 6.5 million people ≥ 65 years were living with AD in 2022, however, this is projected to increase to 12.7 million by 2050.[12] This neurodegenerative disease is ranked as the 7th leading cause of death for all ages and the 5th for individuals older than 65 years in the USA.[12,13] Unfortunately, there is limited data available on the prevalence and impact of dementia on elderly populations in sub-Saharan Africa (SSA), including South Africa (SA). This is ascribed to the limited population-based dementia studies conducted to date.[14–16]

According to the 2016 World Alzheimer's Report, which is the latest report to date, there were 4.4 million people over the age of 60 years in SA, of whom approximately 187,000 were estimated to be living with AD.[16,17] This number is predicted to increase to 250,000 by 2030.[16,17] Alzheimer's disease is ranked as one of the top 50 causes of death, resulting in approximately 2,664 (0.48%) deaths annually in SA.[18] In addition to being a leading cause of death, AD is identified as causing about 2.4% of disability adjusted life years throughout SSA's population aged 70 years and older, leading to an increased burden on health systems. Due to lack of data as mentioned above and limited diagnoses, this estimated number might be lower than the actual number.[5,14,19]

1.2 Pathophysiology of Alzheimer's disease

Despite the global focus on researching AD pathogenesis, its epidemiology as well as its impact on public health, the pathophysiology remains poorly understood.[20,21] This highly complex disease is characterised by extracellular beta-amyloid (Aβ) plaques, intracellular neurofibrillary tangles (NFTs) and a loss of neurons in the brain.[18,22,23] There are several theories and hypotheses on the pathogenesis of AD and the most widely accepted include the amyloid, tangle, cholinergic and excitotoxicity hypotheses.[24,25]

1.2.1 Amyloid hypothesis

The amyloid hypothesis proposes that Aβ deposition is the initial pathological event and major cause of AD.[26,27] The presence of mutations in the β-amyloid precursor protein (APP) and presenilin (PSEN-1 and PSEN-2) genes facilitate accumulation of Aβ.[5,28] Generally, APP is primarily cleaved in a non-amyloidogenic pathway by α-secretase, and further cleaved by γ-secretase.[23] However, due to the aforementioned mutations, APP is abnormally processed through the amyloidogenic pathway. Beta-amyloid precursor protein is cleaved by β-secretases, and then further cleaved by γ-secretase to form amyloidogenic peptides (Aβ1-42). These insoluble peptides aggregate into oligomers and accumulate as amyloid plaques, also known senile plaques in the brain (Figure 1).[24,28,29]

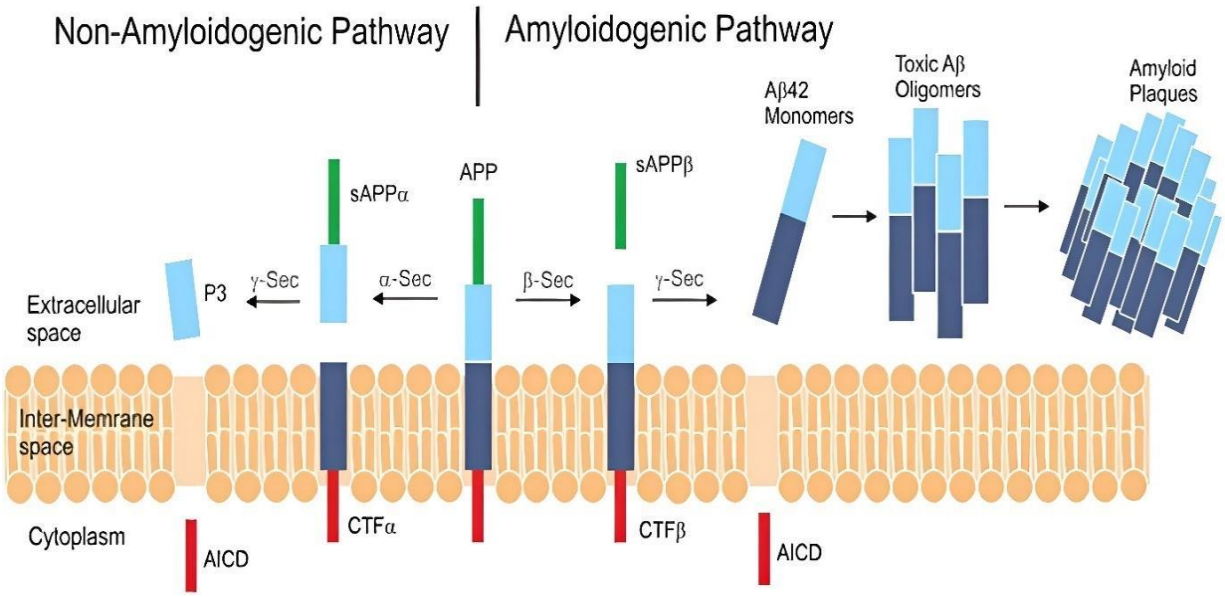

Figure 1: Schematic representation of the beta-amyloid pathway that leads to Alzheimer's disease pathology.[24] APP: amyloid precursor protein, AICD: APP intracellular domain, Aβ: amyloid beta, CTFα: alpha-carboxy-terminal fragments, CTFβ: beta-carboxy-terminal fragments, sAPPα: alpha-soluble amyloid precursor protein, sAPPβ: beta-soluble amyloid precursor protein, P3: soluble N-

terminal peptide fragment, α-Sec: alpha-secretase, β-Sec: beta-secretase, ϒ-Sec: gamma-secretase. [*Reproduced with permission from Wiley Periodicals, Inc., license number: 5190560918613*].

Aggregation of senile plaques may start 10 years before any observable symptoms or the diagnosis of AD.[30,31] High concentrations of these plaques trigger several secondary neuropathological changes that disrupt neuronal homeostasis and promotes AD precipitation, such as the accumulation of NFTs, facilitates synaptic degeneration and neuronal cell death (Figure 2), hence they are considered a principal feature in AD pathogenesis.[5,32,33]

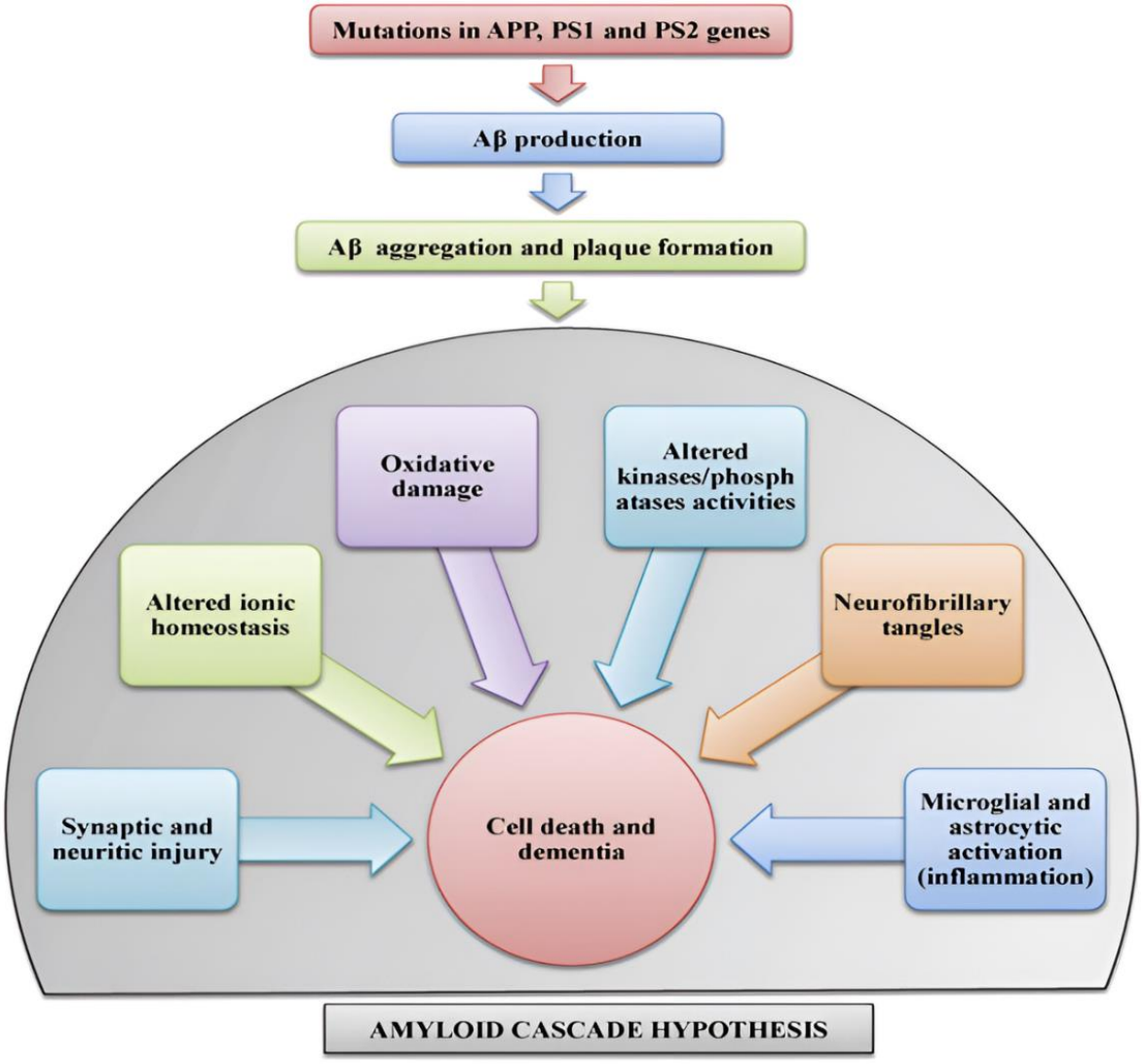

Figure 2: Progression of events leading to cell death and neurodegeneration.[5] Aβ: amyloid beta, APP: amyloid precursor protein, PS1 (PSEN 1): presenilin 1 and PS2 (PSEN 2): presenilin 2. [*Reproduced with permission from Elsevier, license number: 5191890936880*].

1.2.2 Tangle hypothesis

The tangle hypothesis, also known as the tau hypothesis, describes the formation of abnormal tangles by hyperphosphorylated tau protein.[23] Tau proteins are highly soluble peptides found in the neurons, where they play a major role in microtubule stabilisation (Figure 3).[34,35]

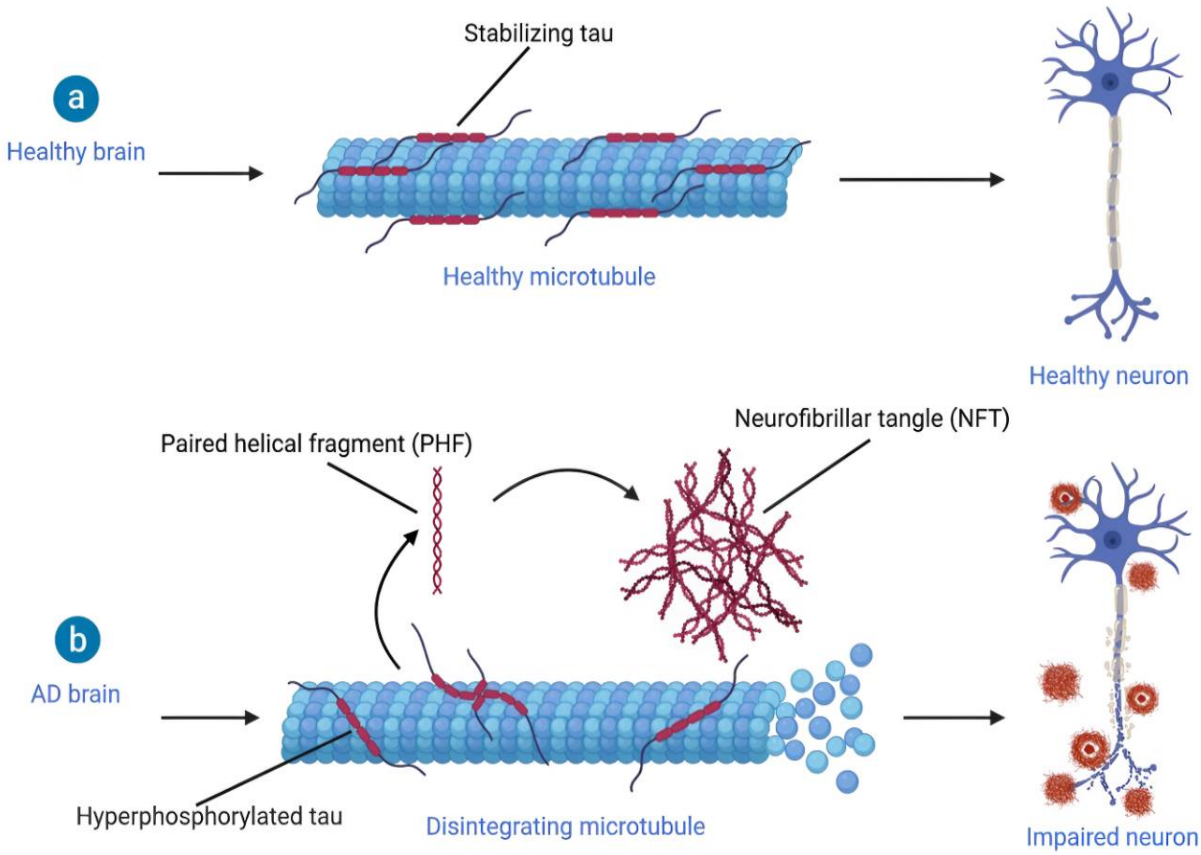

Figure 3: Tangle hypothesis of Alzheimer's disease progression. The role of the tau protein in the (**a**) healthy and (**b**) Alzheimer's disease brain.[36] NFT: neurofibrillary tangles; PHF: paired helical filaments. [*Reproduced with permission from authors (Van Oostveen WM and De Lange ECM) under Creative Commons Attribution (CC BY) license (https://creativecommons.org/licenses/by/ 4.0/)*].

Normally, tau protein phosphorylation plays a role in intracellular trafficking processes which removes these proteins from the microtubule. Tau protein removal allows for transportation followed by dephosphorylation to return tau proteins back to the microtubule.[30] In AD, however, there is an abundance of Aβ plaques in the brain, which results in tau proteins contacting released kinases and resulting in hyperphosphorylation. This hyperphosphorylation results in the removal of the proteins from the microtubule, leading to masses of insoluble paired helical filaments further aggregating into NFTs.[29,34,35] The formation of NFTs destabilises the

cytoskeleton and nerve cell transport system, which eventually causes neurodegeneration and finally apoptosis in neurons.[23,30,35]

1.2.3 Cholinergic hypothesis

In contrast to the amyloid and tangle hypotheses, the cholinergic hypothesis suggests a decreased level of cholinergic neurotransmission in the brain.[23] The importance of cholinergic function in learning and memory processes has been known since the early 1970s.[37] Acetylcholine (ACh) is a neurotransmitter that is responsible for cell-to-cell communication and is synthesised in the nucleus basalis by choline and acetyl coenzyme A (choline acetyltransferase [ChAT]).[38,39] It is transported through the microtubules and released into the synaptic cavity, where it interacts with the cholinergic receptors.[23] The remaining ACh is degraded by the acetylcholinesterase enzyme (AChE) in the synaptic cleft into choline and acetate, which are the bases of its formation (Figure 4).[37] In AD, there is a decreased synthesis and activity of ChAT due to the degeneration of cholinergic neurons, and AChE hydrolysis, consequently leading to ACh deficiency with cognitive and functional symptomatic conditions of AD.[23,37,38]

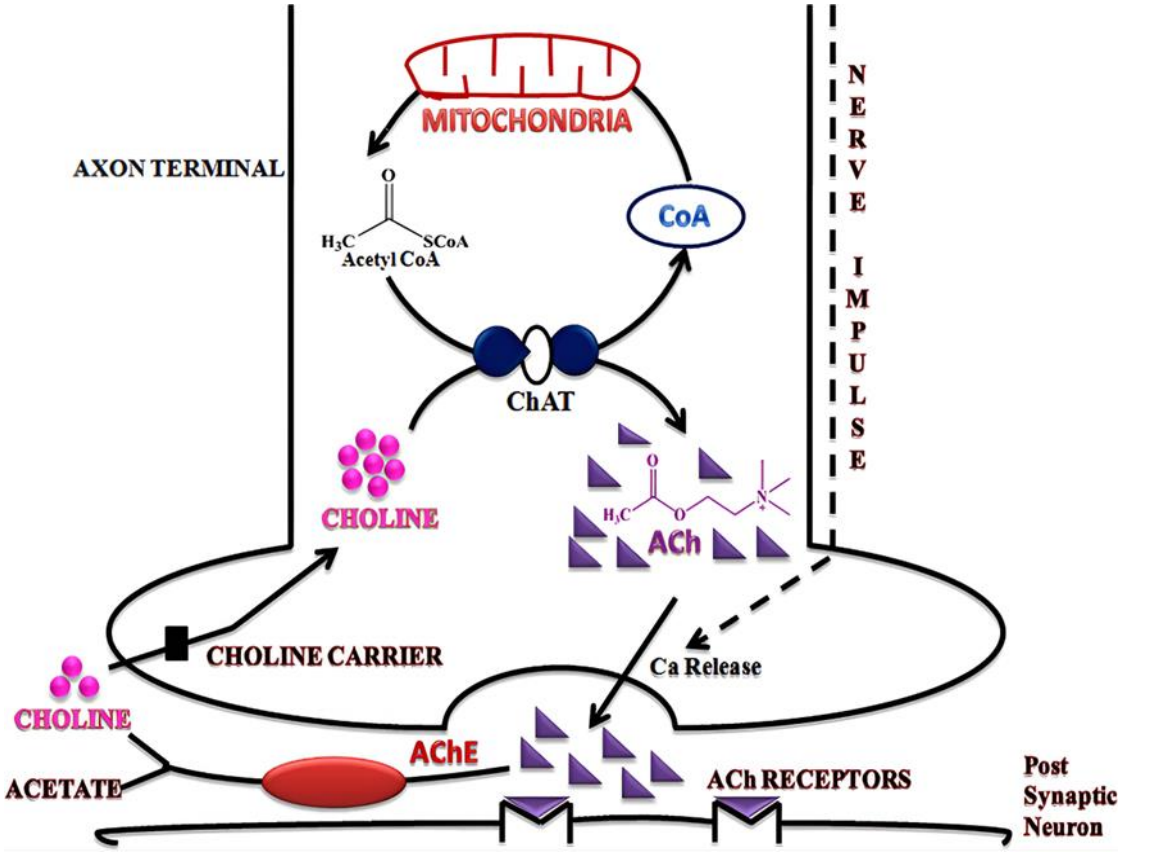

Figure 4: Synthesis of acetylcholine in the axon and its hydrolytic pathway.[40] AChE: acetylcholinesterase enzyme, ACh: acetylcholine, Ca: calcium, ChAT: choline acetyl transferase, CoA: coenzyme A. [*Reproduced with permission from Springer Nature, license number: 5191181303928*].

1.2.4 Glutamatergic hypothesis

The glutamatergic or excitotoxicity hypothesis is explained by the overstimulation of glutamatergic activity in the brain. Briefly, glutamate is an excitatory neurotransmitter that plays a role in all aspects of cognition and higher mental function.[41,42] *N*-methyl-D-aspartate (NMDA) receptors on the other hand play a crucial role in glutamate synaptic transmission and plasticity phenomena such as long-term potentiation.[25,41,43]

In healthy individuals, glutamate level in the neuronal synapses is regulated through metabolite exchange in neuronal, astrocytic and endothelial cells.[41] In AD individuals, the regulation of glutamate is inefficient, thereby leading to elevated levels.[41,44] An increase in and accumulation of glutamate causes excessive NMDA receptor activity, which is known as chronic 'excitotoxicity' and leads to neurodegeneration.[42,44,45] These correlate clinically with the progressive decline in cognition and the development of pathological neural anatomy seen in AD patients.[25,43]

1.2.5 Risk factors associated with types of Alzheimer's disease

In addition to the above-mentioned hypotheses, there are non-modifiable and modifiable risk factors that are thought to increase the chances for the development of AD.[22,46] Non-modifiable risk factors include older age (≥ 65 years), genetics (presence of the ε4-allele of apolipoprotein E) and having a family history (first-degree relative) of AD.[12,47,48] Modifiable risk factors include comorbidities (such as cardiovascular diseases or metabolic diseases), lifestyle factors (such as smoking, excessive alcohol in-take, low physical exercise, and an unhealthy diet) and low education attainment.[48,49]

Depending on the age of the first symptoms of onset and presence of the above-mentioned pathological hallmarks or risks factors, AD can be classified into two types.[38,50] Early-onset AD, also known as familial AD, affects individuals younger than 65 years of age.[35] This dominantly inherited AD is a rare type associated with mutations in the *APP*, *PSEN1* and/or *PSEN2* genes.[7,33,50] The more common type is late-onset or sporadic AD, which manifests in individuals older than 65 years and is mainly associated with non-modifiable risk factors.[7,33,50] Understanding the role of these factors will provide insight into mechanisms that drive AD pathogenesis.[51]

1.3 Progression of Alzheimer's disease

Age of onset, rate of progression and symptoms of AD varies from person to person.[52] There are three primary stages of AD, each with different challenges and symptoms, namely, mild, moderate and severe.[5,28]

1.3.1 Mild stage

The mild stage is also referred to as the early stage, and is the initial stage when AD is first diagnosed. Lasting between two and four years,[53] this stage is characterised by apathy, decreased cognitive ability, depression, and short-term memory loss.[46,53,54] During this stage, individuals have trouble in retaining new information, problem solving, decision making, trouble handling money and paying bills. The individual may start wandering and getting lost, misplacing belongings and take longer to complete normal daily tasks.[54]

1.3.2 Moderate stage

The moderate stage is the longest stage of AD and lasts between two and ten years.[54] During this stage memory continues to deteriorate and individuals cannot create new memories or learn anything new.[28] Patients in this stage, have difficulty identifying and recognising family and friends, performing routine activities, have poor judgement, lose orientation to time and place.[2,18,54] Due to increased memory loss and confusion, patients need help with day to-day activities.[54]

1.3.3 Severe stage

The final or late stage of AD is the severe stage and lasts between one to three years. Cognitive and physical abilities continue to decline severely in this stage.[54] This stage is characterised by impaired communication, disorientation, difficulty in speaking, swallowing and walking.[2,31] When this stage is reached, patients are often placed in nursing homes or other long-term care facilities.[54] As a result of damage occurring to the parts of the brain involved in movement, individuals become bedridden and susceptible to conditions such as pneumonia and septicaemia which lead to death.[2,28]

1.4 Treatment of Alzheimer's disease

Although AD was originally described more than 100 years ago, its pathogenesis has not been elucidated fully, consequently leading to no discovery of curative treatments to date.[37] The Food

and Drug Administration (FDA) has approved acetylcholinesterase inhibitors (AChEIs), NMDA-receptor antagonists and monoclonal antibodies as treatments that are still limited to symptomatic management.[55]

1.4.1 Acetylcholinesterase inhibitors

According to the cholinergic hypothesis described in Section 1.2.3 (page 5), AD patients have low levels of ACh, leading to diminished cholinergic synaptic activity.[37] Acetylcholinesterase inhibitors delay the metabolic degradation of ACh by inhibiting AChE and thus optimise its availability in the brain.[37,56] Currently there are three drugs in use in this class: donepezil (Aricept®), galantamine (Razadyne®) and rivastigmine (Exelon®) (Table 1).[44,53,54]

Tacrine (Cognex®) was the first approved AChEI for the treatment of mild or moderate AD, but it was discontinued due to hepatotoxicity.[44,57] Donepezil, galantamine and rivastigmine are still recommended and used to treat mild to moderate symptoms of AD.[58–60] In 2006, donepezil was approved for the treatment of severe symptoms of AD.[37,48] In addition to AChE inhibition, it is also suggested that these AChEIs have the ability to inhibit the synthesis, deposition and aggregation of toxic Aβ proteins and tau-protein phosphorylation.[48,61,62]

Common side effects which often manifest during initiation or dose escalation of treatment include gastrointestinal disorders, nausea, loss of appetite, diarrhoea, vomiting, fatigue, insomnia, and weight loss.[37,57] Some patients have additionally experienced anorexia, hallucinations, bradycardia, syncope, and muscle cramps.[26]

1.4.2 *N*-methyl-D-aspartate receptor antagonist

As the disease progresses, AChEIs become less effective.[64] Second line treatment, such as the non-competitive NMDA receptor antagonist, memantine (Namenda®), is then prescribed (Table 1).[6,58,64] Memantine inhibits excitotoxicity that develops when excessive amounts of glutamate neurotransmitter is released, as is the case with AD.[40,58] In addition memantine decreases hyperphosphorylation of tau proteins and protects against toxicity induced by Aβ peptides.[26] Memantine is used either as a monotherapy or in combination with an AChEI (donepezil or rivastigmine).[22,59]

As monotherapy, memantine is usually administered at 20 mg which may cause side effects such as dizziness, headache, confusion, and constipation.[64,65] Whereas in combination therapy, consisting of drugs with different targets and modes of action (NMDA receptor antagonist and

AChEI), it provides effective pharmacological management of AD with improved tolerability.[60] Moreover, combination therapy delays AD progression by prolonging the symptomatic benefits and retaining cognitive abilities and functions.[65,66] Due to these beneficial outcomes, combination therapy represents the current gold standard for treatment of moderate to severe AD.[67]

Table 1: Current FDA-approved drugs for the treatment of patients with Alzheimer's disease.[44,63]

Drug name	Chemical structure	Source	Year of approval	Mechanism of action	Daily Dose
Donepezil	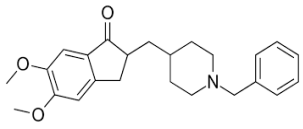	Piperidine derivative	1996	AChEI	5-10 mg
Rivastigmine	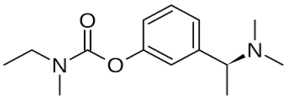	Carbamate derivative	2000	AChEI	3-12 mg
Galantamine	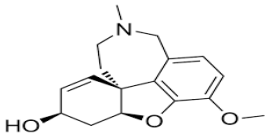	Isolate from *Galanthea woronwii* plant	2001	AChEI	8-12 mg
Memantine	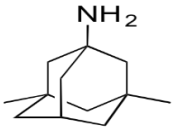	1-aminoadamantane derivative	2003	NMDA receptor antagonist	10-20 mg
Aducanumab	$C_{6472}H_{10028}N_{1740}O_{2014}S_{46}$	Human	2021	Anti-Aβ monoclonal antibody	100 mg/mL
Lecanemab	$C_{6544}H_{10088}N_{1744}O_{2032}S_{46}$	Human	2023	Anti-Aβ monoclonal antibody	10 mg/kg

Aβ: amyloid beta; AChEI: acetylcholinesterase inhibitor; NMDA: *N*-methyl-D-aspartate.

1.4.3 Monoclonal antibodies

In 2021 and 2023, FDA-approved humanised immunoglobulin G1 (IgG1) monoclonal anti-Aβ antibodies, aducanumab (Aduhelm®) and lecanemab (Leqembi®), respectively, entered the market.[68,69] These monoclonal antibodies are used to treat mild AD by binding with high affinity to Aβ aggregates (soluble oligomers and insoluble fibrils), thereby eradicating Aβ plaque load in the brain.[55,70] Side effects such as diarrhoea, confusion, fever, altered mental status, disorientation, headache, microhaemorrhage, and hypersensitivity (angioedema and urticaria) were observed during clinical trials.[71]

1.5 Drug discovery and development

Despite the availability of the above-mentioned drugs, treatment of AD is still unmet.[71] This is since the effectiveness of drugs used to treat AD varies from person to person. Although in some patients these drugs decrease cognitive symptoms by slowing progression, in others there is no response.[71] As AChEIs remain the best treatment of AD due to these drugs increasing ACh levels and decreasing the deposition of Aβ proteins, this pathway remains the target.[40,62,72]

New effective drugs are identified through a multidisciplinary process known as drug discovery and development.[73] Historically, new chemical entities (NCEs) were isolated from natural sources such as plants, animals, and microorganisms.[74,75] A few examples of drugs derived from natural sources include galantamine, quinine, and cocaine. Thyroid hormone, cortisol, and insulin were originally isolated from animals, whereas penicillin was derived from microbes.[76]

Due to the success of NCEs discovered from natural products, their intrinsic complexity and distinctive structural diversity, pharmaceutical companies derived molecules from these products (semi-synthetic analogues) to develop chemical libraries.[76,77] Some of the approved semi-synthetic drugs include artemisinin derivatives, rifampicin, cephalosporins and tetracyclines.[78,79] Synthetic therapeutic entities are the cumulative end-product emerging from an intricate process of hypothesis, design, and synthesis.[80] These include simeprevir, artesunate and chloroquine.[78,79,81]

Identified NCEs (either natural, semi-synthetic or synthetic) must have the required characteristics of druggability in order for them to proceed through the process of drug discovery and development.[76] This process consists of several steps including; target identification, target validation, hit and lead identification, lead optimisation, pre-clinical and clinical testing, new drug application, and drug approval, which depends on the country of origin (e.g., via the FDA, European Medicines Agency approval [EMA] or South African Health Products Regulatory Authority [SAPHRA]) (Figure 5).[82,83]

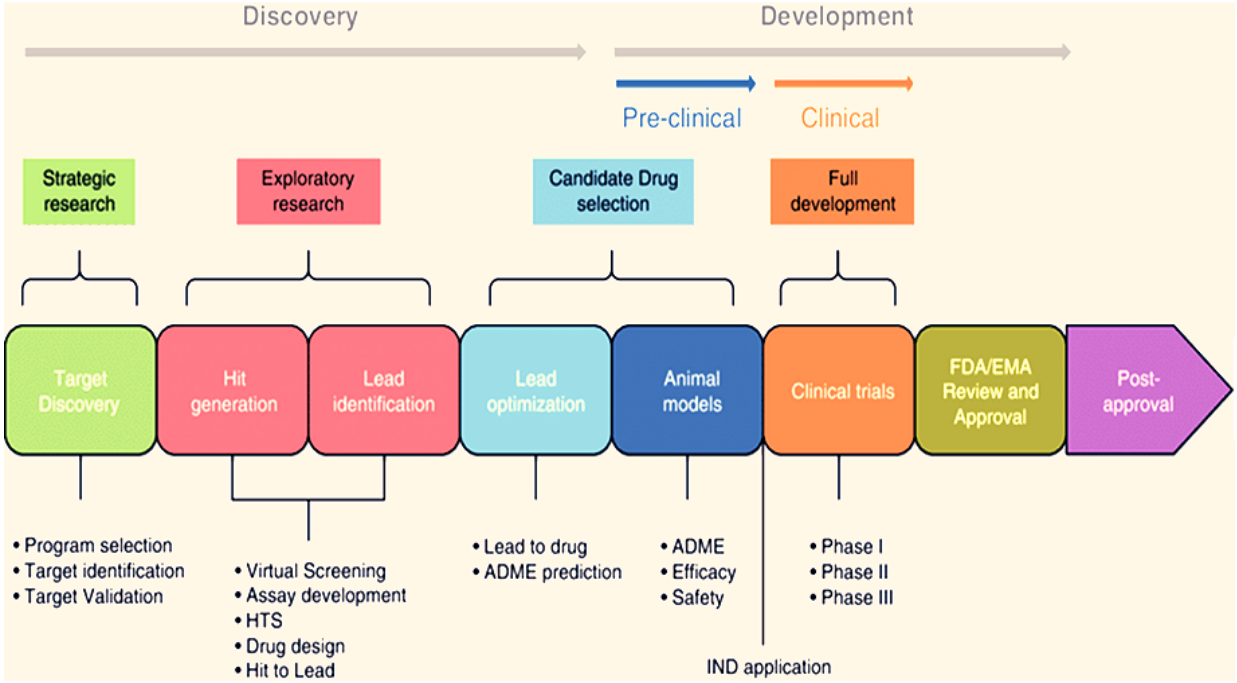

Figure 5: Schematic representation of the drug discovery and development process.[83] ADME: absorption, distribution, metabolism and excretion, EMA: European Medicines Agency, FDA: Food and Drug Administration, HTS: high-throughput screening and IND: investigational new drugs. [*Reproduced with permission from Springer Nature; license number: 5191441370705*].

The multidisciplinary process is expensive due to the high cost of research and development (R&D) and clinical trials. To develop one novel efficacious drug, R&D cost amounts to approximately 900 million to 2 billion US dollars and takes almost 10 to 15 years from when it shows promise to when it is available on the market.[84,85] Despite the significant time and financial investment, this process is still associated with low success rate.[86,87] On average, out of the approximately 1 million compounds entering initial *in vitro* screening, about 250 compounds will enter the pre-clinical testing phase. Of these, only ten will proceed to clinical trials, and may lead to one drug proceeding to approval for the market.[88,89]

1.6 Drug discovery and development for neurodegenerative diseases

The complexity of neurodegenerative diseases such as AD requires an ongoing identification of new effective molecular modulators against specific targets to treat or delay the onset.[90] Sadly, drug discovery and development of novel drugs targeting central nervous system (CNS) disorders is problematic, taking significantly longer to develop (12-16 years compared to 10-12 years for non-CNS targeting drugs), with an overall attrition rate of more than 95%.[91–93] This high rate of failure is caused by factors such as inefficacy, multifactorial aetiology, cytotoxicity, and an inability to cross the blood-brain barrier (BBB).[86,94,95]

1.6.1 Efficacy

The inefficacy of the drugs to treat the disease is considered as the major cause of drug development failure, accounting for about 43% of study terminations.[94,96] Hence assay development and miniaturisation for efficacy screening regarding neurodegenerative diseases has received a great deal of attention over the course of the last decade. These include well-established enzyme based-assays for determination of activity against known targets, such as cholinesterase, Aβ aggregation, β-secretase, and tau-related protein kinases.[97–99]

For AD, drug screening assays such as colorimetry, electrometry, pH-stat, radiometry and tintometry have been and are still used to determine AChE inhibitory activity.[88,100] The colorimetric assay based on Ellman's assay with modifications is the most widely used method for routine determination of AChEI activity, hence it is considered as the gold standard assay. Advantages of this method are that it is inexpensive, rapid, reproducible, and simplistic. This assay has been semi-automated and adapted to microplates.[88,101]

In addition to screening for drug efficacy, Ellman's assay can also be used to assess drug combination treatment. Drug combinations have been extensively explored for enhanced therapeutic efficacies and there are *in silico* tools developed for predicting combination effects.[102] One of the popular dose-effect based methods used is the Chou-Talalay which involves the determination of the drug combination index (CI).[102,103] The Chou-Talalay method, is not time-consuming, nor costly.[102] However, a major limitation is its dependence on accurate and well-defined dose-effect curves, which are not always available.[103]

Predicted CI results facilitate the classification of the compounds combined effect, either as a weaker (antagonistic) or stronger (potentiated, synergistic).[103] The combination of two compounds, for instance AChEIs, that compete for the same enzymatic active site, is expected to have an antagonistic effect. However, due to the ability of one compound to bind allosterically to the enzyme, a synergistic effect can also be observed.[104]

1.6.2 Cytotoxicity

Cytotoxicity is among the main reasons for drug failure, and accounts for almost a quarter of drugs being excluded from further studies.[86,105] Cytotoxicity is the damage caused by the compound on the substructure or function of a cell, often leading to cell death, whereas toxicity refers to the damaging effects of compounds on whole organisms.[106] Cytotoxicity provides a

prediction of the *in vivo* toxicity of compounds and is determined by measuring the ability of a compound to destroy cells.[106]

Drug-induced cytotoxicity is determined by measuring cellular proliferation in mammalian cell lines and a variety of assays such as MTT (3-(4,5-dimethylthiazol-2-yl)-2-5-diphenyltetrazolium bromide), sulforhodamine B, and clonogenic are available.[107,108] Although these approaches can never be accurate enough to replace the *in vivo* environment, they are simple, cheap, reliable, fast, sensitive and reproducible.[107,108] Toxicity testing in pre-clinical research is critical as it provides key information about the recommended dose and safety of a new drug. Should drugs be found to be cytotoxic at any stage, further development is halted leading to decreased drug attrition rate.[109,110]

1.6.3 Blood-brain barrier permeability

One of the leading challenges of developing successful CNS-acting drugs is BBB impermeability.[111,112] The BBB is a centrally located endothelial barrier within the nerve vascular unit, with tight junctions (TJs) between endothelial cells sealing off the vascular lumen from the abluminal side.[113,114] The tightly-sealed endothelial cells provide a unique microenvironment for the brain, allowing communication with the systemic compartment and limits brain penetration of most CNS drug candidates.[115,116] In addition to the endothelial cells, pericytes, astrocytes, and basal lamina (Figure 6), further contribute to the highly selective nature of the BBB.[116,117]

Penetration of molecules into the brain is facilitated and regulated based on their physicochemical properties together with the expression of efflux transporters, such as P-glycoprotein (P-gp).[116,119] As argued by Lipinski, the chemical space is characterised by descriptors (five to six) which are related to molecular size, lipophilicity (presented as Log P), polarity and hydrogen-bonding status.[113,120] The likelihood of a compound crossing the BBB via lipid mediation in pharmacologically significant amounts is dependent on: molecular weight (MW) less than 500 g/mol, Log P less than 5, topological polar surface area (TPSA) less than 80 $Å^2$ and number of hydrogen bond donors (HBD) and acceptors less than 5 and 10, respectively.[119,121,122]

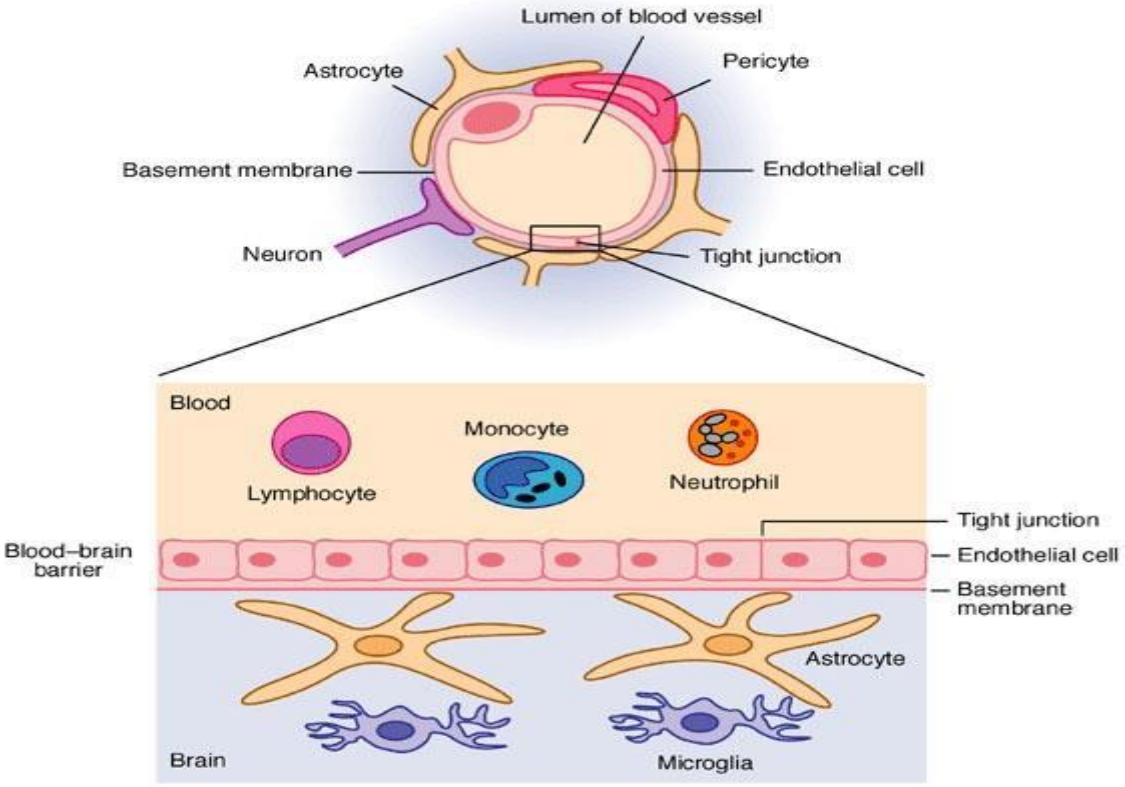

Figure 6: Structure of the blood-brain barrier.[118] [*Reproduced with permission from Springer Nature, license number: 5191481077925*].

Furthermore, these parameters explain molecular properties valuable for a drug's pharmacokinetics in the human body, including absorption, distribution, metabolism and excretion (ADME). If a drug candidate fails to meet the required parameters, then it is unlikely that the drug will cross the BBB in pharmacologically significant amounts.[121,122] It has been noted that approximately 100% of large-molecule neurotherapeutics and over 98% of small-molecule compounds fail to reach the market due to inadequate BBB permeability.[95,111]

Therefore, it is of upmost importance to determine and characterise the BBB permeability of a drug candidate as early as possible in the drug developmental pipeline.[93,95] A variety of models for assessing BBB penetration have therefore been developed and applied to advancing drug candidates with desired properties.[113,122,123] These include *in vivo*, *in vitro*, and computational (also known as *in silico*) models.[111,113] *In silico* prediction methods have gained popularity in drug discovery processes, as they are cheaper and less time-consuming than obtaining experimental data through *in vivo* and *in vitro* methods.[124] These rapid screening tools provide a straightforward interpretation based on chemical structures.[125] It further allows researchers to assess BBB permeability early in the drug discovery process thereby aiding in selection of lead compounds and thus subsequent optimisation.[126,127]

Various *in silico* models are used and SwissADME, a web tool designed for predicting pharmacokinetics parameters, is among them.[128] This method evaluates the intestinal and brain permeation of drugs in tandem based on computed lipophilicity according to the atomistic method developed by Wildman and Crippen (WLogP), and polarity of drugs with good accuracies of approximately 83-93% for intestinal absorption and 90% for brain permeation.[129] It permits a clear and informative graphical representation of data using the brain or intestinal estimated permeation (BOILED-Egg) method, which corresponds to a descriptive graphical approach discriminating between well and poorly absorbed molecules intestinally, P-gp substrate possibilities and between non- and brain-permeable molecules.[129] With these benefits, this physicochemical descriptors-based method can be applied in a variety of settings, from the filtering of chemical libraries at the early steps of drug discovery, to evaluation of drug candidates for development.[130]

Besides *in silico* and *in vivo* models, a variety of cellular *in vitro* BBB models such as Transwell models, dynamic flow-based hollow-fiber models, or microfluidic devices are available.[131] Much effort is dedicated to the development of brain endothelial cell (BEC, from different origins such as murine, porcine, bovine, or human) culture systems, which could be used for quantitative permeability studies and as a drug discovery screening aid.[113] The BEC culture models uses the Transwell insert system, where an endothelial cell monolayer is grown to confluence on collagen/fibronectin-coated, removable polycarbonate filter inserts separating lumen and abluminal chambers.[113]

The Transwell system is popular primarily because of its simplicity which allows relative HTS at moderate costs.[93] Lack of stimulating factors derived from other cellular components of the neurovascular unit (astrocytes and pericytes) and cell-to-cell communication are the major limitations of this monolayer model.[93,119,132] Thus, cell monolayer quality and TJs formation monitoring is of importance and various techniques such as transendothelial electrical resistance (TEER) measurement and permeability to hydrophilic markers are used.[113,133] Of these, TEER is the most widely used technique, due to its high sensitivity, rapidness, ease, and convenient use.[134,135] This non-invasive method has proven to be an excellent indicator of barrier integrity since the electrical impedance across an endothelium barrier is related to the formation of TJs.[136–138]

TEER measurements increase as cells proliferate and it reaches the highest value at confluence, suggesting intactness of the cell layer. A reduced TEER value is an indicator of a compromised

barrier either paracellular or transcellular.[139,140] However, an immense heterogeneity of absolute TEER values tends to be produced even though similar cell types are cultured under comparable conditions.[135] Furthermore, TEER values obtained from *in vitro* studies are in the range of 20 to 200 Ωcm^2, which are considerably lower compared to those of *in vivo* studies ($\geq$ 1000 Ωcm^2).[138]

With the aforementioned, none of these models fully replicates *in vivo* conditions as each has its advantages and disadvantages, thus there is no perfect BBB model.[119,132] However, these models do serve as strong tools in the drug discovery process and are important to distinguish drug candidates that must be eliminated or structurally modified from the promising candidates that can move forward in the development process.[111,131] The early exclusion of drugs with potential toxicity, inactivity or BBB impermeability minimises both the costs, resources and time of further development. Subsequently, this also enhances the success rate in CNS-targeting drug discovery. As such, screening of compounds for efficacy, BBB permeability and toxicity in the early stages of drug discovery and development is of utmost importance.

1.7 Aims and objectives

The aim of this study was to identify novel pharmacophores with the potential to be developed further as treatments for Alzheimer's disease.

An insight into the novel pharmacophores investigated in this study, these pharmacophores are from a commercial compound library (Charles River Laboratories/BioFocus, United Kingdom [UK]).

The objectives of the study were to:

- determine the AChEI activity of selected pharmacophores using the Ellman's colorimetric assay;
- predict the BBB permeability of the biologically active pharmacophores using SwissADME software;
- determine the combinatorial effect of the biologically active and *in silico* BBB permeable pharmacophores with donepezil using the Ellman's colorimetric assay;
- investigate the cytotoxicity of biologically active pharmacophores in SH-SY5Y neuroblastoma and bEnd.5 brain endothelial cells using the sulforhodamine B assay;
- determine the cellular AChEI activity of biologically active, *in silico* BBB permeable and non-toxic pharmacophores using SH-SY5Y based Ellman's colorimetric assay; *and*
- assess the BBB permeability of the biologically active pharmacophores using the bEnd.5 monolayer cellular *in vitro* BBB model and UPLC-MS.

Chapter 2: Materials and methods

Ethics approval was obtained from the Research Ethics Committee (780/2019) of the Faculty of Health Sciences of the University of Pretoria to carry out the study (Appendix I). A list of reagents, as well as details of their preparation, is provided as Appendix II.

2.1 Compound selection and collection

This study accessed an existing commercial 20,000 compound library (Charles River Laboratories/BioFocus, UK) housed at the Council for Scientific and Industrial Research (CSIR) on behalf of the Department of Science and Innovation (DSI) and the Technology Innovation Agency (TIA). The library is stored at -20°C in 96-well plates containing 80 compounds per plate. Three subsets of compounds were selected and collected as 10 mM aliquots dissolved in dimethyl sulfoxide (DMSO).

Previous work within our collaborative group has focused on the use of computer-aided drug discovery techniques to identify novel inhibitors of AChE (performed by Dr Carl Johan van der Westhuizen from the Department of Chemistry, University of Pretoria, in fulfilment of the requirements for his PhD).[141] High-throughput virtual screening was employed to screen the library of 20,000 compounds and predict potential inhibitors of AChE. Further development of the docking protocol was performed with the use of a machine learning approach, Random Tree Forest (RTF). The approach is largely based on SIEVE-Score which takes the interaction energies between the ligand and residues in the active pocket into account. Using this approach, the top 400 compounds were identified using the Schrödinger RTF (n = 200) and Qvina RTF (n = 200) models respectively, and these 400 compounds formed the primary library screen.

Once the hits were identified from the primary screen, a structural analysis was performed on the entire library to identify structurally similar compounds that could be subjected to secondary "structure-activity relationship"-like screening. Thus, the second and third subsets (508 and 545 compounds, respectively) were selected based on the structural similarities to the hits identified from the first subset. In total, 1,453 compounds were selected and assayed in this study (Appendix III).

2.2 Acetylcholinesterase inhibitory activity

2.2.1 Micro-plate assay miniaturisation and optimisation

Acetylcholinesterase inhibitory activity was determined using Ellman's method,[142,143] with modifications to the volumes used. This modification was required due to the limited volume that could be extracted from the compound library-stock. This assay entails the hydrolysis of acetylthiocholine iodide (ATCI) by AChE to produce thiocholine, which reacts with 5,5-dithiobis-2-nitrobenzoic acid (DTNB) to create the yellow 5-thio-2-nitrobenzoate (TNB) anion. The anion production measured is directly proportional to the AChE activity in the biological system (Figure 7).[144,145]

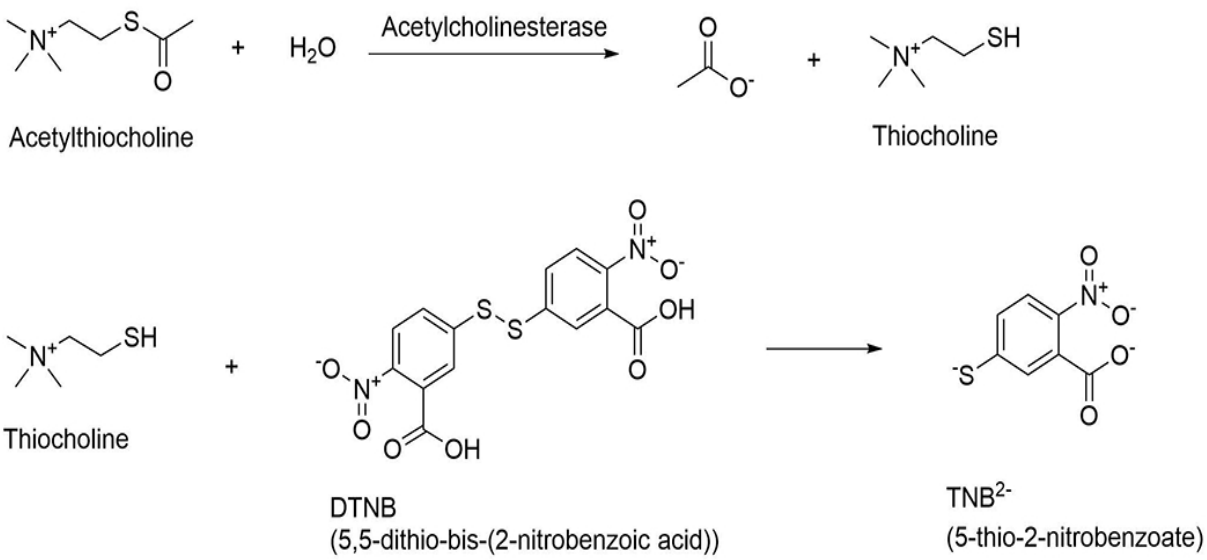

Figure 7: Chemical principle of Ellman's method.[146] DTNB: 5,5-dithiobis-2-nitrobenzoic acid, TNB: 5-thio-2-nitrobenzoate. [*Reproduced with permission from Li S et al.*[146] (*authors*), *licensed under Creative Commons Attribution 4.0 License* (*https://creativecommons.org/licenses/by/ 4.0/*)].

Additional modifications that were implemented included the reduction of the assay volume and buffers, and inclusion of a pre- and post-incubation step. The volume was reduced from 250 µL to 100 µL, however the ratio of all constituents was kept the same, as well as the in-reaction concentrations. The number of buffers was decreased from three [buffer A: 0.05 M Tris-HCl; buffer B: bovine serum albumin (0.1% (BSA) in buffer A) and buffer C: 0.1 M NaCl and 0.02 M $MgCl_2.6H_2O$] to one mix-buffer (0.045 M Tris-HCl, 0.071 M NaCl and 0.014 M $MgCl_2.6H_2O$ supplemented with 0.07% BSA, 2.14 mM ATCI and 2.14 mM DTNB), while ensuring that in-reaction concentrations were similar to the original method. Degradable reagents (BSA, ATCI and DTNB) were added on the same day of the assay to avoid risk of

contamination or spontaneous conversion. To allow the reaction to take place, 5 min pre-enzyme and 5 min post-enzyme incubation at room temperature were introduced.

To a 96-well plate was added: 10 µL of mix-buffer (blank and negative control), 0.1% DMSO (vehicle control for positive controls), galantamine or donepezil (1 pM to 10 µM; positive controls) (Merck/Sigma-Aldrich, St. Louis, USA), or DMSO (0.0001% to 0.5% given the potential enzyme inhibitory potential thereof), as well as 70 µL of mix-buffer. Blank control wells received 70 µL of buffer without DTNB. Plates were incubated for 5 min at room temperature and absorbance was measured spectrophotometrically (ELx800 UV plate reader, BioTek, USA) at 405 nm three times consecutively every 45 s (read-out 1). Thereafter, 20 µL of electric eel AChE (eeAChE) (0.1 U/mL, type VI-S, Merck/Sigma-Aldrich, St. Louis, USA) was added to each well and incubated for 5 min. After the post-enzyme incubation period, absorbance was measured five times consecutively every 45 s (read-out 2). This initial rate kinetic run provided the maximum velocity (MaxV) values for both measurements, from which AChE activity was inferred. Background activity was corrected for by subtracting MaxV values for read-out 1 from read-out 2, after which AChE activity was determined relative to the negative control:

$$\text{AChE activity (\%)} = (\text{MaxV}_s/\text{Average MaxV}_c) \times 100$$

Where, MaxV_s is background-adjusted MaxV of the sample, and Average MaxV_c is the background-adjusted average of the MaxV of the negative control. The concentration providing 50% inhibition (IC_{50}) was obtained from the dose-response curve generated with the use of a log(inhibitor) vs. response function using GraphPad Prism 6 (GraphPad Software, USA).

2.2.2 Assay validation

Assay variability, quality and signal differences were assessed by determining the coefficient of variation (CV), Z'-factor (Z') and signal window (SW), respectively[142,143] using the following equations:

$$\text{CV (\%)} = \text{SD}/\text{A} \times 100$$

$$\text{Z'} = 1 - (3[\text{SD}_s + \text{SD}_b]/[\text{A}_s - \text{A}_b])$$

$$\text{SW} = \text{A}_s - \text{A}_b - (3[\text{SD}_s + \text{SD}_b]/\text{SD}_s$$

where, A_s and SD_s represent the absorbance and standard deviation of the AChE activity signal, respectively; A_b and SD_b represent the absorbance and standard deviation of the background signal, respectively.

Acceptance limits for these parameters were defined as CV ≤ 20%, 0.4 ≤ Z' ≤ 1, and SW ≥ 2. These statistical parameters were used to monitor changes in assay performance during assay miniaturisation, optimisation and validation.

2.2.3 Single-point and dose-response screening of compounds

Acetylcholinesterase inhibitory activity of the compounds was determined using the optimised micro-plate assay protocol as described in Section 2.2.1 (page 19). A total number of 1,453 compounds were screened at 5 µM, with a ≥ 60% inhibitory activity cutoff used to define biologically active candidates. A blank, negative (mix-buffer), vehicle (0.05% DMSO) and positive controls (5 µM donepezil) were included. Any compounds that were defined as biologically active were further screened between 3 200 pM to 32 µM to determine their IC_{50} value.

2.3 Pharmacokinetics prediction

Blood-brain barrier permeability of the active compounds was predicted and assessed using the Swiss Institute for Bioinformatics pharmacokinetic prediction tool, SwissADME. Simplified molecular input line entry system (SMILES) of the compounds were collected from the compound library database. A list of SMILES was then captured using the online SwissADME web tool (http://www.swissadme.ch)[128,129] to generate a prediction of BBB penetration. These predictions were done using the BOILED-Egg method (Figure 8), which corresponds to a descriptive graphical approach which discriminates between BBB-permeable and BBB-non-permeable molecules.[128] A compound is predicted to be BBB-permeable if the TPSA is < 80 Å and the WLogP limit is ~6. The yellow and white regions in the BOILED-Egg plot represents BBB-and gastrointestinal-permeable compounds, respectively, and thus overlapping areas are considered permeable for both. Blue dots are indicative of compounds that are substrates for the P-gp transporter, while red dots suggest that the compounds are not substrates for the P-gp transporter.[128]

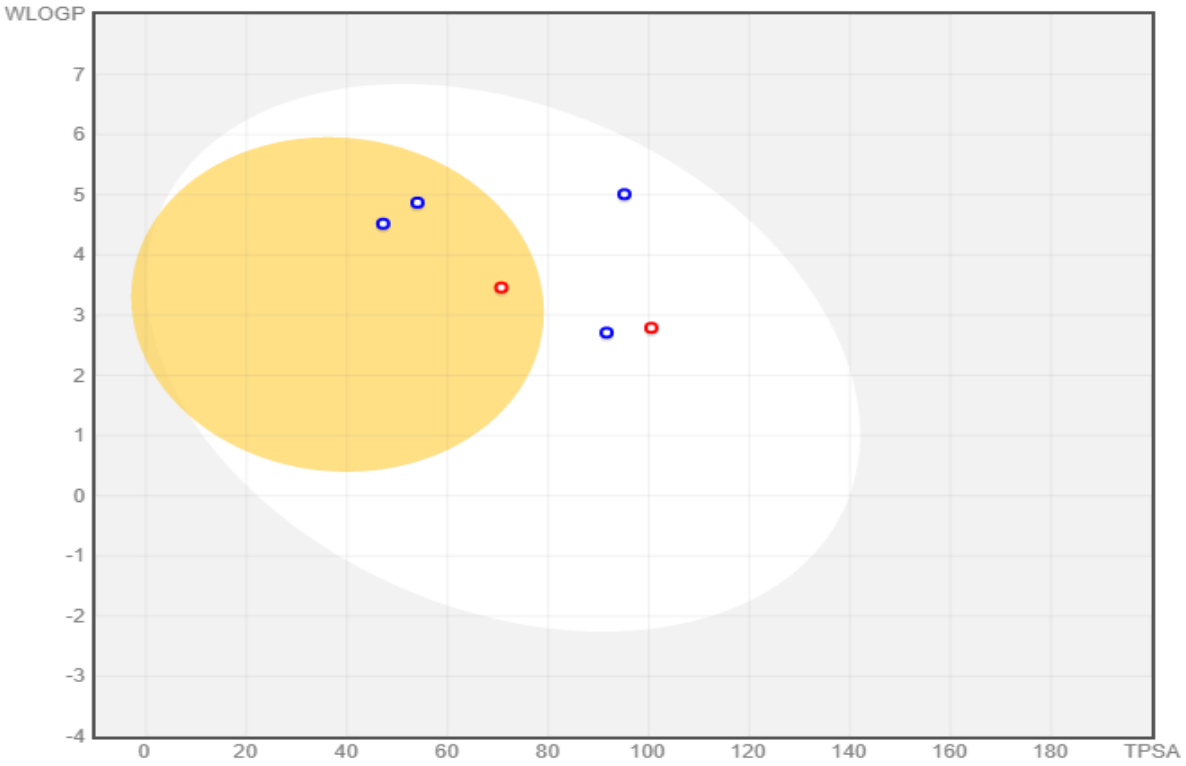

Figure 8: The SwissADME results presented as brain or intestinal estimated permeation plot.[128] [*Reproduced with permission from SwissADME web tool, licensed under Creative Commons Attribution 4.0 International License* (*https://creativecommons.org/licenses/by/ 4.0/*)].

2.4 Combinational inhibitory effects of compounds with donepezil

The activity of the biologically active compounds in combination with donepezil was assessed using the optimised and validated assay as described in Section 2.2.1 (page 19), however, the sample aliquot consisted of 5 µL of the compound and 5 µL of donepezil. The assay was conducted using a checkerboard layout with nine different combinations per compound (Figure 9). The fraction affected (*fa*) of each combination in relation to their individual compounds was analysed using CompuSyn (PD Science LLC)[147] to generate CI values, where a CI < 1 indicates synergism, equal to 1 indicates additivity, and > 1 indicates antagonism.

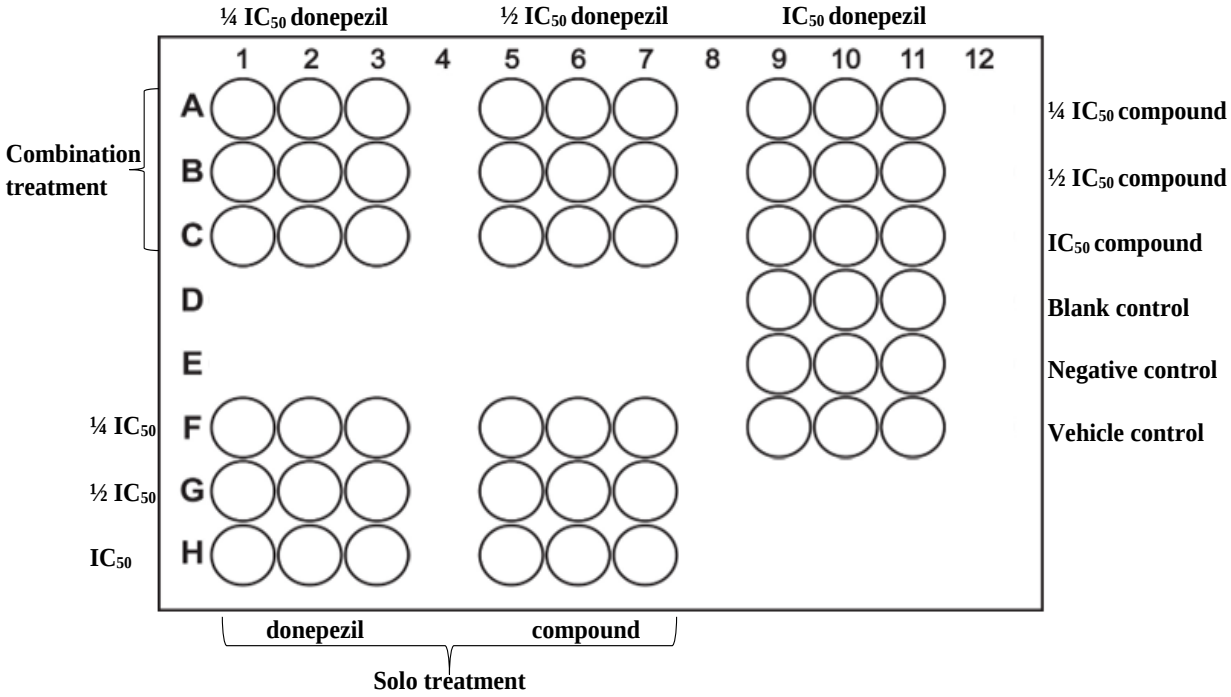

Figure 9: Plate layout used to determine the combinatorial effect of donepezil and the active compound. IC_{50}: concentration resulting in 50% inhibitory effect.

2.5 Cytotoxicity screening of biologically active compounds

2.5.1 Cell culture and maintenance

The human neuroblastoma (SH-SY5Y) cell line (CRL-2266) was originally purchased from the American Tissue Culture Collection (ATCC) by the Department of Pharmacology at the North-West University and was gifted to the Department of Pharmacology at the University of Pretoria. The immortalised mouse brain endothelial (bEnd.5) cell line was purchased from the European Collection of Authenticated Cell Cultures (Cat no. 96091930) by the Department of Medical Biosciences at the University of Western Cape. Cells were cultured in 75 cm^2 cell culture flasks (Greiner Bio-One, USA) using a 1:1 mixture of Dulbecco's Modified Eagle's Medium (DMEM, Gibco, Invitrogen, USA) and Ham's F-12 nutrient mixture (Gibco, Invitrogen, USA) supplemented with 1% penicillin/streptomycin (Pen-strep) (Gibco, Invitrogen, USA) and 10% heat-inactivated foetal calf serum (FCS) (Gibco, Invitrogen, USA) for SH-SY5Y cells and further supplemented with 1% nonessential amino acids (BioWhitakker/Lonza, Thermo-Fischer, USA) and 1% sodium pyruvate (Gibco, Invitrogen, USA) for bEnd.5 cells. Cells were grown to a confluence of 70% to 80% at 37°C in a humidified incubator (HF212 UV Heal Force, China) with a 5% CO_2 atmosphere, washed with sterile phosphate-buffered saline (PBS) (Gibco, Invitrogen, USA) and chemically detached using

TrypLE™ Express (Gibco, Thermo-Fischer, USA). Detached cells were transferred to a 15 mL centrifuge tube (Thermo-Fischer, USA) alongside 10% FCS-supplemented growth medium to make up the volume. Cells were centrifuged (Allegra X-22 centrifuge, Beckman Coulter, USA) at 200 *g* (SH-SY5Y) and 700 *g* (bEnd.5) for 5 min. The supernatant was discarded, and the pellet was re-suspended in 1 mL of 10% FCS-supplemented medium. Cells were counted using the trypan blue (Merck/Sigma-Aldrich, St. Louis, USA) exclusion assay (0.4% *w/v*) and diluted to 5 x 10^4 or 400 x 10^4 cells/mL (SH-SY-5Y) and to 1.5 x 10^4 or 50 x 10^4 cells/mL (bEnd.5) in 10% FCS-supplemented growth medium.

2.5.2 Cell seeding and exposure

A volume of 100 µL of the cell suspension was seeded into sterile round-bottomed 96-well plates (Merck/Sigma-Aldrich, USA) at a seeding density of 5 000 and 1 500 cells/well for SH-SYSY and bEnd.5 cells, respectively. Seeded plates were incubated overnight at 37°C and an atmosphere of 5% CO_2 to allow for cell attachment. Attached cells were exposed to 100 µL medium (negative control), 1% DMSO (vehicle control), 1% saponin (positive control), donepezil (1 000 pM to 100 µM) (Merck/Sigma-Aldrich, USA) or the test compounds (1 000 pM to 100 µM) prepared in serum-free medium. The plates were incubated at 37ºC in a humidified incubator with 5% CO_2 for 72 h.

2.5.3 Sulforhodamine B colorimetric assay

The cytotoxicity of the biologically active *in silico* BBB-permeable compounds was assessed by cell density determination using the sulforhodamine B (SRB) staining assay as described by Vichai and Kirtikara[148] with minor changes to volumes used.

After the exposure period, 50 µL of a 50% trichloroacetic acid (TCA) (Merck/Sigma-Aldrich, USA) solution was added to each well and the plates were incubated at 4ºC for 24 h. After fixation, plates were washed three times with slow-running tap water and dried in an oven (EcoTherm, Labotec, South Africa) at 40°C to 45°C. A volume of 100 µL of 0.057% SRB solution (Merck/Sigma-Aldrich, USA) was added to each well and the plates were incubated at room temperature for 30 min in the dark. After 30 min, unbound dye was removed by washing the plates three times with 150 µL of 1% acetic acid (Merck/Sigma-Aldrich, USA) and dried in the oven.

The bound dye was extracted from fixed cells by adding 200 µL of 10 mM Tris-base (Merck/Sigma-Aldrich, USA) solution (pH 10.5) to each well. Plates were shaken on a gyratory

shaker (VRN-200, Gemmy Industrial Corporation, Taiwan) for 1 h to solubilise the protein-bound dye. After the dye had solubilised, the optical density (OD) was measured at 540 nm (reference: 630 nm) using an ELX800 microplate reader (BioTek instruments Inc, Highland Park, USA). All values were blank-subtracted, and the cell density (%) calculated using the formula below:

$$\text{Cell density (\% relative to negative control)} = OD_{sample}/\text{Average } OD_{negative} \times 100$$

Where 'OD_{sample}' refers to the corrected optical density of the sample and '$OD_{negative}$' is the corrected optical density of the negative control.

2.6 Michaelis-Menten kinetics assay

The non-cytotoxic, active (≥ 60% AChEI), *in silico* BBB-permeable compounds were subjected to an in-house miniaturised AChE inhibitory assay to determine Michaelis-Menten kinetics. The AChE inhibitory assay was performed as described in Section 2.2.1 (page 19); however, compounds were tested at the IC_{50} against a substrate concentration range (ATCI; 0 to 2.14 mM). The negative control consisted of mix-buffer to determine the upper plateau of enzyme saturation. Two additional controls were included to monitor inter-reagent interactions: DTNB without ATCI, and ATCI without DTNB. The substrate concentration at half the maximum reaction rate (K_m) versus the reaction rate (measured maximum velocity of reaction at each concentration being equivalent to initial velocity, where acceleration/gradient is steepest, to obtain the maximum velocity [V_{max}] at the concentration with the highest initial velocity) was plotted using GraphPad Prism 6 (GraphPad Software, USA). Results were further processed as Lineweaver-Burk plots.

2.7 Chemical stability analysis

The non-cytotoxic, active (> 60% AChEI), *in silico* BBB-permeable compounds were subjected to quality control analysis using ultra-performance liquid chromatography (UPLC) coupled to exact mass spectrometry (MS), to ensure the chemical integrity. Quality control analysis was conducted at the CSIR by Prof Paul Steenkamp. A Waters UPLC coupled in series to a Waters SYNAPT G1 HDMS mass spectrometer was used to generate accurate mass data. Optimisation of the chromatographic separation was done using a Waters HSS T3 C18 column (150 mm x 2.1 mm, 1.8 µm) and the column temperature controlled at 60°C. A binary solvent mixture consisting of water (eluent A) containing 10 mM formic acid (natural pH of 2.4) and acetonitrile (eluent B) containing 10 mM formic acid was employed. The initial conditions were 95% A at

a flow rate of 0.4 mL/min which was maintained for 30 s, followed by a linear gradient to 5% A at 6 min. The conditions were kept constant for 1 min and then reverted to the initial conditions. The runtime was 10 min, and the injection volume was 1 µL. Samples were kept at 6°C in the Waters Sample Manager during the analysis.

The SYNAPT G1 mass spectrometer was used in V-optics and electrospray mode to enable detection of all electrospray ionisation (ESI)-compatible compounds. Leucine enkephalin (50 pg/mL) was used as reference calibrant (Lock Mass) to obtain typical mass accuracies between 1 and 5 mDa. The mass spectrometer was operated in both ESI-positive and -negative modes with a capillary voltage of 2.0 kV, the sampling cone was set at 30 V and the extraction cone at 4.0 V. The scan time was 0.1 s covering the 50 to 1 000 Da mass range, with an interscan time of 0.02 s. The source temperature was 120°C and the desolvation temperature was set at 450°C. Nitrogen gas was used as the nebulisation gas at a flow rate of 550 L/h and cone gas was added at 50 L/h. The software used to control the hyphenated system and to do all data manipulation was MassLynx 4.1 (SCN 872).

A Waters UPLC-compatible photodiode array detector was operated in front of the mass spectrometer without any splitting of the column eluent. The detector was operated in full scan mode covering the 200 – 500 nm wavelength range with a wavelength accuracy of 1.2 nm.

Each compound was analysed in both positive and negative ionisation modes and full scan UV data collected simultaneously. The data was firstly evaluated to determine whether the compound preferably ionised in ESI-positive or ESI-negative mode. The best ionisation mode was selected, and the presence of the target compound confirmed. Thereafter the UV data was evaluated to determine whether the compound contained chromophores and displayed a usable UV spectrum. Compounds with UV-active, a MaxPlot chromatogram were evaluated, and all relevant compounds integrated to determine the purity of the target compound.

2.8 *In situ* acetylcholinesterase inhibitory activity of compounds

The assay was carried out according to the method of Ellman *et al.* [142,143] as described in Section 2.2.1 (page 19) with minor modifications. SH-SY5Y human neuroblastoma cells were cultured and seeded as described in Section 2.5.1 (page 23), however, cells were seeded at 400 000 cells/well in a 24 well plate. After the cells had attached, culture medium was aspirated and replenished with 300 µL of the specific compound in buffer at 1/5 IC_{50}, IC_{50} and 1.5×IC_{50} and incubated for 5 min at room temperature. Post-exposure, 100 µL mix-buffer (pH 8) containing

aqueous 0.045 M Tris-HCl, 0.050 M NaCl and 0.010 M $MgCl_2.6H_2O$ supplemented with 0.05% BSA, 1.5 mM ATCI and 3 mM DTNB (Sigma-Aldrich, St. Louis, USA) was added. Plates were incubated for 5 min and read spectrophotometrically at 405 nm over a 1 h period at 3 min intervals. The AChE activity was determined relative to the negative control (Section 2.2.1; page 19).

2.9 Blood-brain barrier permeability assessment

2.9.1 The *in vitro* bicameral system

The bicameral chamber system was used for the *in vitro* model of BBB, where the basolateral (the well) assumes the abluminal side of the capillary endothelium, while the apical chamber (the insert) assumes the luminal side of the capillary (Figure 10). The measurement was performed as described by Srinivasan *et al*.[136] The *in vitro* BBB model was used to determine bEnd.5 peak values and the effect of three biologically active *in silico* BBB permeable, non-cytotoxic compounds on bEnd.5 monolayer TEER.

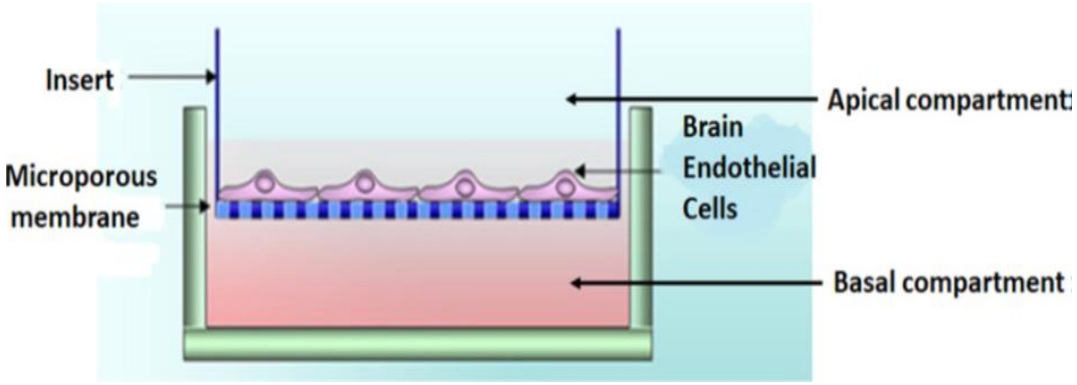

Figure 10: A bicameral system.[149] [*Reproduced with permission from Mentor and Fisher 2022 (authors), licensed under Creative Commons Attribution License (http://creativecommons.org/licenses /by/4.0)*].

Briefly, the bEnd.5 cells were cultured and maintained as described in Section 2.5.2 (page 24). A volume of 300 µL bEnd.5 cell suspension was seeded at a density of 50 000 cells into the apical chamber of a Transwell® insert (pore size of 0.45 µm, filtration diameter of 12 mm, and an effective surface area of 0.6 cm^2) (Merck-Millipore, UK) placed in sterile 24-well plates (Bio-Smart Scientific, SA). Monolayer seeded plates with 500 µL growth medium (Bio-Smart Scientific, SA) in the basolateral side (well), were incubated at 37ºC and 5% CO_2 for 24 h to attain cell confluence.

To establish TEER peak values, after 24 h seeding incubation, TEER was measured using the EVOM TEER measurement system (Millipore, Germany) daily for six days, and the medium was changed daily after measurement. The measurement was performed by connecting the electrodes to either side of the cell monolayer and measuring the resistance. The resistance of the blank (inserts without cells) was subtracted from the resistance value of the cell monolayer (inserts with cells), and the resultant value was multiplied by the surface area of the inserts to standardise the TEER value.

The effect of the compounds on monolayers of bEnd.5 endothelial integrity was tested by determining the TEER. Post-seeding and incubating, the bEnd.5 cells in the inserts were treated at peak TEER (day 3) with compounds at their IC_{50} and $1.5\times IC_{50}$ concentrations. Plates were incubated at 37ºC, and 5% CO_2 and TEER was carried out and monitored for 12 h, 24 h, and 48 h periods. After 24 h exposure, the apical and basolateral medium was collected for UPLC-MS analysis (as described in Section 2.7; page 25) to determine whether the compounds penetrated through the bEnd.5 monolayer. No sample preparation or validation was done, medium was tested as it was collected. However, since compounds were present in a low concentration in the medium, the preferred MS data channel was selected. In this case a base peak intensity chromatogram was generated, and all relevant compounds integrated to determine the presence of the target compound.

2.10 Statistical analysis

Experiments were conducted with technical and biological triplicates to obtain at least six to nine data points per test. All data processing was conducted using Microsoft Office Excel 2019 (Microsoft, USA) and GraphPad Prism 6 (GraphPad, Software, USA). Data points estimated to be outliers were excluded using Grubb's testing. The IC_{50} was calculated by nonlinear regression analysis of the response-concentration (log) curve. Results were reported as mean ± standard error of mean (SEM). The student's t-test was used to determine significance ($p < 0.05$) relative to the comparator.

Chapter 3: Results and discussion

3.1 Acetylcholinesterase inhibitory activity

3.1.1 Assay miniaturisation and optimisation

Acetylcholine deficiency due to AChE catalysis is one of the major pathophysiological features of AD. Inhibition of the catalytic activity prevents metabolism, thus increasing ACh availability for synaptic transmission.[150,151] Hence, AChE has received much attention as the prime target for drug discovery and rapid assay development, to identify novel AChEIs to treat not only AD, but also other cognitive-related disorders associated with ACh deficiency.[152,153]

Several conventional methods, such as spectrophotometric and fluorometric assays, have been developed for AChEIs screening.[154–159] Of the assays, Ellman's method is considered the gold standard for AChE inhibitory activity quantification. The latter method has been employed with the introduction of various modifications leading to the improvement of its throughput.[160–162] To date, the Ellman's colorimetric method modified by Eldeen *et al.*[143] for microplates is the most widely used method. Eldeen and his colleagues introduced the use of three buffers (Buffer A: 50 mM Tris-HCl, pH 8; Buffer B: 50 mM Tris-HCl, pH 8, containing 0.1% bovine serum albumin (BSA); Buffer C: 50 mM Tris-HCl, pH 8, containing 0.1 M NaCl and 0.02 M $MgCl_2 \cdot 6H_2O$) with a total assay volume of 250 µL.[143]

In the present study, the AChE microplate assay was modified further, optimised and validated while maintaining its robustness by using the same kinetic protocol as Ellman with Eldeen's modification, though creating a single assay buffer with a smaller volume (45 mM Tris-HCl). Single-buffer assay methods have been developed and found to have reproducible results. Similar to this study, single buffers were employed by Järvinen *et al.*[162] (50 mM Tris-HCl buffer; pH 8.0, containing 0.1 M NaCl and 0.02 M $MgCl_2.6H_2O$) and Ingkaninan *et al.*[163] (50 mM Tris-HCl; pH 8.0).

In addition to the single buffer, the assay was adapted to make use of smaller volumes. Miniaturisation of AChE assays, using microtiter plates is not new, but has been in existence since the 1980s.[164] Assay miniaturisation allows not only for the reduction in sample volume and concentration (to nanoscale), but also reduction in reagent volumes.[165] In this study, the total assay volume was reduced from 250 µL to 100 µL. Assay volume reduction (to 200 µL) has been employed by French-Constant *et al.*[166] Although the volume reduction wasn't as low as in the present study, reproducible results were obtained. Reduction of total assay volume to

55 µL and 50 µL were reported by Järvinen and colleagues in 2010 and 2011, respectively.[167,168] These and the current study have indicated that assay volume reduction and combination is feasible, resulting in reproducible results.

Donepezil and galantamine, known AChE inhibitors, were used in the development, optimisation and validation of the miniaturised AChE assay as positive controls. Both compounds inhibited AChE dose-dependently, with donepezil displaying greater potency (IC_{50} of 0.06 ± 0.07 µM) compared to galantamine (IC_{50} of 1.99 ± 0.10 µM) (Figure 11).

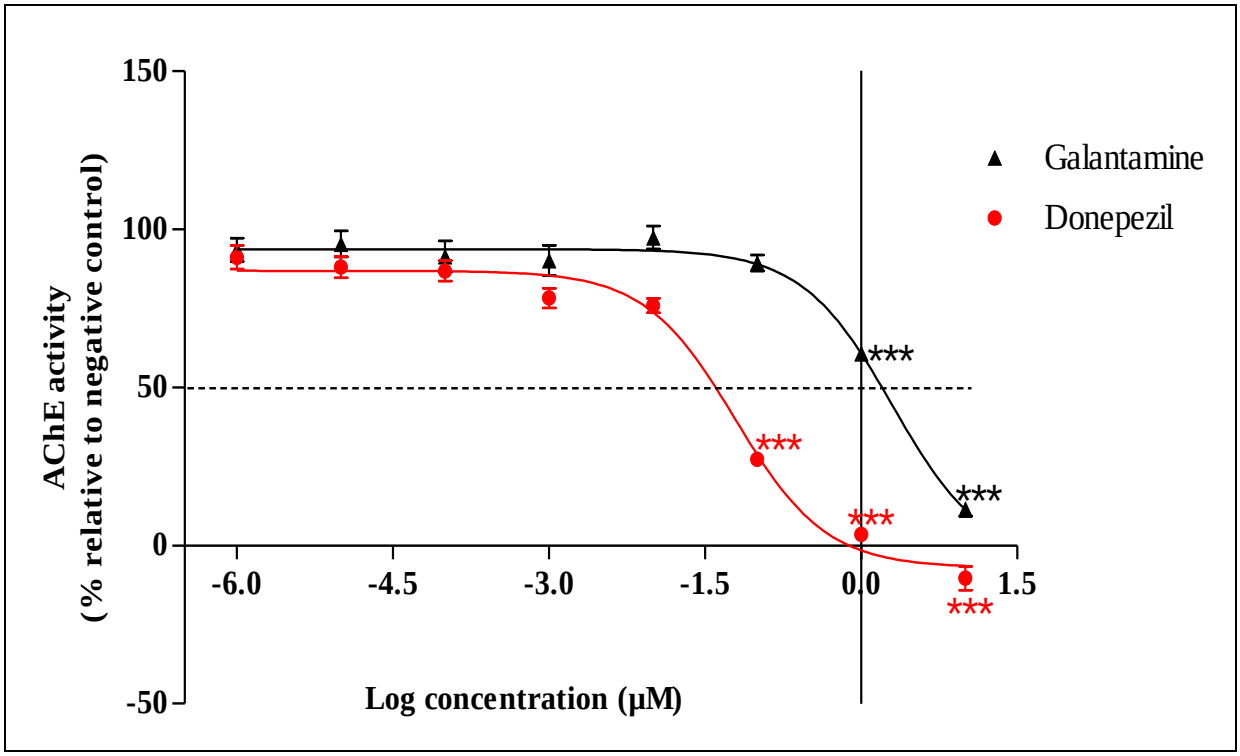

Figure 11: Dose-dependent inhibition of acetylcholinesterase by donepezil and galantamine. The dotted line indicates 50% acetylcholinesterase activity. Significance of changes relative to negative control are indicated as *** $p < 0.001$.

These results in the current study were similar to those reported by other authors, where similar IC_{50s} of donepezil and galantamine were noted.[143,169–171] Despite assay changes such as, using one buffer instead of three, reduced assay volume or substrate concentrations, there was no change in the potency of the FDA approved drugs when compared to those reported by other authors who used the original method.[170,171] The results indicated that the AChE assay was successfully miniaturised and optimised in the current study.

Dimethyl sulfoxide is an organic solvent used commonly for preparing stock solutions in the drug discovery process.[172] Despite its wide use, DMSO is known to interact with several

enzyme classes, including cholinesterase, causing either enhancement or inhibition of activity.[172,173] There is no particular concentration range defined for the use of DMSO in assays; usually concentrations in the range of 0.1 to 1% (v/v) are recommended.[174,175] As part of assay optimisation and validation, the inhibitory activity of 0.0001% to 0.5% DMSO was assessed to determine confoundment and the optimal dilutions that could be used. At a concentration ≥ 0.1%, DMSO significantly ($p < 0.05$) inhibited AChE by ≥ 21% (Figure 12).

Given the results, a final concentration of 0.05% DMSO was deemed appropriate to use in AChE assays. These results are in accordance with those of Kumar and Darreh-Shori[173] who found that DMSO at a concentration of 3.3% (v/v) induced 50% inhibition of the human AChE enzyme activity.[173] Novales and Schwans,[176] assessed the effect of various solvents at final concentrations of 1 and 2% on eeAChE. In agreement with the current findings on eeAChE enzyme, 1% DMSO decreased AChE activity by 75%. This clearly indicates the importance of determining solvent-compatibility of assay reagents at an early stage of assay development.[177]

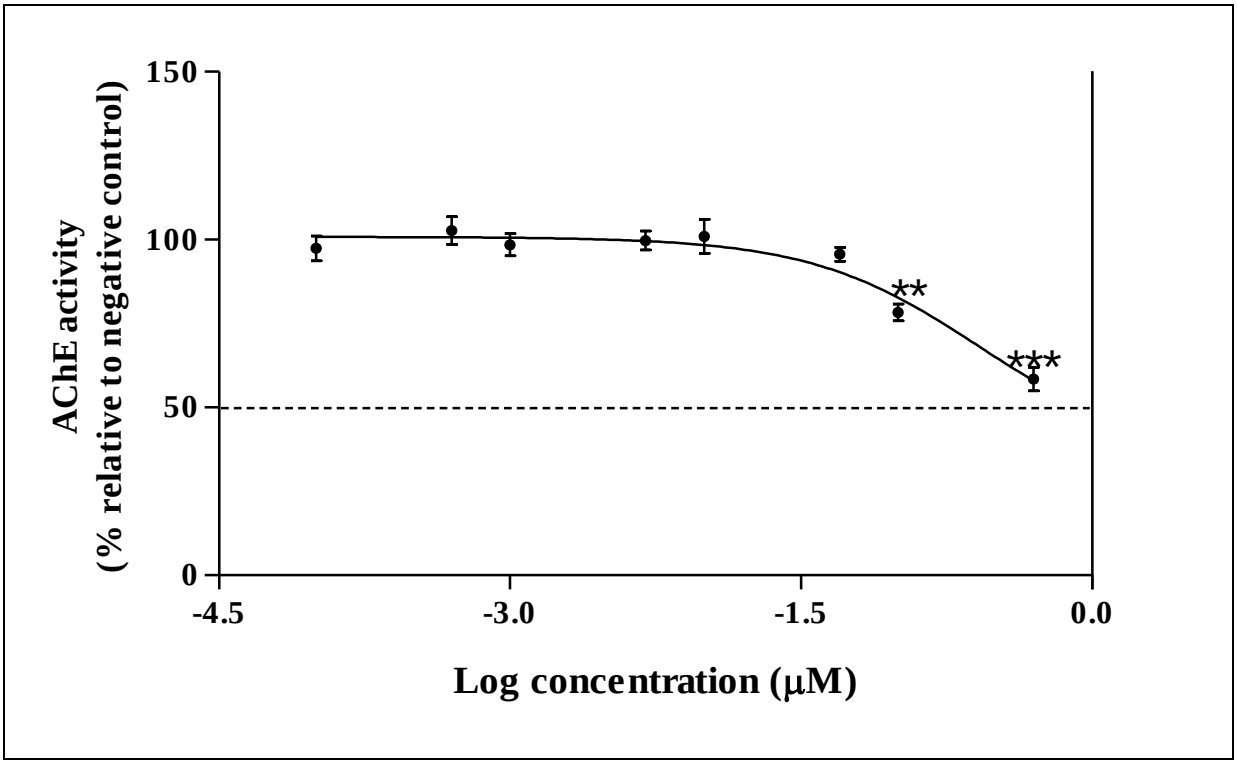

Figure 12: Dose-dependent inhibition of acetylcholinesterase by dimethyl sulfoxide. The dotted line indicates 50% acetylcholinesterase activity. Significance of changes relative to negative control are indicated as ** $p < 0.01$, *** $p < 0.001$.

3.1.2 Assay validation

To ensure that assays are consistent and suitable for the intended use, they must be validated.[178] This is usually carried out using a consistent three day plate experiment of control compounds during which computation of critical statistical parameters [coefficient of variation (CV), Z' factor (Z') and signal window (SW)] are determined daily for all experiments.[179]According to Zhang *et al.*[180] the Z' is the main statistical parameter as it assesses the quality of the assay. The CV provides information on assay variability (intra-assay and inter-assay variabilities) and can uncover pipetting errors especially at low volume densities.[181] Difference between the maximum and minimum signal is measured by the SW parameter.[181,182]

For assay validation, acceptance criterion for CVs of each signal must be ≤ 20% per plate, while the SW must be ≥ 2 and Z' must be between zero and one (with one indicating optimal assay performance).[177,183] The aforementioned assay validation values were calculated to assess how the miniaturised AChE assay performed over three consecutive days. All parameters were found to be within acceptable ranges (Table 2). This therefore allowed for the screening of a large number of compounds i.e. high throughput.

Table 2: Statistical parameters (intra- and inter-assay) for the miniaturised acetylcholinesterase assay.

Acceptable range	Coefficient of variation (%)	Z' factor	Signal window
	≤ 20	**≥ 0.4 ≤ 1**	**≥ 2**
Day 1	10.59	0.58	73.94
Day 2	5.68	0.73	68.93
Day 3	8.93	0.56	75.62

3.1.3 Acetylcholinesterase inhibitory activity screening of the compounds

In the search for potential AChEIs, an initial single-point concentration (5 µM) screen was carried out on 1,453 selected synthetic compounds from a Charles River Laboratory/Biofocus compound library (listed in Appendix III). Donepezil served as the standard due to its potent inhibition of AChE (IC_{50} value of 0.03 µM), adequate safety, and tolerability. Moreover, it has a long half-life, which allows the use of lower doses, hence it is one of the most prescribed treatments for AD to date.[184,185]

Compounds were grouped into three subsets (**A**, **B** and **C**). Compounds for each subset were numbered with the subset letter as the prefix, followed by the compound number in the subset (e.g., **A1** for compound 1 in subset **A**). Acetylcholinesterase inhibitory activity results for all compounds in the three subsets are provided in Appendix III. Compounds with ≥ 60% AChEI

activity were considered biologically active. Such compounds were only present in subset **A** and **C** (Figures 13A and 13B; Tables 3 and 4).

Of the 400 compounds from subset **A**, only six compounds (**A8**, **A51**, **A73**, **A136**, **A175** and **A176**) were considered biologically active (Table 3). All active compounds, apart from compound **A8**, contained a donepezil-like scaffold, benzo-fused heterocycle, albeit with different atom substituents within itself as depicted below (Table 3). To note that changes to the rings and positions of the heteroatoms result in scaffold name changes.

Table 3: Compounds in subset **A** that inhibited acetylcholinesterase activity by ≥ 60%.

Main scaffold: benzo-fused heterocycle core		
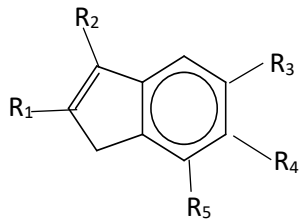		
Compound	**Chemical structures**	**AChE inhibition (%) ± SEM**
A8	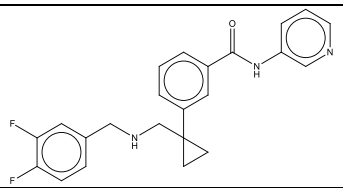	59.87 ± 3.04
A51	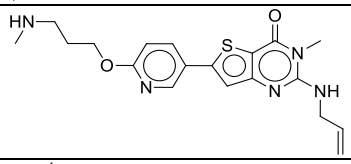	66.53 ± 4.67
A73	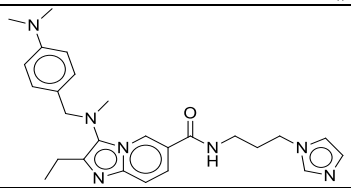	77.98 ± 4.13
A136	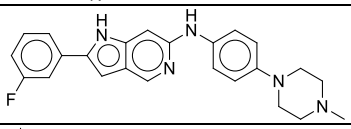	62.33 ± 3.75
A175	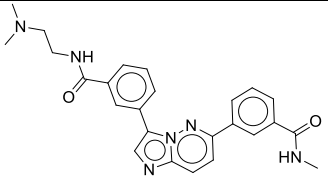	65.28 ± 8.20
A176	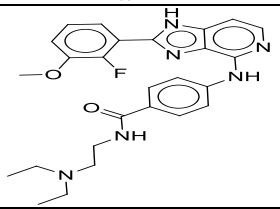	77.08 ± 6.09

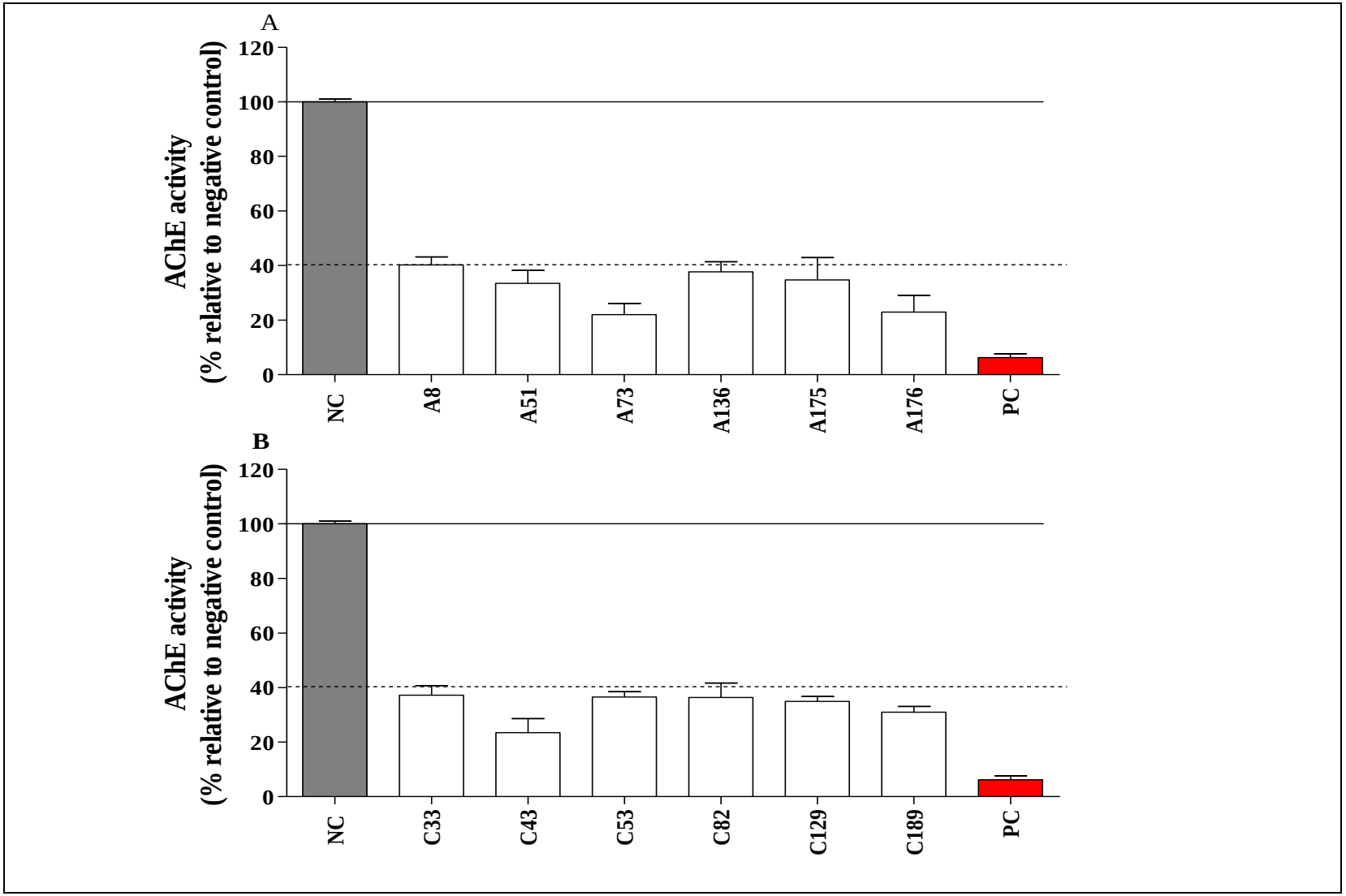

Figure 13: The acetylcholinesterase inhibitory activity of active compounds from subsets **A** and **C**. The solid line indicates 100% acetylcholinesterase activity, whereas the dotted line indicates 40% acetylcholinesterase activity (selected bioactive threshold). NC: negative control; PC: positive control (donepezil, 5 µM); vehicle control (DMSO, 0.05%).

Heterocyclic (particularly benzo-fused heterocyclic) scaffolds are essential structural backbones for novel and selective drugs used to treat various illnesses.[186–188] Due to their stability and ubiquitous occurrence in natural as well as synthetic compounds, five or six-membered heterocycles with one, two, or three heteroatoms in their nucleus have attained special interest.[189] Hence many biological compounds, such as vitamins, hemoglobin, hormones, deoxyribonucleic acid, and ribonucleic acid, contain these heterocyclic rings as a key structural constituent.[189]

Although fused ring scaffolds are widely implemented in the treatment of various diseases, their incorporation in drugs for the treatment of neurodegenerative diseases such as AD, is still lower. This is possibly due to their limited physicochemical properties.[188] Despite this, a number of heterocyclic molecules incorporating various heterocyclic rings, such as imidazole, pyrazole, thiazole, thiophene, pyridine, pyrimidine and triazine have been evaluated against AChE activity in search of new anti-Alzheimer's agents.[189,190] Among them, triazolothiadiazoles, triazolothiadiazines, tacrine-benzothiazole and heptylene-linked bis-tacrineor bis(7)-tacrine are some potent heterocyclic molecules reported and further described in reviews by Hiremathad and Piemontese[187] and Saini and Saxena.[190]

Among the active compounds identified in the present study, one compound (**A8)** did not contain the benzo-fused heterocycle scaffold and was regarded as structurally unique (Figure 14). Further studies are required to determine which part of this unique structure is responsible for the observed AChEI activity.

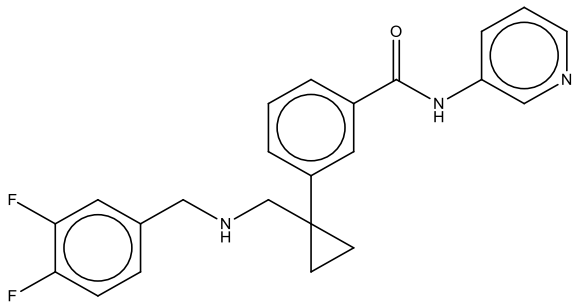

Figure 14: Unique structure of compound **A8**.

Structural analysis was performed on the entire compound library to identify compounds that were structurally similar to actives of subset **A**. Additionally, *in silico* BBB permeability predictions were performed to refine the selection of these subsets. Subsets **B** and **C** were selected based on their structural similarities and BBB permeability predictions to actives **A8**

and **A73**, respectively. Surprisingly, all compounds belonging to subset **B** (n = 508) were found to be inactive and thus this subset was excluded from further assessment.

Six compounds (**C33**, **C43**, **C53**, **C82**, **C129** and **C189**) from subset **C** (n = 545) were determined to be active. Active compounds identified from subset **C** possessed the imidazo[1,2-*a*]pyridine scaffold (similar to the parent compound **A73**, Table 4), i.e. these are a subset of the aforementioned benzo-fused heterocycles.

Table 4: Compounds in subset **C** that inhibited acetylcholinesterase activity by ≥ 60%.

Scaffold: imidazo[1,2-*a*]pyridine		
	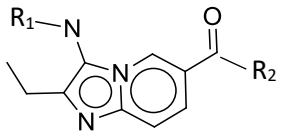	
Compound	**Chemical structures**	**AChE inhibition (%) ± SEM**
C33	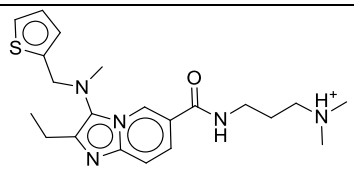	62.77 ± 3.50
C43	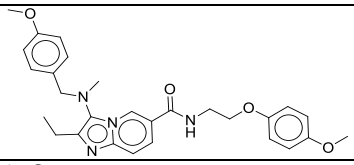	72.16 ± 3.14
C53	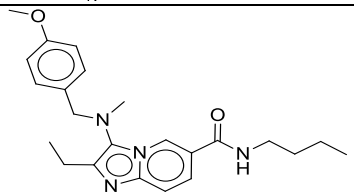	63.41 ± 1.89
C82	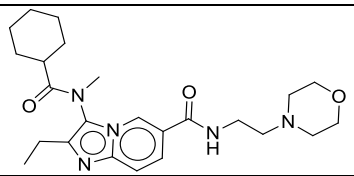	68.66± 1.87
C129	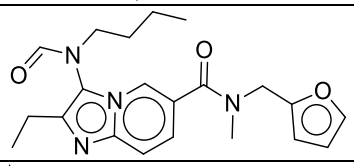	65.03 ± 1.75
C189	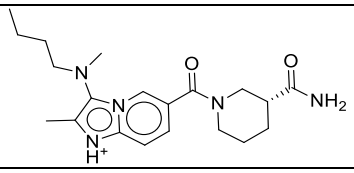	69.00 ± 2.04

AChE: acetylcholinesterase; SEM: standard error of the mean

The imidazo[1,2-*a*]pyridine scaffold noted in the active compounds in subset **C**, are considered as one of the most potent bicyclic 5-6 heterocyclic rings, and recognised as a "drug prejudice" scaffold.[191] The reason being that this scaffold is found in lead molecule discovery of novel synthetic drugs with a variety of targets, including AChE.[192,193] To attest to this, the imidazo[1,2-*a*]pyridine scaffold has been evaluated for AChEI since the 1990s.[194] A series of imidazo[1,2-*a*]pyridines derivatives (2-arylimidazo[1,2,-*a*]pyridinium salts) compounds were found to inhibit AChE with IC_{50} values ranging from 0.20 to 50.0 μM.[194]

In a study conducted by Mohsen *et al.*[195], *N*-(benzylidene)imidazo[1,2-*a*]pyridine derivatives were shown to have potential AChE inhibition. Furthermore, Gurjar and colleaques[196] also reported cholinesterase inhibition activity of designed imidazole analogues. Activity of these analogues was determined and confirmed through computational studies, pharmacological evaluation using animal model and mechanistic *in vitro* cholinesterase inhibition.[196] Even though the structures of these compounds are not exactly the same as those reported in the current study, it should be noted that the main scaffold played a role in the AChEI activity observed.

Active compounds from both subsets **A** and **C**, were further compared and clustered. Only two compounds from subset **A** (**A73** and **A175**) were found to be within the same cluster as the rest of subset **C** compounds (Figure 15). It was expected that compound **A73** would be in the same cluster as compounds from subset **C** since it is the parent compound with exactly the same main scaffold albeit different substitution sites. With the majority of subset **A** compounds not found within the same cluster as subset **C**, this suggests substituents' variability and structural diversity of these hits.

The 12 active compounds were further analysed to determine their dose-response activity and IC_{50} values. Compounds displayed reproducible dose-response curves with correlation coefficient values ranging from 0.78 to 0.93, which is indicative of good trend fits (Table 5). Of the six active compounds in subset **A**, **A51** was the most promising compound (Table 5). For subset **C**, **C129** was found to be the least active (Table 5). None of the compounds achieved a potency comparable to that of donepezil, with IC_{50} inhibitory activities being 6.7 to 556.0-fold lower than any of the actives.

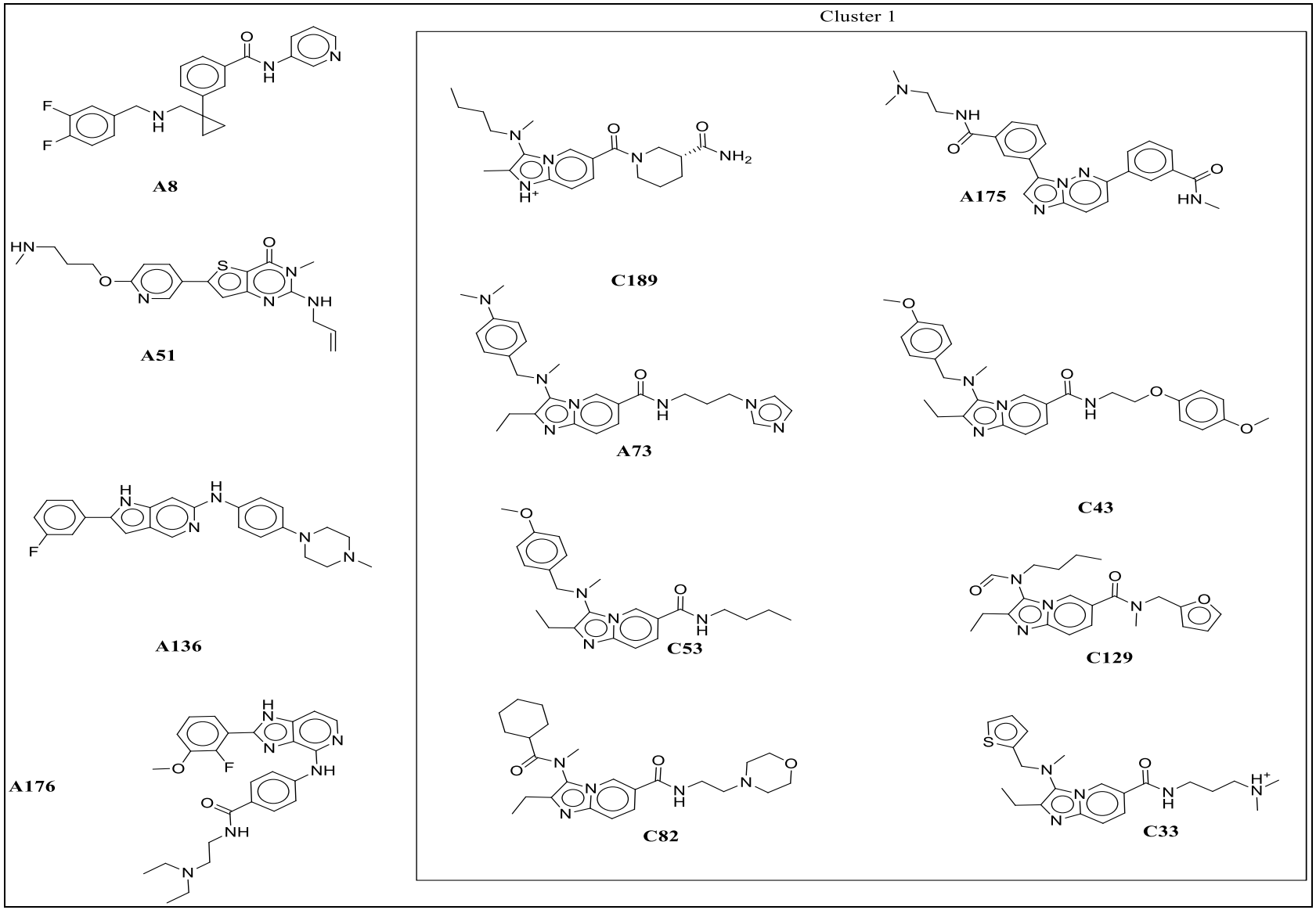

Figure 15: Chemical structures of the active compounds.

Table 5: Half maximal inhibitory concentration values and coefficient correlation of active compounds.

Compounds	IC_{50} values ± SEM (µM)	R^2
A8	5.86 ± 0.01	0.88
A51	0.20 ± 0.06	0.86
A73	3.56 ± 0.09	0.89
A136	16.68 ± 0.04	0.87
A175	15.37 ± 0.23	0.78
A176	2.78 ± 0.08	0.93
C33	3.71 ± 014	0.80
C43	3.37 ± 0.11	0.87
C53	3.36 ± 0.12	0.85
C82	7.34 ± 0.14	0.88
C129	12.52 ± 0.12	0.92
C189	4.49 ± 0.08	0.86

IC_{50}: concentration resulting in 50% inhibitory effect; SEM: standard error of the mean; R^2: correlation coefficient.

Compound **A51**, containing the thieno[3,2-*d*]pyrimidinone scaffold was the most potent compound at IC_{50} concentration. Thienopyrimidine is one of the opulent fused heterocycles and emerges as an attractive scaffold in drug discovery.[197,198] Several thienopyrimidine derivatives, thieno[2,3-*d*]pyrimidine and thieno[3,2-*d*]pyrimidine in particular, have proven to elicit a broad spectrum of pharmacological effects such as kinase inhibition, antibacterial, anticancer, and CNS protection activity.[199,200] However, not much is reported in literature about the implementation of the thieno[3,2-*d*]pyrimidinone scaffold in AD treatment.

Few studies have reported on other thienopyrimidine derivatives, one such study was conducted by Eissa *et al*.[201] where 12 S-substituted tetrahydrobenzothienopyrimidines were designed and one compound showed to have the greatest AChE inhibitory activity. Additionally, Tanarro and Gütschow[202] reported that tetracyclic thienopyrimidine showed a mixed-type inhibition of human AChE with an IC_{50} value of 5.69 µM. In another study in search of AChEIs, Chiriapkin and colleagues[203] screened a series of compounds with 2-substituted 5,6,7,8-tetrahydrobenzo[4,5]thieno[2,3-*d*]pyrimidine-4(3*H*)-one. Heterocycle pyrimidine-4(3H)-one with thienopyrimidines in the second position were found to be the most potent AChE inhibitors. From literature as well as the results for compound **A51** it is evident that the thienopyrimidine scaffold contributes towards the AChEI activity observed. With this scaffold being one of the opulent fused heterocycles, it is clear that these compounds play a vital role in the discovery of novel effective pharmacophores.[189]

Subsequent structural searches of the active compounds using literature found that the majority of the active compounds' analogues are used as building blocks and/or are patented as inventions in other drug development projects (Table 6).

Table 6: Analogues of active compounds reported in literature.

Compound	Literature finding	Target	Reference
A8	Patent	AGC kinases inhibitors	204
	Aurora building block 7 and 9	-	205
A136	Patents	Fyn kinase inhibitors	206
		G protein-coupled receptor kinase 5 (GRK5) modulators	207,208
A175	Patent	Novel Fyn kinase inhibitors	206
A176	Patent	GRK5 modulator	207
C33, **C43**, **C53**, **C82**, **C129**, **C189**	Aurora building block 6	-	205

Analogues of compound **A51** have been reported to be dual histamine H_3 receptor (H_3R) antagonist/serotonin 5-HT_4 receptor (5-HT_4R) agonists, which are considered a novel treatment for degenerative disorders associated with impaired cholinergic function.[209] Presynaptic autoreceptors, H_3R modulates histamine release and regulates the release of neurotransmitters such as norepinephrine, dopamine, and serotonin. Serotonin receptors are targeted emerging AD therapies, and 5-HT_4R agonists are suggested to provide both symptomatic alleviation of cognitive impairment as well as neuroprotection by reducing Aβ generation and toxicity.[209]

It has also been shown that it is feasible to combine H_3R and 5-HT_4R activities in a single molecule (named benzo[h][1,6]naphthyridine derivative 17).[209] This dual H_3R antagonist/5HT_4R agonist, in a single molecule, has the potential for use in the treatment of neurodegenerative diseases such as AD.[209] This compound may act synergistically, exerting both symptomatic and disease modifying effects. In the light of these findings and for the purpose of this study, **A51** and its analogues are considered as promising leads for AD drug development as a dual-acting inhibitor with polypharmacological properties.

3.2 Pharmacokinetics prediction

The BBB permeability of compounds presents a major challenge for the development of new drugs targeting neurodegenerative diseases.[210,211] This is due to its highly restrictive nature

making it harder for drugs to enter and reach their therapeutic targets in the brain.[210,212] High attrition rate caused by BBB impermeability can be reduced by screening of CNS targeting drugs at an early stage of the drug discovery process for favourable pharmacokinetic parameters.[212] Various BBB models, including *in silico* models, are used at early stages of drug discovery research to predict the brain's uptake of the drug, based on simple molecular and physiochemical parameters.[113,213]

One of the easiest and most commonly used computational models, SwissADME, facilitates the evaluation of pharmacokinetic properties. For a drug to be predicted as BBB-permeable, it must possess a WlogP between 0.4 and 6, HBD of < 8, MW less than 400 g/mol, and a TPSA < 80 Å^2.[127,128,134] Of the 12 active compounds, only five displayed good drug-likeness according to Lipinski's rules. Analysis using the BOILED-Egg plot of TPSA and WlogP indicated that compounds **A8**, **A73**, **A136**, **C53** and **C129** were predicted to be BBB-permeable (Figure 16). Compounds **A8**, and **C129** were the most attractive as lead compounds and this is mainly because the parameters fit perfectly within the BBB-permeability range (MW [382.46 to 393.43 g/mol], TPSA [54.02 to 71.06 Å^2], WLogP [3.37 to 4.87] and HBD [< 8]) (Table 7).

The MW threshold of BBB transport is a more prominent issue in modern CNS drug discovery.[122,214] According to literature, if the MW of the drug exceeds 400 g/mol, it will not be transported across the BBB in pharmacologically significant amounts.[122] This is in accordance with *in silico* prediction results for compounds **C43** and **C82** with computed TPSA (< 80 Å^2), WLoP (< 6) and HBD (< 8) within the acceptable range, however, due to the greater MWs (488.58 and 441.57 g/mol), these compounds were predicted as being non-BBB permeable.

Interestingly, **A73**, **A136** and **C53** were predicted as BBB-permeable with MWs between 400.51 and 459.59 g/mol, indicative thereof that they can penetrate the BBB, and additionally the other parameters fall within the acceptable range (Table 7). This may relate to the fact that BBB permeability decreases 100-fold when the TPSA of a drug is increased from 50 to 100 Å^2, which would be the case when the MW of a drug is increased from 300 to 450 g/mol.[122] If the TPSA of the drug exceeds 80 Å^2, which corresponds to a MW of 400 g/mol, then BBB transport is minimal.[215] Unfortunately, this was true for the most potent compound of the study, **A51,** which was predicted to be non-BBB permeable due to the TPSA value being beyond the acceptable range (Table 7).

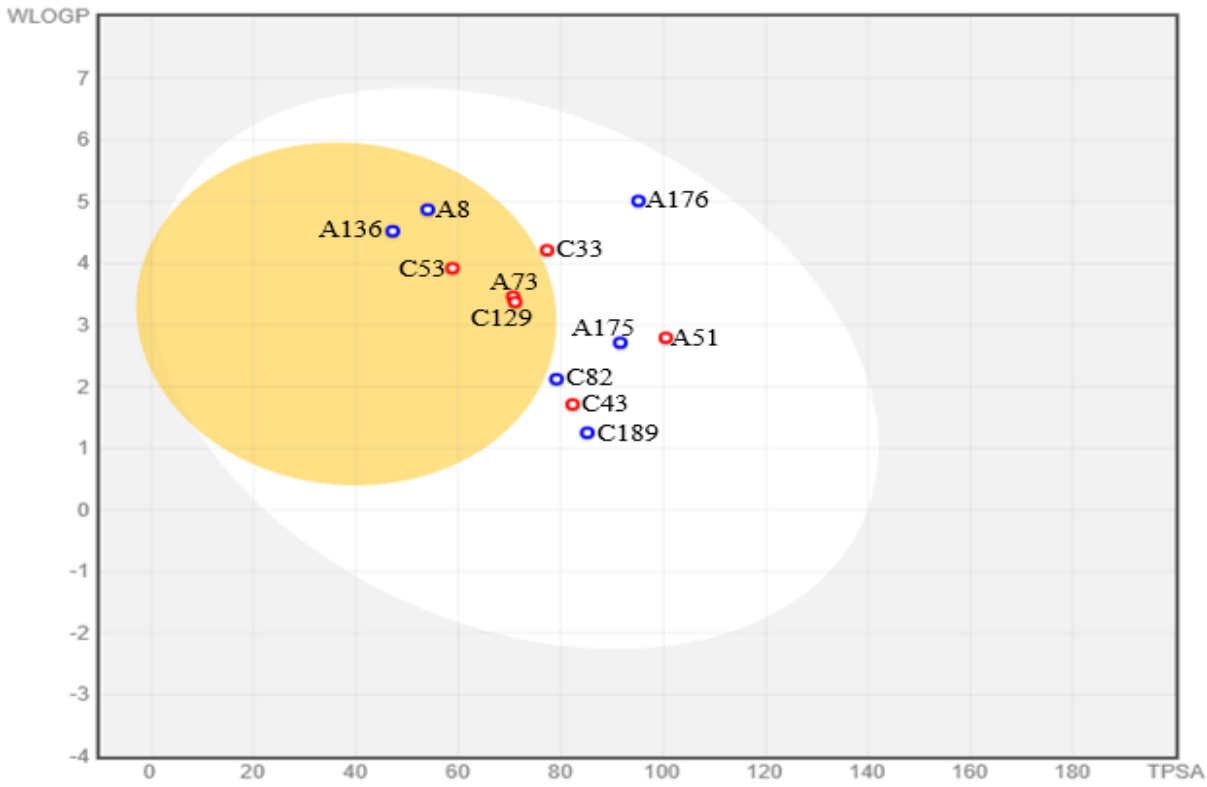

Figure 16: A brain or intestinal predicted permeation plot of the 12 compounds with acetylcholinesterase inhibitory activity. The compounds in the yellow circle are considered blood-brain barrier permeable, and in the white circle as gastrointestinal-permeable. The compounds with a blue circle are predicted to be P-gp substrates, whereas those with a red circle are not P-gp substrates.

Table 7: Physiochemical descriptors for the compounds containing acetylcholinesterase inhibitory activity.

Compounds	MW (g/mol)	TPSA (Å^2)	WLogP	BBB permeable	P-gp substrate	H-bond acceptors	H-bond donors
A8	393.43	54.02	4.87	Yes	Yes	5	2
A51	399.51	100.52	2.79	No	No	5	1
A73	459.59	70.7	3.46	Yes	No	3	1
A136	401.48	47.19	4.52	Yes	Yes	3	2
A175	442.51	91.63	2.71	No	Yes	5	2
A176	476.55	95.17	5.01	No	Yes	6	3
C33	394.51	82.32	1.71	No	No	2	2
C43	488.58	77.33	4.21	No	No	5	1
C53	400.56	58.87	3.92	Yes	No	3	1
C82	441.57	79.18	2.12	No	Yes	5	1
C129	382.46	71.06	3.37	Yes	No	4	0
C189	372.48	85.19	1.25	No	Yes	2	2

MW: molecular weight; TPSA: topological polar surface area; BBB: blood-brain barrier; P-gp: P-glycoprotein; H: hydrogen.

The number of hydrogen bonds a drug can form with a solvent (e.g., water), is inversely related to the lipid solubility.[122] Highly lipid-soluble drugs, characterised by low hydrogen bonding

and TPSA, can readily cross the hydrophobic phospholipid bilayer into the brain.[216] Similar to TPSA, this parameter works in tandem with the MW of a drug. If the MW of a drug is ≥ 400 g/mol and the drug forms more than eight hydrogen bonds, then the drug is too polar to cross the BBB.[215] This was true for compound **A176**, which contains 8 hydrogen bonding capabilities and a MW of 476.55 g/mol and predicted to be BBB impermeable.

Based on the BOILED-Egg results of the 12 AChEI active compounds, five compounds (**A8**, **A73**, **A136**, **C53** and **C129**) were predicted to be BBB-permeable, whereas seven compounds (including **A51**), were predicted as BBB-impermeable. Compounds predicted as BBB-impermeable were excluded from further investigation. Even though some compounds were predicted to be BBB-permeable, they might be effluxed immediately from the brain back to the blood if the drug requires active efflux transporters (e.g., P-gp) to cross the BBB.[217,218] The P-gp transporter serves as one of the important pharmacokinetic factors that influences the rate and extent of drug penetration into the brain by extruding lipophilic compounds back into the blood.[133,219] Lipophilic molecules with a low molecular weight tend to be substrates for P-gp and thus may be subject to low intracellular accumulation.[220]

Of the five compounds predicted to be BBB-permeable, only two, **A8** and **A136**, were found to be P-gp substrates. For these compounds, absorption across the BBB may be compromised as they may be effluxed, and thus bioavailability will be decreased. Physicochemical property modulation alone during lead optimisation cannot overcome all the BBB parameters; instead, it helps mainly to optimise the passive diffusion and the P-gp activity.[218] As much as the BOILED-Egg method predicts drug transfer across the BBB with high accuracy, the results should further be confirmed. Further BBB permeability assessment was conducted in Section 3.7 (page 59).

3.3 Combinational treatment effects

Combination therapy, consisting of dual-drugs or multi-targeting drugs at lower dosing regimens, provides effective pharmacological management of AD with improved tolerability.[221,222] For instance, the use of the FDA approved fixed-dose combination of donepezil and memantine, has primarily proven to be more clinically effective for the treatment of moderate to severe stages of AD.[22,66,67] Hence there is a growing enthusiasm for combination therapy as the most promising avenues toward treating multifactorial diseases.[223]

It should be noted that drug combinations may interact in unexpected ways, and therefore have different outcomes.[224] These interactions can be classified as antagonistic, additive/non-interactive, or synergistic, according to whether the combined effect of the drugs is larger than, equal to or smaller than the effect predicted by their individual activities.[225] Among these, the combined booster effect of drug efficacy, is regarded as the positive interaction and highly sought for combinational drug development.[223,224,226] A synergistic effect observed in a case where combined compounds target the same site, might be due to one of the compounds binding allosterically to the enzyme.[104] For instance, AChEIs used for the treatment of AD, inhibit AChE via direct binding to the catalytic anionic site (CAS), also known as esteratic site or via binding to a peripheral anionic site (PAS) known as allosteric binding.[171,222] This implies that AChE can potentially accommodate two AChEI molecules simultaneously.[222]

In the present study, AChEI activity of the five active compounds with predicted BBB permeability was combined with donepezil at their ¼IC_{50}s, ½IC_{50}s and IC_{50}s (Table 8). The CI value was used as a measure of combinational activity. A CI of 1 is indicative of additive activity, whereas a CI > 1 or CI < 1 is considered antagonistic or synergistic, respectively. A total of 45 combinations were assessed with five combinations displaying synergistic activity, 15 combinations antagonistic activity, and 25 combinations additive activity (Table 9).

Table 8: The concentrations of the compounds and donepezil used to determine the combination index.

Compound	IC_{50} (µM)	½IC_{50} (µM)	¼IC_{50} (µM)
A8	5.87	2.94	1.47
A73	3.83	1.92	0.96
A136	16.68	8.34	4.17
C53	3.37	1.69	0.84
C129	12.52	6.26	3.13
Donepezil	0.03	0.015	0.007

IC_{50}: concentration resulting in 50% inhibitory effect.

Table 9: Combination index values obtained when combining the compounds with donepezil.

Compounds		CI values when combined with donepezil		
		¼ IC_{50}	½ IC_{50}	IC_{50}
A8	¼ IC_{50}	0.97315	1.10127	1.36008
	½ IC_{50}	1.13606	1.14178	1.35792
	IC_{50}	1.34679	1.2734	1.38135
A73	¼ IC_{50}	1.49738	1.07627	1.31801
	½ IC_{50}	1.11742	1.42789	1.28898
	IC_{50}	1.52648	1.30244	1.55634
A136	¼ IC_{50}	2.6799	1.16448	1.22352
	½ IC_{50}	**0.61572**	**0.81085**	1.03392

Compounds		CI values when combined with donepezil		
		¼ IC_{50}	½ IC_{50}	IC_{50}
	IC_{50}	**0.81611**	**0.69063**	1.00737
C53	**¼ IC_{50}**	**0.82461**	1.11644	3.26654
	½ IC_{50}	1.20981	1.66732	1.80658
	IC_{50}	1.36329	1.92501	2.63125
C129	**¼ IC_{50}**	1.24306	0.98440	1.88882
	½ IC_{50}	1.20119	1.57913	2.81944
	IC_{50}	1.84031	2.70451	3.86729

IC_{50}: concentration resulting in 50% inhibition; CI: combination index.

The strongest synergistic activity was achieved when the ¼IC_{50} of donepezil and ½IC_{50} of **A136** were paired (CI = 0.61). As solo treatment, donepezil had high AChEI activity (IC_{50} = 0.03 µM) compared to **A136** (IC_{50} = 16.68 µM). To achieve the AChEI synergistic response observed, a higher concentration (½IC_{50}) of **A136** was required compared to that of donepezil (¼IC_{50}). In another study where the ability of donepezil, tacrine, berberine, and galantamine alone and in combination were determined to inhibit human or *Torpedo californica* acetylcholinesterase (tcAChE), the most effective synergism (CI = 0.575) was observed for the berberine and galantamine combination which were found to be the least active AChEIs when tested individually.[222] This was contradictory to what was observed in the current study as the greatest synergism effect was observed between a combination with high AChEI (donepezil), and one with the lowest AChEI activity (**A136**).

It has been reported that synergistic activity between two compounds is usually noted when lower concentrations of each compound are combined.[227,228] This theory supports the synergic effect observed in this study between donepezil and **C53** at their lowest concentrations (¼IC_{50}). Advantage of such synergistic drug pairs provides the opportunity to lower the dosage of individual drugs, thereby reducing toxicity while maintaining the desired effect.[229]

Synergistic effects observed might be as a result of complementary drug action (different targets sites on the same enzyme or protein are hit), anti-counteractive actions (one drug affects the biological response of the other one), or facilitation actions (one drug potentiates the effect of the other).[229,230] To this point, the specific binding site(s) and mechanism of action of compounds screened in this study are unknown besides those of donepezil, as reported in literature. To further explain and understand the mechanisms by which these combinations exert synergistic effects, Michaelis-Menten kinetics was carried out. Michaelis-Menten kinetics elucidate the mechanism of inhibition in relation to specific binding sites of the compounds (refer to Section 3.5; page 51).

Additivity/potentiation which indicates that the combined effect is a pure summation effect [226] was observed for the majority of combinations tested. A drug combination is considered to be additive when the effect of each drug neither masks nor increases the efficacy of the other drug. This is also known as non-interaction.[227,229] An additive effect may occur if the intrinsic activities and affinities of the two drugs are identical.[231] Combined drugs may bind to the same binding site either orthosterically or allosterically. In the study of Amatur-ur-Rasool *et al.*[222] an additive effect was observed between tacrine and donepezil as drug combination, both of which possessed the highest activity as single drugs. Furthermore, both drugs are said to bind to the same (PAS) active site.[222] As both compounds compete for the same binding site, when one compound binds first, the second drug increases the total amount of compound present in the biological environment causing an increase in the inhibitory effect observed.[227]

On the other hand, antagonism, defined by interaction resulting in a less than additive effect was observed. This interaction was mostly observed when the concentration of donepezil was higher (IC_{50}) than the combination compound's concentration. This results in a strong form of antagonism, which is characterised by a single agent dominance, which may lead to limited efficacy when in a drug combination.[232] Similar to a synergistic effect, an antagonistic effect is also observed when two compounds act on the same target (AChE) and compete for the same enzymatic binding sites (either active or allosteric sites).[104] Therefore, this effect might be due to negative allosteric effects, or competition for the orthosteric site.

When the inhibitor binds to either site, it "deactivates", thus prohibiting the generation of the end product.[233] Furthermore, this type of antagonism manifests when the compound with the lowest intrinsic activity possesses higher affinity for the target and is the first to bind to the target.[104] Another factor leading to apparent synergy or antagonism is the effect some drug may have on uptake, metabolism and clearance of other drugs.[227] For most diseases including AD, drug antagonism is often undesirable, but could be useful in some diseases such as cancer.[224] An explanation to support the observed effects in relation to mechanism of inhibition is provided later in Section 3.5 (page 51).

Combination treatments for AD are a necessity and preferred to monotherapy and can be achieved by seeking synergistic responses.[22,223] Moreover, synergistic combinations can overcome toxicity and other side effects associated with high doses of single drugs used for AD treatment.[223]

3.4 Cytotoxicity screening

Currently, there is a wide variety of *in vitro* models used for cytotoxicity screening based on primary cell cultures, immortalised cell lines and induced or embryonic stem cells. Advantages, and limitations should be considered when selecting an assay.[106,234] The SRB assay is one of the most used assays, as it is rapid and sensitive. In addition to its sensitivity, this colorimetric method provides good linearity with cell number, and has high reproducibility. An aspect of importance is ensuring that a homogeneous cell suspension is maintained.[108] The SRB assay was therefore chosen to assess the cytotoxicity of *in silico* predicted BBB-permeable compounds with AChEI activity, using the SH-SY5Y neuroblastoma cell line. As much as this cell line is cancerous, it has been shown to exhibit similar biochemistry and morphology to human neuronal cells hence it is commonly used for neurotoxicity testing.[171,235]

Most of the compounds, except for **A136** and **C129**, presented with a cell density > 100% over a concentration range of 0.001 and 10 µM (Figure 17). At a concentration of 100 µM, **A8**'s effect on cell density was comparable to the negative control, while **A73** and **C53** displayed low cytotoxicity at 100 µM, with a cell density reduction of 27% and 49%, respectively. Donepezil and **C129** were found to be cytotoxic, with IC_{50} values of 43.00 and 13.64 µM, respectively, resulting in cell reduction of 90.76 and 65.86%, respectively, at 100 µM.

Although **A136** increased cell density (> 100%) between 1 and 3.2 µM, it reduced cell density at concentrations ≥ 10 µM to ~0%. An IC_{50} of 4.99 ± 1.31 µM was calculated for **A136**, being the compound that was the most cytotoxic of the batch tested. The initial increase in cell density was suggestive thereof that a hormetic effect was present at lower concentrations. A hormetic effect, also known as hormesis, is defined as a biphasic dose response characterised by exhibiting stimulatory or beneficial effects at low doses, and inhibitory or toxic effects at high doses.[236,237] Low doses of toxins or stressors are not only harmless, but also initiate and activate an adaptive stress response.[238] In neuroscience, the adaptive process is a reflection that neuronal cells respond to an induced moderate level of stress, but that their ability to resist a more severe stress might cause cell death, dysfunction or enhance disease.[239,240]

The adaptive response further induces changes in gene expression and activates molecular pathways that ultimately lead to the expression of a hormetic dose response.[241] It has been reported that key signalling pathways of cell survival/proliferation and oxidative stress response are involved in the processes of hormesis.[236,239]

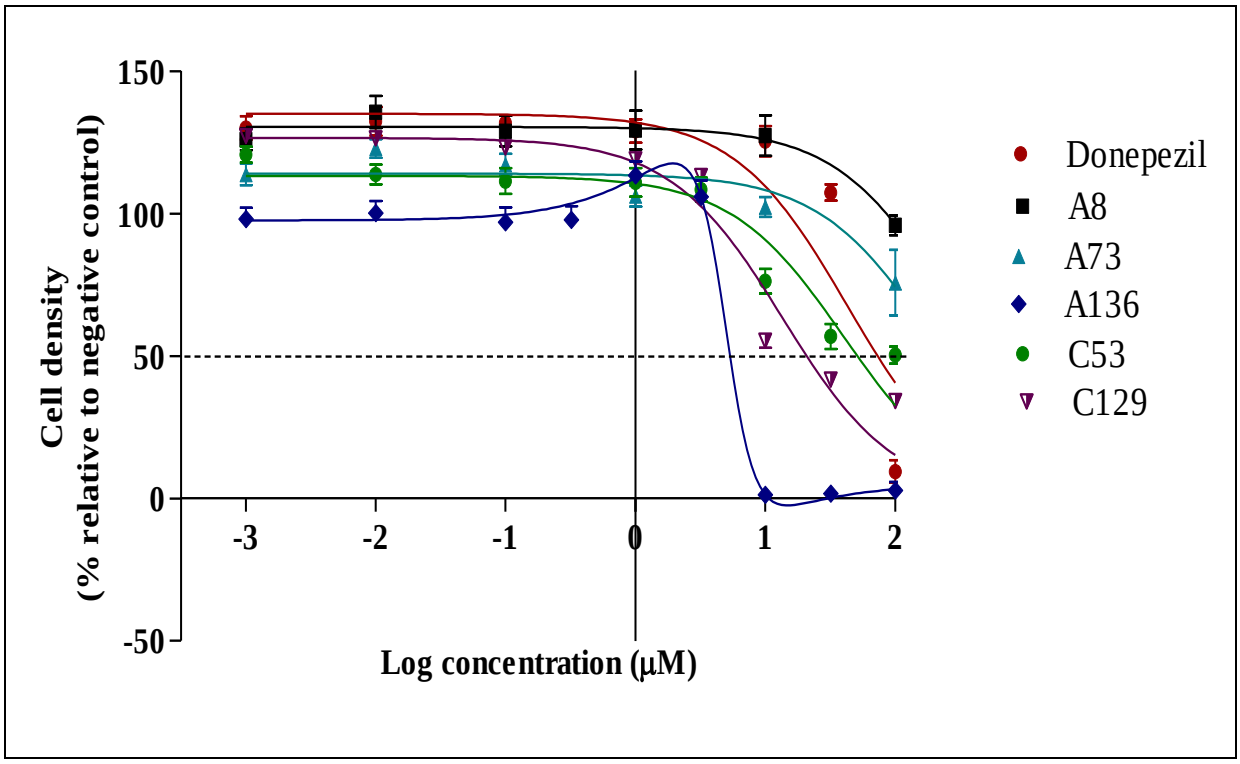

Figure 17: The effect of compounds with acetylcholinesterase inhibitory activity and donepezil on SH-SY5Y cell density after 72 h exposure

Authors such as Pallas[241] and Mattson[240] summarised the mechanisms of hormesis induced by resveratrol and these include; activation of cell-survival signalling kinases, nuclear factor-erythroid 2p45 (NF-E2)-related factor (NRF2), cAMP response element-binding protein, components of sirtuin family, and AMP-activated protein kinase.[236] Demirovic *et al.*[242] also reported that curcumin induced a hormetic dose response in wound healing via the oxidative stress response pathway, Nrf2/ antioxidant response element (ARE)/HO-1. These reported pathways might have also contributed to the hormetic effect exerted by **A136**. As much as compounds **A136** and **C129** inhibited the AChE activity, these compounds were excluded from further assessment due to their cytotoxicity.

Cytotoxicity of the combinations which indicated synergistic AChEI activity (CI < 1) were assessed to determine whether this resulted in cytotoxicity. Of the five combinations that indicated synergistic effect, the combination of **C53** (¼IC_{50}) and donepezil (¼IC_{50}) was the only combination to display low cytotoxicity, with cell density reduction of 23% (Figure 18). However, it should be noted that the cytotoxicity of the combination was higher than that observed for the individual compounds. The combinations of **A136** and donepezil showed cytotoxicity and were therefore not investigated further, irrespective of their strong synergistic effect.

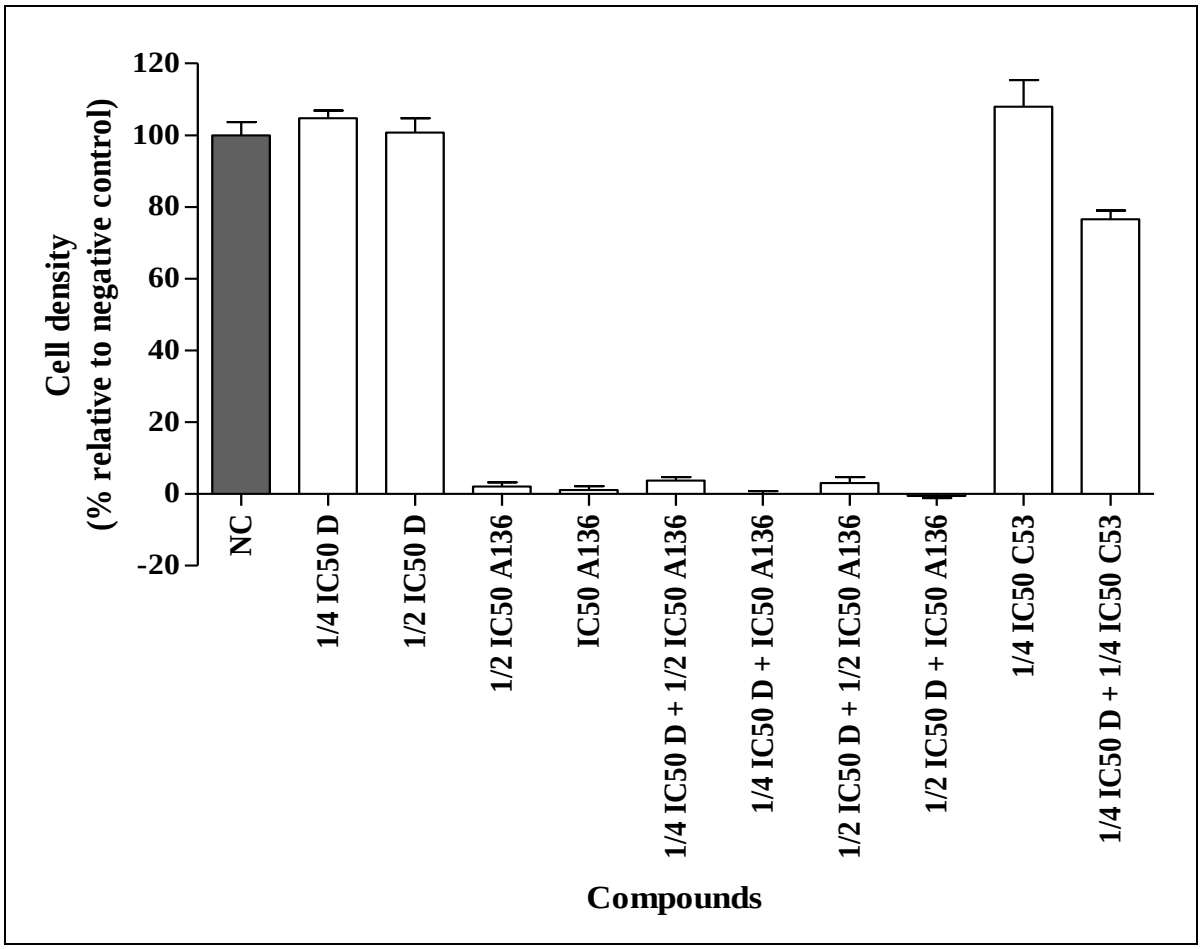

Figure 18: Cytotoxicity of the combinations which indicated synergistic effect. D: donepezil; IC_{50}: concentration resulting in 50% inhibition; NC: negative control.

It should be kept in mind that all compounds had a similar scaffold and exhibited some sort of cytotoxicity, with the exception of **A8** (Table 3). This compound has a unique structure and promoted cell growth even at the highest concentration tested. Due to structure variability of these compounds and the scope of this study, at this point it is impossible to identify which scaffolds or substituents were responsible for the cytotoxicity observed.

Compounds **A8**, **A73** and **C53**, did not possess cytotoxicity activity at the concentrations tested and were further assessed for their purity and stability to identify if any decomposition of the compounds had occurred since the library was purchased. No degradation or decomposition was noted for the three compounds (stored at -20°C) over time when UPLC-MS analysis was performed (Appendix IV).

Prior to assessing the effect of non-cytotoxic compounds on the integrity of endothelial monolayers, cytotoxicity of these compounds in bEnd.5 cells was investigated. All compounds including the synergistic combinations resulted in a cell density > 100% over a concentration

range of 0.001 and 10 µM (Figure 19). At concentrations ≥10 µM, the effect of compounds **A8** and **A73** on cell density were comparable to the negative control, while donepezil and **C53** displayed low cytotoxicity at 100 µM, with low cell density reduction of 36% and 10%, respectively. The combination containing synergistic activity (**C53** [¼IC_{50}] and donepezil [¼IC_{50}]) displayed cell density comparable to the negative control (Figure 20).

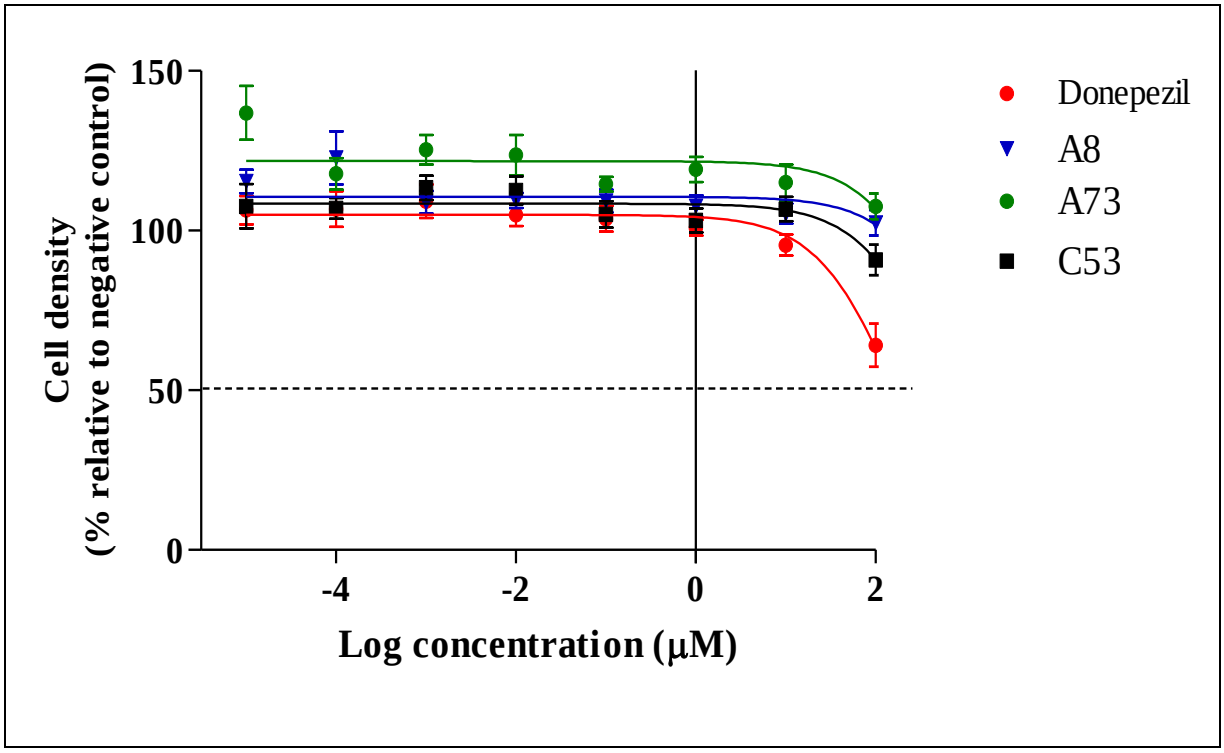

Figure 19: The effect of compounds and donepezil on bEnd.5 cell density after 72 h exposure.

All the compounds exhibited lower cytotoxicity in bEnd.5 cells than in the SH-SY5Y cells. These results are in accordance with findings reported by Michaelis *et al.*[243] where human umbilical vein endothelial cells showed a lower sensitivity to the anti-cancer drugs doxorubicin, vincristine, or cisplatin, compared to a panel of seven neuroblastoma (UKF-NB-2, UKF-NB-3, UKF-NB-6, IMR-32, NLF, IMR-5 and MS-KAN) cell lines. Zaremba-Czogalla *et al.*[244] reported that six of the 12 resynthesed derivative compounds screened had high cytotoxicity against pancreatic cancer cells (BxPC-3 and AsPC-1), with low toxicity against normal human dermal fibroblasts cells (control cells). This affirms the necessity for cytotoxicity assessment using at least two cell-lines in the early stages of CNS targeting drug discovery.

Despite the use of different cell lines and modulators it is evident from this and other studies that non-cancerous (normal) cells have a high tolerance for toxicity compared to cancerous cells.[234,245] This might be ascribed to the metabolic changes of tumour cells and the loss of

membrane integrity, rendering them more sensitive to compound toxicity than 'normal' cells.[216,217] On the other hand, normal cells, especially endothelial cells, contain additional defence mechanisms against constant exposure to toxins or stress-inducing elements. Therefore, exposure to drugs activate survival pathways and defence mechanisms making them less sensitive.[243,246]

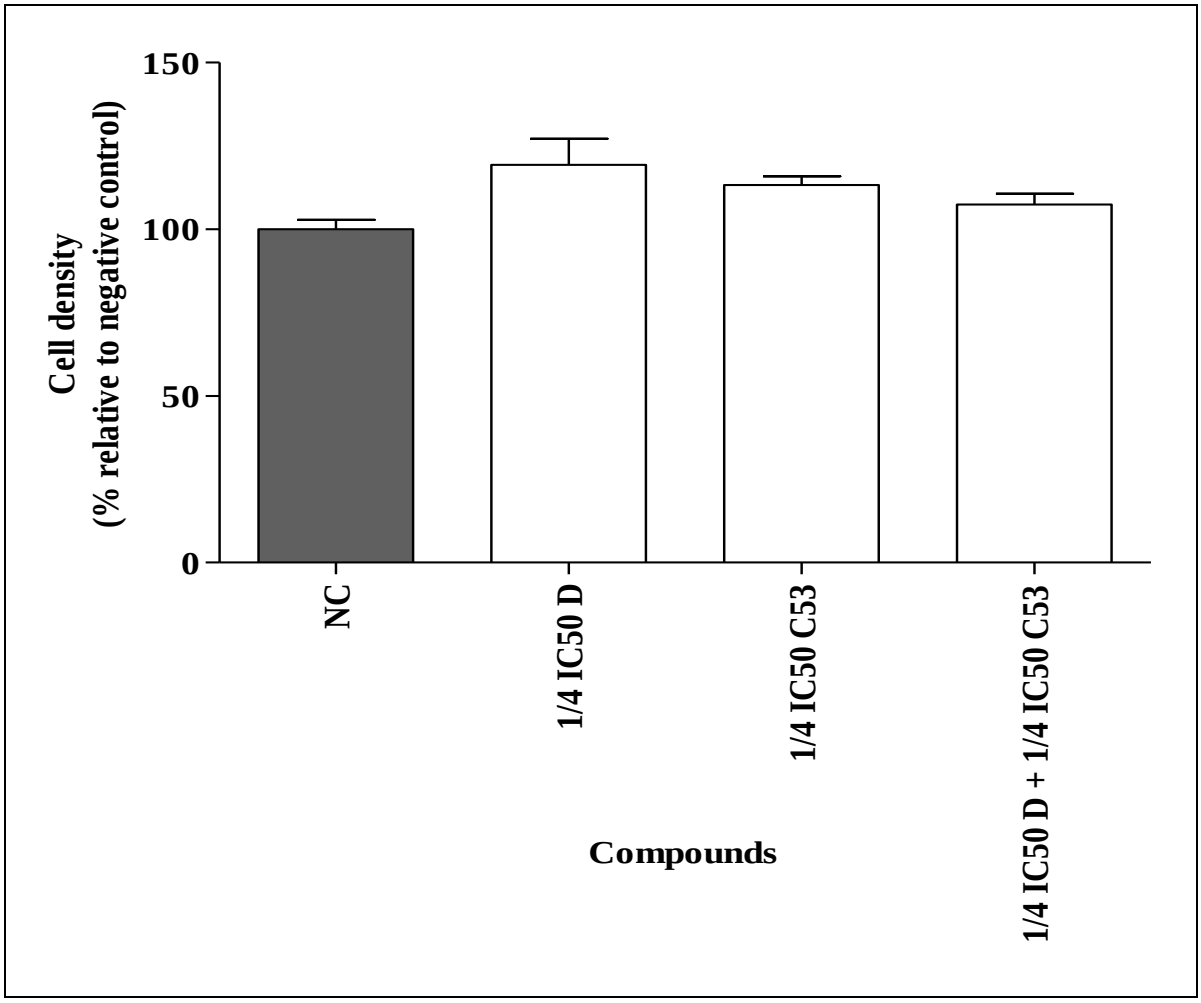

Figure 20: Cytotoxicity of the combinations which indicated a synergistic effect. D: donepezil; IC_{50}: concentration resulting in 50% inhibition; NC: negative control.

The low cytotoxicity observed in both cell lines for the compounds which were predicted to be BBB-permeable and contained AChEI activity, **A8**, **A73** and **C53**, as well as the synergistic combination of **C53** (¼IC_{50}) and donepezil (¼IC_{50}), make them ideal candidates for further investigation for drug development.

3.5 Inhibition kinetics of acetylcholinesterase enzyme

Determining a potential candidate's mechanism of action is an essential step in the drug discovery process. [232] Depending on changes in the values of the Michaelis constant (K_m) and

maximal rate of reaction (V_{max}) using Lineweaver-Burk plots, enzyme inhibition mechanisms can be classified as either competitive, non-competitive or mixed, as indicated in Figure 21.

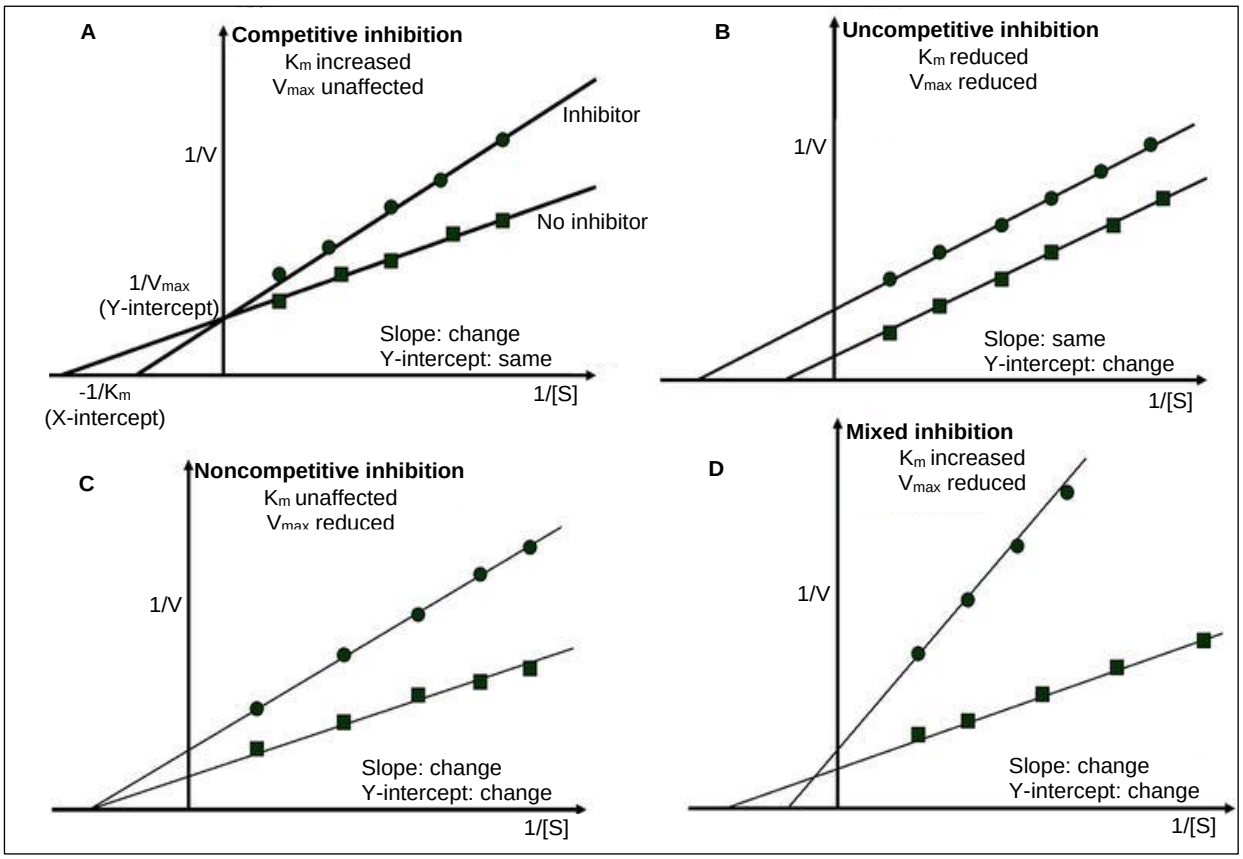

Figure 21: Lineweaver-Burk plot for enzyme inhibition.[247] Graph A: competitive inhibition; B: uncompetitive inhibition; C: noncompetitive inhibition and D: mixed inhibition. V_{max}: maximum rate of reaction when the enzyme is saturated with substrate. K_m: concentration of substrate which permits the enzyme to achieve half V_{max}. v: reaction velocity; [S]: substrate concentration. *[Reproduced with permission from Lopina, 2017 (author), licensed under Creative Commons Attribution License (http://creativecommons.org/licenses/by/3.0)].*

The mode of enzyme inhibition of the potential hits identified in this study was analysed by Michaelis-Menten kinetics (Figure 22A) using the in-house AChE miniaturised assay and confirmed using the Lineweaver-Burk plot (Figure 22B). The known AChEI, donepezil, was used as the positive control. Donepezil is a mixed competitive and non-competitive inhibitor that binds to the PAS.[248,249] This mode of inhibition was confirmed in the current study (Figure 23A). Competitive inhibitors typically compete with substrates for binding to the same active site of an enzyme and this binding is said to be mutually exclusive.[250,251] On the other hand, non-competitive inhibitors bind equally to both the free enzyme and the enzyme-substrate complex.[106,252]

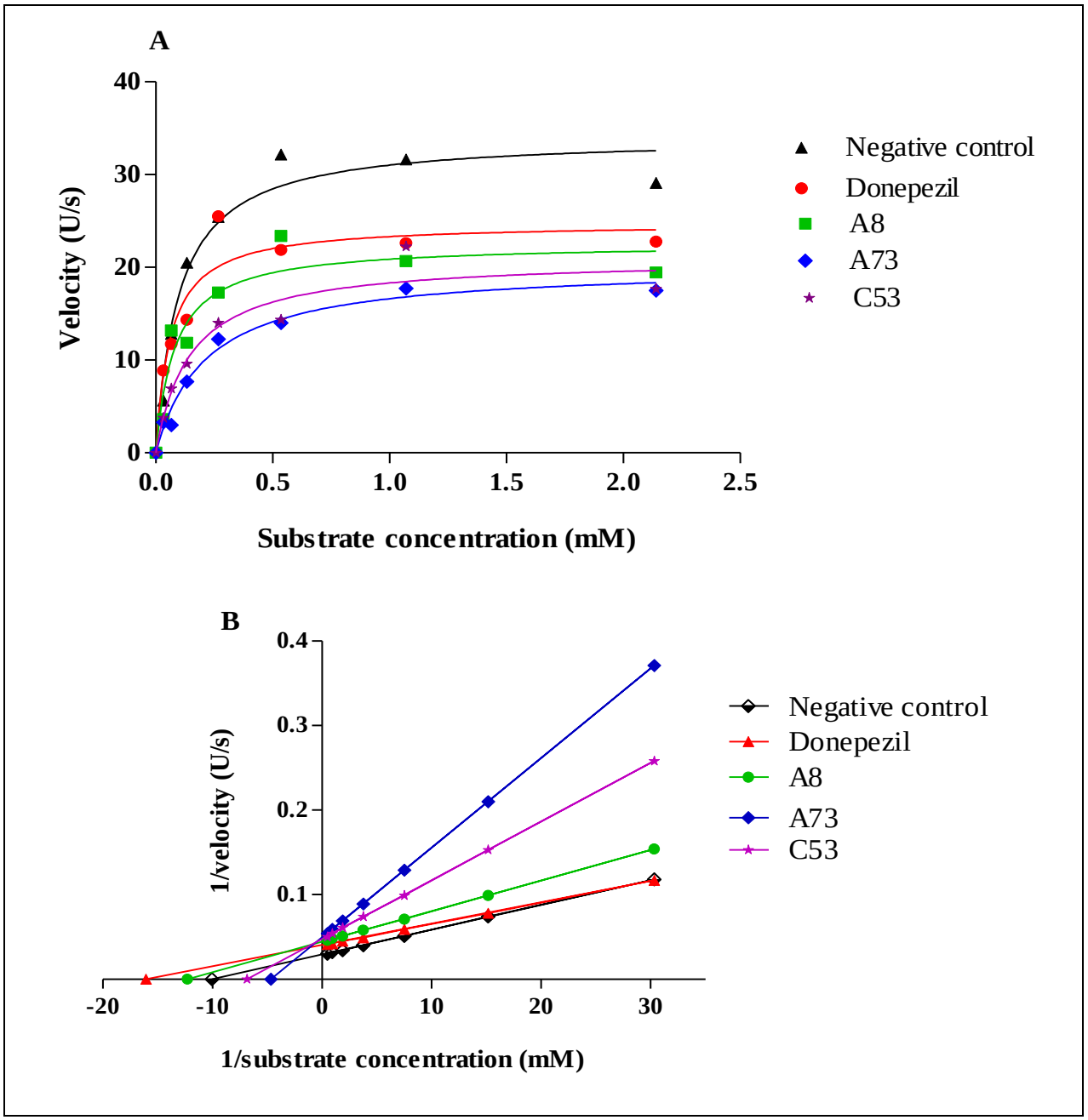

Figure 22: A) Michaelis-Menten graph and B) Lineweaver-Burk plot for compounds with acetylcholinesterase inhibitory activity and predicted blood-brain barrier permeability.

However, this type of inhibitor tends to bind exclusively to a site distinct from the enzyme's active site and by so doing it confers an allosteric inhibition.[106,252] Features of a non-competitive inhibitor include; having no effect on substrate K_m while decreasing the V_{max}. Competitive inhibitors maintain a constant V_{max}, whereas there is a change in K_m.[106] Since donepezil is a mixture of these two mechanisms, changes in both parameters were noted (Figure 23A). The V_{max} reduced from 34.11 to 24.76 and the k_m from 0.09 to 0.06 (U/s). In relation to the compound's structures, the hydrophobic aromatic part (5,6-dimethoxyindan-1-one) of

donepezil is reported to bind to the PAS, whereas the *N*-benzyl piperidine residue binds to the CAS of AChE.[253,254]

Compound **A8** is an uncompetitive inhibitor, as characterised by a decrease in both K_m and V_{max}.[171] The V_{max} decreased to 22.27 [s] and K_m to 0.08 (U/s) (Figure 23B). This mode of action is promising for drug design as the inhibitor only recognises and binds exclusively to the enzyme-substrate complex.[250,251] Similar to donepezil, **A73** and **C53** displayed mixed inhibition. The competitive effect resulted in an increase in K_m (0.21 and 0.15), whereas the non-competitive effect led to a decrease in V_{max} (20.17 and 21) as is evident in Figures 23C and D, respectively. If the value of K_m increases, then the inhibitor is said to have a higher affinity for the free enzyme than for the enzyme-substrate complex.[249]

As the mechanism of inhibition of the potential hit compounds was determined, the results could be related to those of the combinational effects. The combination of donepezil (mixed competitive and non-competitive inhibitor) and **A8** (non-competitive inhibitor) exerted additive effects across all the concentrations tested, and this is attributed to the fact that the compounds bound to the same binding site. Even though donepezil can bind to both the enzyme and enzyme-substrate complex, it tends to have a higher affinity for the enzyme-substrate complex (the only binding site for **A8**). For instance, if either compound binds first, then the other compound won't bind, leading to a higher amount of the compound in the microenvironment which will be observed as a greater extent of inhibition (additive effect).

Similarly, the combination of donepezil and **A73** (both mixed inhibitors, binding to the same site) resulted in additive effects at all concentrations tested. Since the compounds bind to the same site, when one compound binds to the enzyme, it might be completely inactive for the next compound to bind. Thus, the additive effect observed is exerted due to the presence of an unbound inhibitor. A synergistic effect was observed for the combination of donepezil and **C53** at the lowest concentration, even though they both displayed mixed inhibition. This might be due to the fact that donepezil has a high affinity for the enzyme-substrate complex (indicated by the decreased K_m), whereas **C53** (increased K_m) has a high affinity to the free enzyme. These compounds may bind simultaneously (mutually non-exclusive) to different sites, giving rise to the synergistic inhibition observed. With this said, it proves that a reduced dosage of each compound or accessing context-specific multitarget mechanisms, might lead to synergistic combinations, which overcome toxicity and other side effects associated with high doses of single drugs.[223,255]

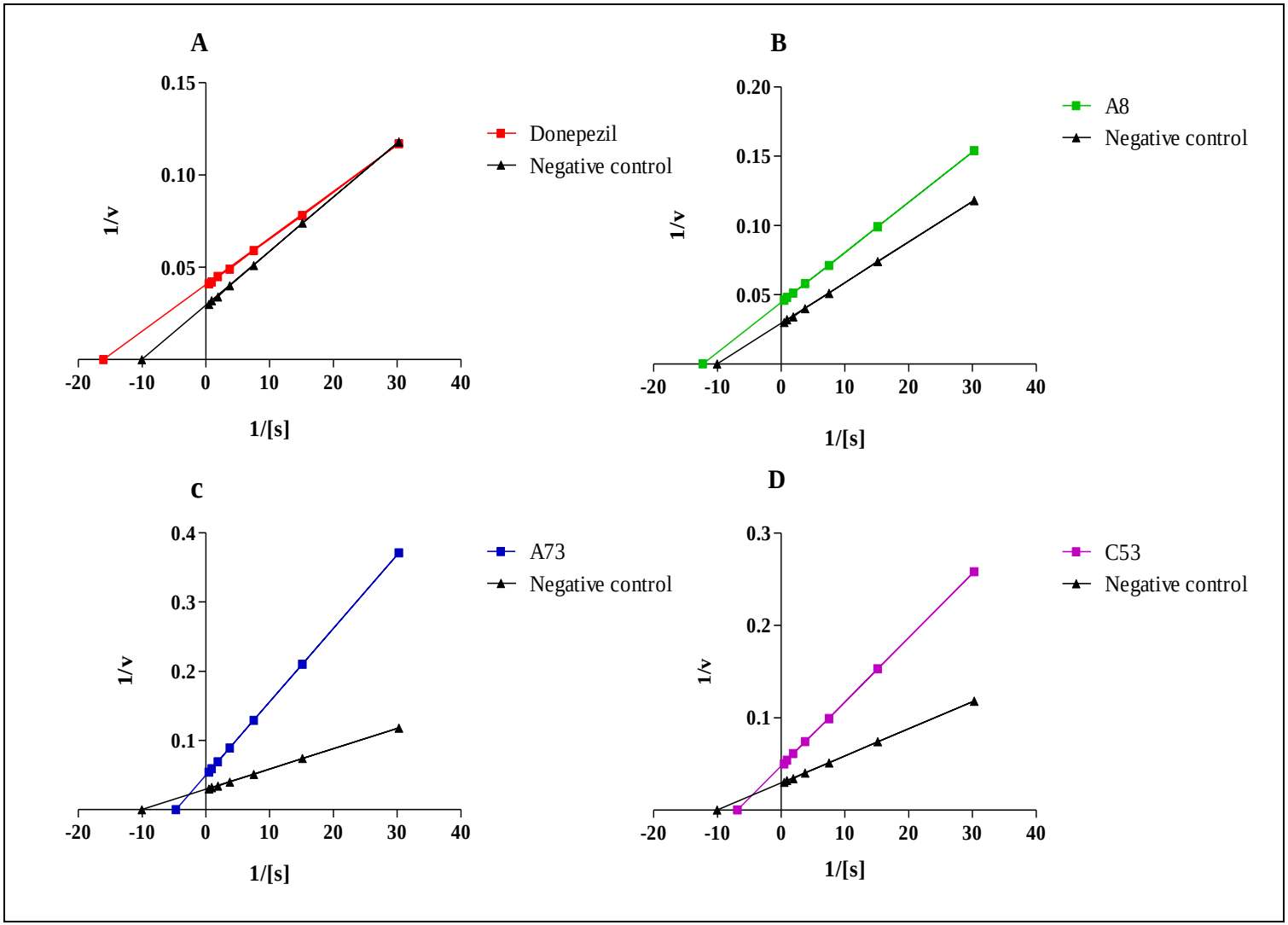

Figure 23: Lineweaver-Burk plots of compounds with acetylcholinesterase inhibitory activity and predicted blood-brain barrier permeability. A) donepezil, B) **A8**, C) **A73** and D) **C53**. v: reaction velocity; [s]: substrate concentration.

3.6 *In situ* acetylcholinesterase inhibitory activity of compounds

Neuroblastoma cells can be used either in the undifferentiated or differentiated form. The important difference between the undifferentiated and differentiated SH-SY5Y human neuroblastoma cell line is the polarisation and proliferation rate of the cells.[138,256] For instance, differentiated cells have a decreased proliferation rate, extended neurites and are more pyramidal shaped.[245,256] In addition to this, differentiated cells have the ability to reflect a mature neuron-like phenotype characterised by the expression of neuronal markers.[256,257] There are several methods used to differentiate SH-SY5Y cells such as the use of retinoic acid and phorbol esters.[256] However, a standardised protocol with regards to ingredients of mediums and treatment period to provide better differentiation, is still debatable.[138,256]

Due to this, several studies especially in the field of neurobiology tend to use undifferentiated SH-SY5Y cells as a functional model for human neurons.[245] Undifferentiated SH-SY5Y cells are able to proliferate rapidly, even though they grow in clumps and are non-polarised.[245,256] Despite some innate limitations, these cells can express esterase enzymes such as AChE at higher cell densities.[66] For this reason, undifferentiated cells have been tested and used as an *in vitro* model to study the effects of various compounds on esterase activity.[66] In this study, compounds were screened at the concentration of 1.5/IC_{50}, IC_{50} and 1.5×IC_{50} together with the synergistic combination compounds at their ¼IC_{50}s. Of these, compound **A73** was the only compound that inhibited AChE dose-dependently (Figure 24).

Donepezil significantly ($p < 0.1$ and $p < 0.001$) inhibited AChE at all concentrations with the IC_{50} and 1.5×IC_{50} showing comparable inhibition of 68% and 67%, respectively. Compound **A8** showed low AChEI activity, comparable to that of the negative control at both concentrations (IC_{50} and 1.5×IC_{50}; Figure 24). Although **A73** possessed a dose-response inhibitory response, this compound had low AChEI activity with 10% AChE inhibition at IC_{50}. Similar to donepezil at all concentrations (1/5IC_{50}, IC_{50} and 1.5×IC_{50}), **C53** significantly ($p < 0.01$, $p < 0.001$ and $p < 0.0001$) inhibited AChE by 40, 61 and 60%, respectively (Figure 24). The synergistic combination, **C53** (¼IC_{50}) and donepezil (¼IC_{50}) inhibited AChE significantly ($p < 0.1$) by 69% compared to the individual compounds (Figure 25). Given the results, **C53** as single treatment and in combination with donepezil, should be assessed further as potential treatment.

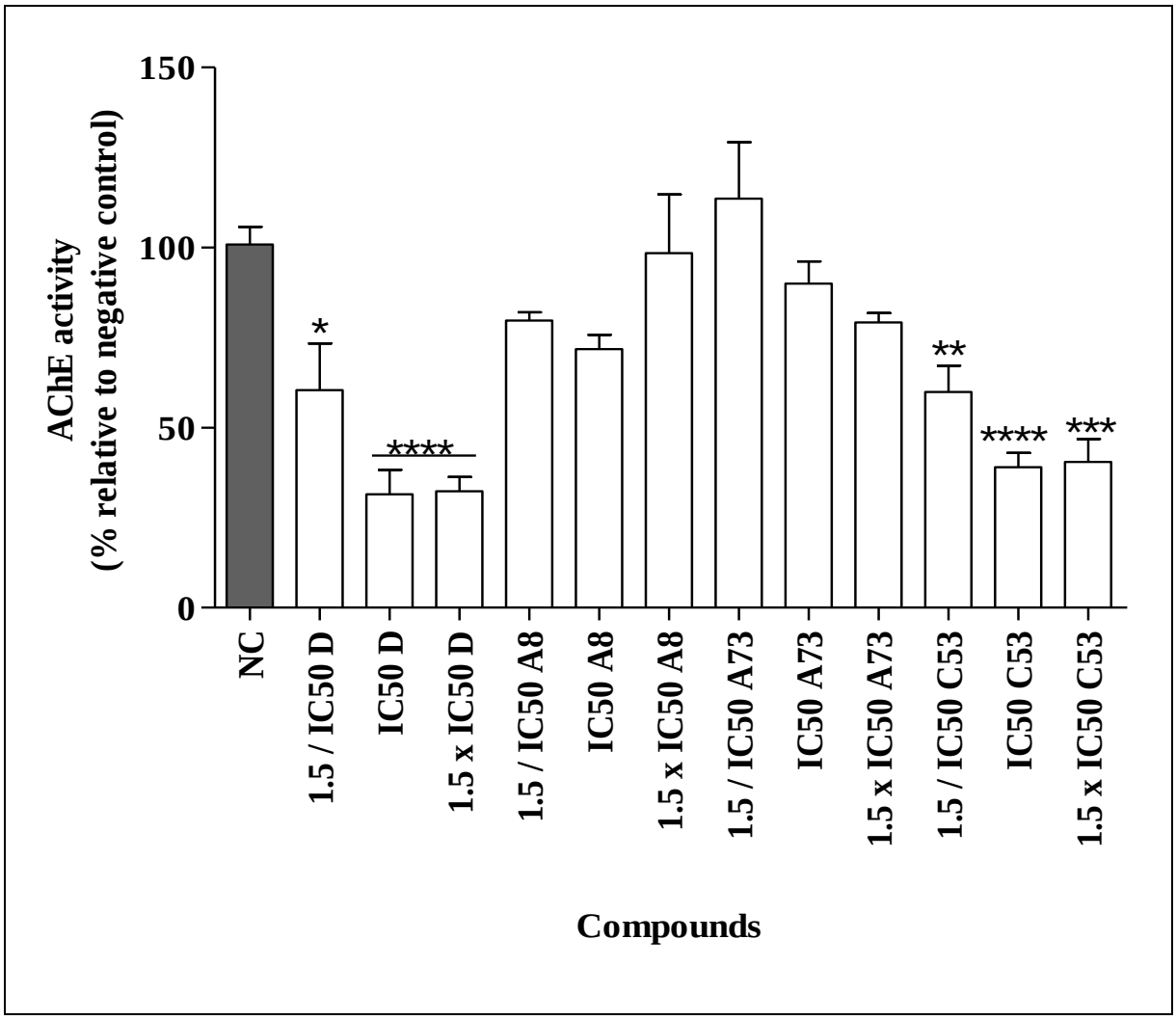

Figure 24: Cellular acetylcholinesterase inhibitory activity of compounds with potential acellular acetylcholinesterase inhibitory activity. Significance of inhibition relative to negative control is indicated as * $p < 0.1$, ** $p < 0.01$, *** $p < 0.001$, **** $p < 0.0001$. D: donepezil; IC_{50}: concentration resulting in 50% inhibition; NC: negative control.

Acetylcholinesterase inhibitory activity exhibited by these compounds especially at IC_{50} and $1.5 \times IC_{50}$, may be ascribed to the altered environment; acellular (enzyme-based) versus cellular (cell-based). Although AChE enzymes are well conserved in evolution, interspecies differences in activity and inhibition do exist.[258,259] It is reported that there are species differences for brain AChE inhibition between birds, fishes and mammals, including rats, particularly for compounds such as organophosphates, oxon and carbamates.[144,258,260]

Differences in factors such as affinity, the rate of phosphorylation of AChE and steric arrangement in the active site can contribute to species differences, resulting in different inhibitory activity and species sensitivity distributions dependent on the compounds.[258,261] For instance, human and eeAChE share the same acyl pocket that is characterised by two Phe

residues (Phe288 and Phe290), however, there are still structural differences that may lead to potency differences.[144,262] Based on the observed results, eeAChE was more sensitive as the potency of all compounds tested in eeAChE was greater than those in human AChE.

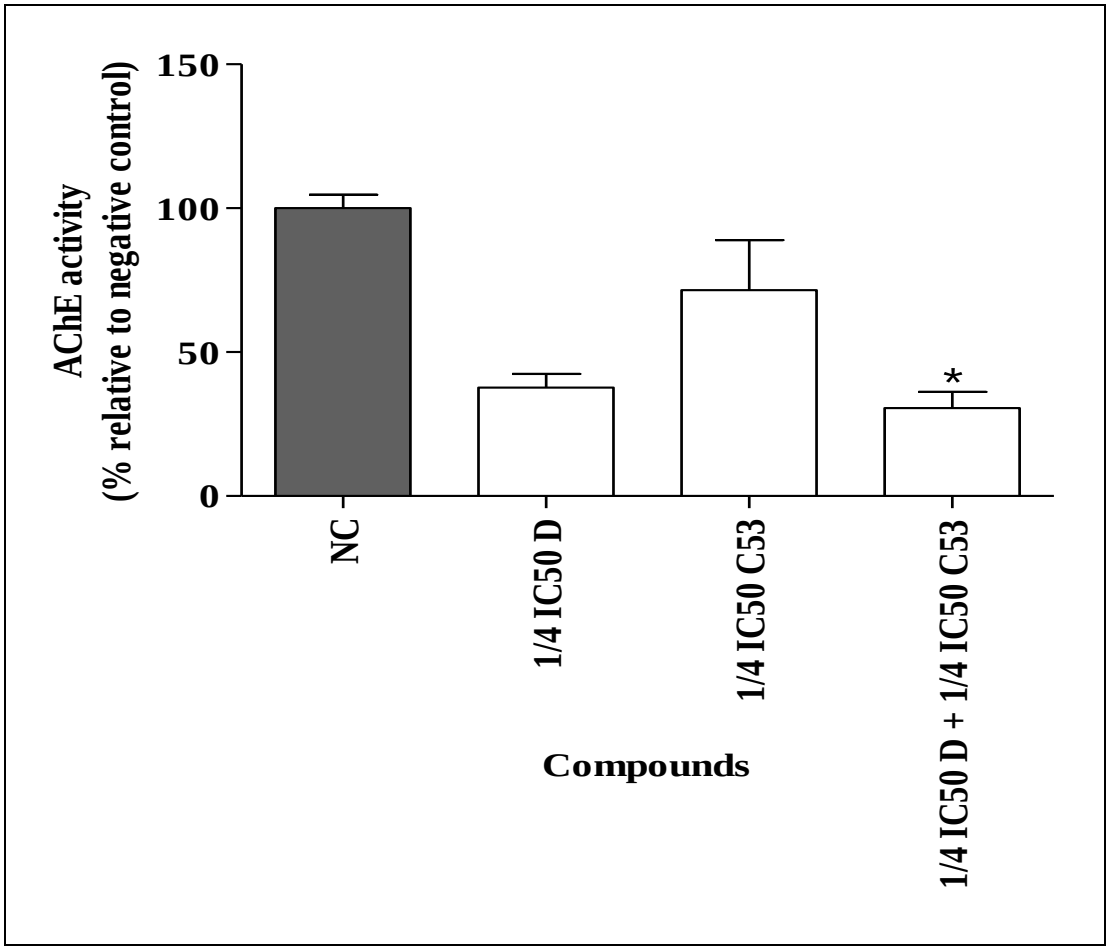

Figure 25: Cellular acetylcholinesterase inhibitory activity of individual compounds and the synergistic combination. Significance of changes relative to negative control are indicated as * $p < 0.1$. D: donepezil; IC_{50}: concentration resulting in 50% inhibition; NC: negative control

Human neuroblastoma (SH-SY5Y) cells were used to produce human AChE enzyme and these cells can also express another type of ChE, namely butyrylcholinesterase (BChE).[258,263] Test compounds might have bound to BChE instead of AChE, thereby limiting AChE inhibition. Additionally, the enzyme-based assay did not include FCS medium, whereas the cell-based technique required FCS (10%) supplemented medium. High protein concentrations in FCS can bind to test compounds, lowering their free concentrations and therefore reducing their inhibitory potency towards AChE activity.[144,264]

Another important aspect that may be responsible for some differences observed between cell and enzyme-based results, might be metabolic activities present in cells.[144] Cytochrome P450-

2D6, for example, is expressed in SH-SY5Y cells, which metabolises neurotoxic compounds such as 1-methyl-4-phenyl-1,2,3,6-tetrahydropyridine, and β-carbolines.[265] Moreover, SH-SY5Y cells contain dehydrogenases and reductases which could metabolise test compounds, yielding potency differences between cell-based and enzyme-based assay formats.[144,266]

The above-mentioned differences are compound-specific, which is clear from the results reported here for electric eel and human AChE. These results suggest that compounds **A8** and **A73** may specifically and effectively inhibit the electric eel form of AChE instead of the human AChE enzyme. This implies that these compounds (**A8** and **A73**) may not inhibit AChE significantly *in vivo*. The most promising compounds of all the screened compounds were **C53** at the IC_{50} and the combination of donepezil and **C53** at their ¼IC_{50} concentrations and was included in further assessments.

3.7 *In vitro* blood-brain barrier permeability assessment

Brain endothelial cells connected by TJs, play a key role in BBB barrier functioning and integrity.[267,268] Hence *in vitro* modelling of BBB is based on isolating and culturing primary BECs or using immortalised BEC lines.[269] The selection of BEC type (primary vs. Immortalised, and which species) to be used for *in vitro* modelling is critical, since each offers benefits but has limitations.[269] Advantages of immortalised BEC derived from mouse, rat, and human tissues, include; their simplicity of use, expression of tight junction proteins, and other BBB-specific proteins.[269] Furthermore, these cell lines are usable over many passages with higher reproducibility of results, yielding a large number of cells with the same genetic and phenotypical characteristics.[131,270] Thus immortalised BECs are more beneficial and mimic the BBB more closely.[271]

Immortalised BECs cultured on a Transwell insert is the most widely used *in vitro* model to evaluate the BBB endothelial monolayer integrity and permeability using TEER.[271] The TEER measurements constitute a simple, non-invasive method to monitor the barrier integrity of endothelial monoculture cell layers hence it is considered as the “gold standard” method for the measurement of permeability across *in vitro* monolayers.[272,273] In the present study the effect of AChEI active, non-toxic, *in silico* BBB permeable predicted compounds was tested using monolayers of bEnd.5 cells and determination of the TEER using the *in vitro* BBB model.

The TEER measurements across the control monolayers followed a typical profile for bEnd.5 endothelial monolayer with a biphasic response where TEER initially increases to a peak at day

0 to 3, plateaus on day 3 to 4 and then gradually decreases on day 5 to 6.[274] Peak TEER responses on days 3 and 4 were compared to bEnd.5 monolayers exposed to selected concentrations of the compounds (IC_{50} and $1.5\times IC_{50}$). All compounds, apart from **A8**, increased TEER, suggesting a decrease or tightening in the permeability across the BEC monolayer over the 48 h period (Figure 26).

After 12 h of exposure, neither donepezil, **A8**, **A73**, or the combination of donepezil and **C53** at both concentrations (IC_{50} and $1.5\times IC_{50}$) displayed any significant difference in TEER values when compared to the negative control, whereas compound **C53** significantly increased ($p < 0.001$) the endothelial resistance at $1.5\times IC_{50}$ (Figure 26). After 24 h, donepezil (IC_{50}) together with compound **A73**, **C53**, as well as the combination of donepezil and **C53**, slightly increased TEER at both concentrations (IC_{50} and $1.5\times IC_{50}$).

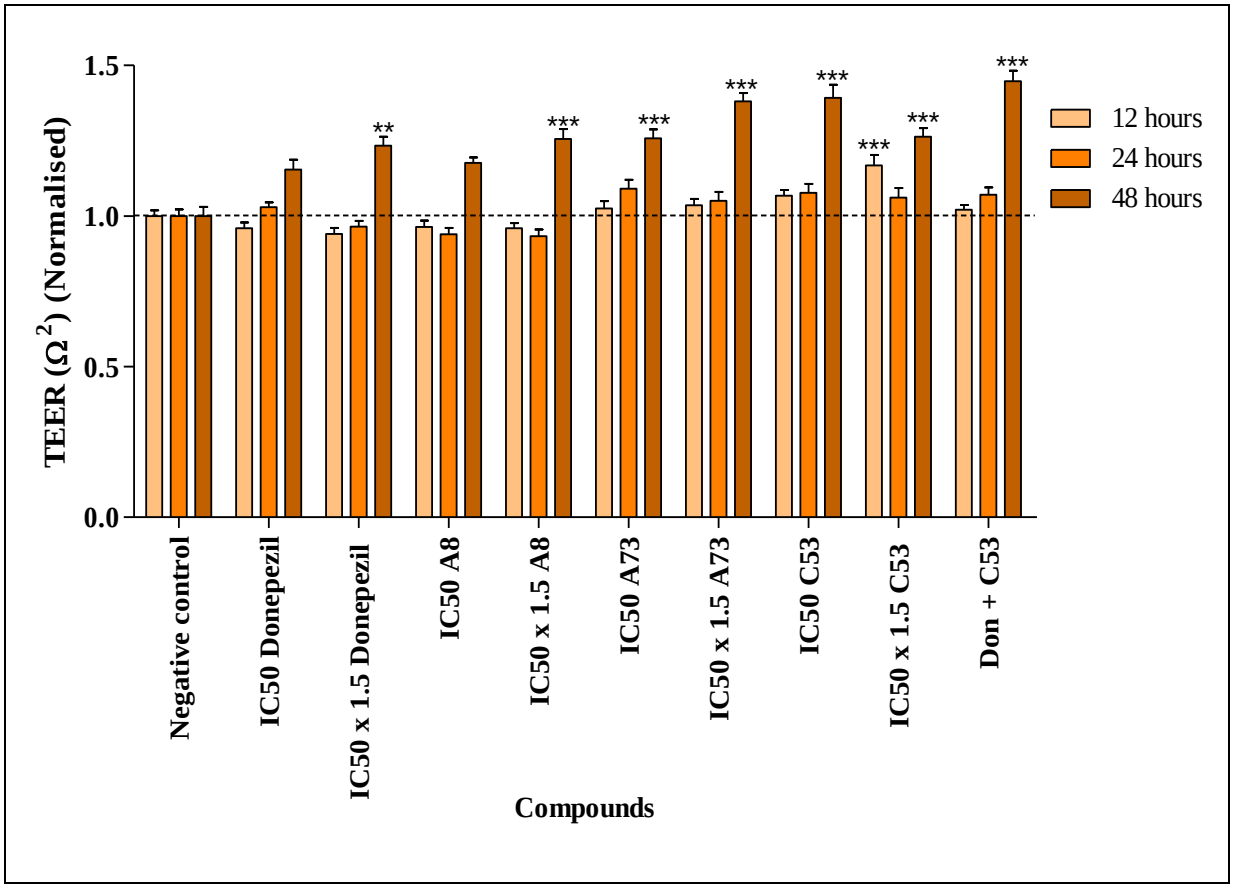

Figure 26: A graphical representation of the effect of acetylcholinesterase inhibitors, *in silico* blood-brain barrier predicted and non-cytotoxic compounds on bEnd5 permeability upon 12 h, 24 h, and 48 h treatment. IC_{50}: concentration resulting in 50% inhibition. The significance of changes relative to the negative control is indicated as ** $p < 0.01$, *** $p < 0.001$

As presented in Figure 26, **A73** (IC_{50} and $1.5\times IC_{50}$), **C53** (IC_{50} and $1.5\times IC_{50}$), and the combination of donepezil and **C53** showed a constant increase in TEER after 24 h and significantly increased ($p < 0.001$) after 48 h. Interestingly, donepezil and **A8** at $1.5\times IC_{50}$ also significantly ($p < 0.01$ and $p < 0.001$, respectively) elevated TEER of bEnd.5 monolayers after 48 h exposure. Based on the results observed, initial treatment (12 - 24 h) of monolayer cells with these compounds didn't display any significant effect, with the TEER being indicative of no effect on the BBB integrity. Following 48 h exposure, increased TEER was observed, and this suggests that all the compounds including the combination, decreased BBB permeability.

This may be ascribed to bEnd.5 cells indicating adaptation to the presence of the compounds. Alternatively, treatment with these compounds might have led to endogenous antioxidant production and TJs proteins which stimulated decreased permeability in the bEnd.5 cells.[275–278] It is known that improved BBB integrity might be brought about by down-regulating multiple pro-inflammatory genes, such as cytokines, enzymes, and adhesion molecules.[279–281]

High TEER values indicate restricted ionic transport through the BBB and optimal barrier function.[282] Furthermore, the higher TEER observed might suppress polar and ionic substances from entering the brain.[283] Although TEER measures both solute permeability and TEER transport across the BBB, it is negatively correlated and tend to be difficult to translate to a functional estimate of tightness.[270,282] Tightness of the endothelial monolayer depends both on the integrity of the tight junction complexes and on the size of the compound of interest.[270]

Validation of functional tightness can be performed by permeability studies with hydrophilic tracer molecules such as Lucifer yellow (444 g/mol), sodium fluorescein (376 g/mol), sucrose (342g/mol), or mannitol (180 g/mol).[270] TEER correlates with permeability for a given small hydrophilic molecule, but the correlation depends strongly on the size of the molecule and the experimental design (shaking/no shaking, change of medium, sampling during the experiment, single point estimation/steady state calculations). Thus, the optimal characterisation of paracellular permeability should include both TEER and tracer flux.[270] In this study compound transport and permeability was further evaluated by detecting the compounds in the basolateral chamber using UPLC-MS.

After 24 h treatment of the bEnd.5 monolayer cells with the compounds of interest, apical and basolateral medium were collected and subjected to UPLC-MS analysis to determine the *in vitro* BBB permeation potential of the compounds. All compounds at both concentrations (IC_{50}

and 1.5×IC_{50}) displayed peaks in both the apical and basolateral chambers (Appendix V). As for the combination of donepezil and **C53** at their ¼IC_{50s}, two peaks were detected in both chambers comparable to those of their respective individual compounds (Figure 27).

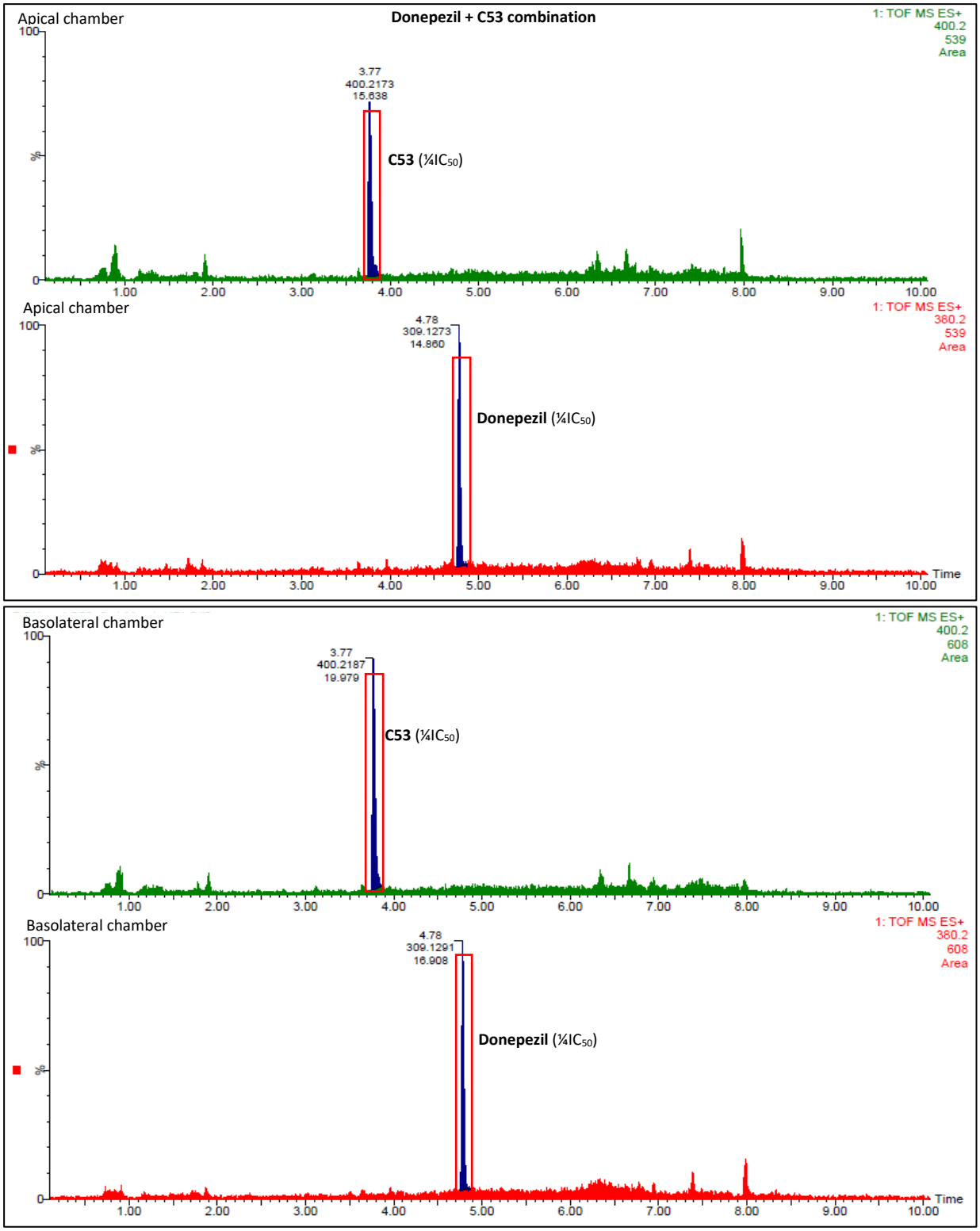

Figure 27: The positive electrospray ionisation chromatograms for the combination of donepezil and **C53**. IC_{50}: concentration resulting in 50% inhibition.

The latter results indicate the presence of all compounds including the combination in the basolateral chamber of the Transwell *in vitro* BBB model. This further suggests that these compounds were able to penetrate and cross the *in vitro* BBB monolayer. These results support and confirm the *in silico* BBB permeability prediction results described in Section 3.2 (page 40). However, as quantification of these compounds in the basolateral chamber were not determined, no inference to the ease and completeness of permeation can be done.

As much as these compounds were able to permeate the *in vitro* BBB monolayer, all compounds including the combination, also decreased the BBB monolayer permeability (as shown by the increased TEER) over 48 h of treatment. As mentioned above, barrier function and tight integrity of the BBB is primarily a result of TJs between adjacent BECs. However, as a consequence of the presence of these TJs, paracellular passive diffusion (between the BECs) of polar compounds is almost impossible.[284] With this said, the observed *in vitro* BBB permeation of the study compounds might be through transcellular passive diffusion (through the BECs). Transcellular passive diffusion also known as lipophilic pathway allows small, lipophilic compounds to passively permeate across the BBB through the BECs directly.[285] This pathway is commonly used for BBB transport and has been considered as the main route.[285,286]

The ability of compounds to passively (diffusion by concentration differences across the cell membrane) cross the BBB depends on the MW, charge (hydrogen bonding capabilities) and drug lipophilicity (log P).[287,288] The use of the log P as a reliable index of BBB transport of lipid-soluble small molecules has been shown to be valid only when the MW of a compound is less than a threshold of approximately 400-600 Da.[287,289] Furthermore, the less the degree of hydrogen bonding with water (less than 10 hydrogen bonds), the greater the possibility of partitioning of the compounds to the membrane.[287,290]

This study is in agreement with the reported literature mentioned above. Reflecting back to the *in silico* pharmacokinetics predictions (Section 3.2; page 40), the study compounds were predicted to have MWs in the range of 373,43 and 459,59 Da with WLogP of less than 5 and less than 10 hydrogen bonds. It is also worth mentioning that MWs of these compounds correlated with those detected by UPLC-MS (Appendix V). Therefore, the observed results, both *in silico* and *in vitro*, infer that these compounds permeated the *in vitro* BBB monolayer via transcellular passive diffusion.

Although these small, lipophilic and uncharged compounds diffused through the BBB membrane, their brain uptake is often restricted by active efflux transporters such as P-gp.[284] P-

glycoprotein is highly expressed at the apical membrane of the BECs and accounts for the poor BBB permeability for certain drugs by pumping them actively back into the blood.[284,287] Amongst the screened compounds, **A8** was the only compound predicted to be P-gp substrate (refer to Table 7).

This suggests that as much as **A8** might permeate into the BBB membrane, absorption may be compromised as it may be effluxed, leading to decreased bioavailability and therapeutic effectiveness. However, this is contradictory to the observed results as this compound was detected in the basolateral chamber by the UPLC-MS indicating its permeation and presence (Appendix V, Figure 29). Further studies such as detecting the presence of P-gp expression genes might assist in conforming the P-gp functions in the BECs used for this study.

Even though the *in vitro* BBB monolayer system cannot fully emulate the ionic transport and permeability,[282] the supporting *in silico* results together with *in vitro* data confirms that the single compounds and combination reduced BBB permeability and are BBB permeable. With this said, these compounds and the combination can be assessed further as potential treatment.

Chapter 4: Conclusion

The search for curative treatments for AD has long been and is still a priority with AChE enzyme as the primary target. An overall attrition rate of more than 95% has been noted for novel drugs targeting neurodegenerative diseases, and this is mainly due to a lack of efficacy, BBB permeability, multifactorial nature and/or toxicity. This reinforces the rationale for assessing a broad spectrum of effects of pharmacophores that show potential for therapeutic use at a preclinical level to reduce the high attrition rate. The aim of the study was to identify novel pharmacophores with the potential to be developed further as treatments for AD.

In vitro screening of 1,453 synthetic compounds, belonging to three subsets, was undertaken to determine AChEI activity using the optimised in-house miniaturised Ellman's assay. Subset **A** and **C** possessed six compounds each with AChEI activity ≥ 60% and IC_{50}'s ranging from 0.2 to 16.68 µM. All the compounds had a donepezil-like scaffold, benzo-fused heterocycle, except for compound **A8**, with a unique structure. Of the 12 active compounds identified, only five were predicted to be BBB-permeable (excluding **A51**) and of the five compounds, two, **A8** and **A136**, were found to be P-gp substrates which might lead to reduced bioavailability. Furthermore, two *in silico* BBB-permeable predicted compounds, **A136** and **C129**, were found to possess noteworthy cytotoxicity. Due to the cytotoxicity observed, these compounds were considered therapeutically unsuitable and are not recommended for further investigation.

The combination of donepezil and **C53** at their ¼ IC_{50}s indicated the most prominent synergistic effect. Three non-cytotoxic compounds and the synergistic combination were further assessed for cytotoxicity and found to be non-toxic at the concentrations tested in bEnd.5 cells. No decomposition was observed for the active *in silico* BBB permeable non-toxic compounds, indicating these compounds were stable. A non-competitive mode of inhibition was noted for compound, **A8**, whereas compounds **A73** and **C53**, as well as donepezil, were found to be mixed inhibitors. This suggests that these compounds might bind simultaneously to the CAS and PAS active sites of AChE.

Even though compounds **A8** and **A73** had no effect on the bEnd.5 monolayer cells, possibly due to the low *in situ* AChEI activity, they might not inhibit AChE efficiently *in vivo*. All compounds increased TEER which indicated decreased BBB permeability of the bEnd.5 monolayer over a period of 48 h. All compounds were detected in the basolateral chamber of the *in vitro* BBB model, suggesting that these compounds including the combination have

permeated the BBB monolayer. Compound **C53** as monotherapy and as synergistic combination with donepezil, appears to be most promising for further investigation, given the noteworthy acellular and cellular AChEI activity, *in silico* BBB-permeability, absence of cytotoxicity in both cell lines and their ability to cross the *in vitro* BBB monolayer.

Chapter 5: Limitations and future recommendations

The initial objective of this study was to optimise and validate the miniaturised AChE assay on an automated liquid handler to conduct high-throughput screening. Due to time and unforeseen instrumental downtime, selected compounds were screened manually. As future work, it is recommended that a liquid handler at the CSIR used for fast primary screening of compounds. Furthermore, comparison between the manual and automated screening should be done using relevant controls to ascertain whether validity is maintained.

In silico testing was used to predict the BBB permeability of the AChE active compounds and the most potent compound was predicted to be non-BBB permeable. Due to this, the compound was excluded from further investigation. Even though this was an excellent example of what happens in CNS drug discovery and development process, more than one *in silico* method (such as parallel artificial membrane permeability assays and machine learning methods) should be used in future to confirm BBB predictive results. Furthermore, structure modification studies are required for this potent compound to be investigated further as it might be a promising hit.

Even though kinetic results and supporting literature suggests the binding sites of the active compounds, additional molecular docking studies need to be carried out to confirm the exact binding sites. These studies will further give an insight as to which substituents and moieties bind to the enzyme and confer to the activity observed. Furthermore, molecular docking together with screening of more libraries of similar analogue compounds might assist to identify which group within a scaffold is responsible for toxicity observed.

Transendothetial electrical resistance results suggested that these compounds tightened or improved BBB integrity and as mentioned above, this might have been through broad spectrum of aspects such as down-regulating multiple inflammatory genes, the ability to enhance antioxidant production and functioning of TJs. Based on these reported possibilities, antioxidant assays, determination of the expression of TJs proteins and inflammatory genes need to be carried out for confirmation. The *in vitro* BBB co-culture of bEnd.5 and SH-SHSY cells was not feasible due to time constraints. This should be setup in future to determine whether the AChEI activity observed *in situ* is similar to that after the compounds penetrate through the bEnd.5 monolayer.

Additionally, undifferentiated neuroblastoma cells lacking mature neuronal markers were used in this study, requiring a high cell density to produce sufficient AChE enzyme. Further

investigation *in vivo* or using differentiated cells which have the ability to reflect a mature neuron-like phenotype with the expression of neuronal markers, is required to confirm these findings. With all the compounds being detected in the basolateral chamber of the *in vitro* BBB model, quantitative studies should be performed to determine how much of the compound is available. Currently, no information is available on how much of the sample was lost during preparation, which impacts on the interpretation of results.

The selected compounds were only screened for one target (AChE enzyme) in this study, and it is reported that AChEIs might have the ability to further inhibit Aβ plaques and NFTs. These or other compounds from the same library should further be screened against other AD targets and be used as multi-target modulators.

Due to time, costs and the scope of the current study, UPLC-MS was only used to detect the presence and to confirm the compounds' *in vitro* BBB permeation. No qualitative or validation studies were done. Furthermore, given the small samples size and lack of validation, quantification could not be done. It is therefore recommended for future studies to include and conduct the above-mentioned as they will assist to determine any matrix effects (such as quenching or binding to the compounds) on the compounds as well as compound concentrations in basolateral chamber.

References

1. Xu W, Ferrari C and Wang HX. Epidemiology of Alzheimer's Disease.2013. Available from: http://dx.doi.org/10.5772/54398. (Accessed: 21 April 2023).

2. Alzheimer's Association. Alzheimer's disease facts and figures. Alzheimer's and Dementia.2018; 14:367-429.

3. World Health Organization. global action plan on the public health response to dementia.2017. Available from: http://apps.who.int/bookorders. (Accessed: 25 April 2023).

4. Cao Q, Tan CC, Xu W, Hu H, Cao XP, Dong Q, Tan L and Yu JT. The prevalence of dementia: A systematic review and meta-analysis. Journal of Alzheimer's Disease. 2020; 73:1157–1166.

5. Awasthi M, Singh S, Pandey VP and Dwivedi UN. Alzheimer's disease: An overview of amyloid beta dependent pathogenesis and its therapeutic implications along with in silico approaches emphasizing the role of natural products. Journal of the Neurological Sciences. 2016; 361:256–271.

6. World Alzheimer Report. The state of the art of dementia research: New frontiers. Alzheimer's Disease International. 2018. Available from: www.alz.co.uk. (Accessed: 30 April 2023).

7. Bondi MW, Edmonds EC and Salmon DP. Alzheimer's Disease: Past, present, and future. Journal of the International Neuropsychological Society. 2017; 23:818–831.

8. Cummings J, Lee G, Ritter A and Zhong K. Alzheimer's disease drug development pipeline: 2018. Alzheimer's & Dementia: Translational Research & Clinical Interventions. 2018; 4:195–214.

9. Kuo YC and Rajesh R. A critical overview of therapeutic strategy and advancement for Alzheimer's disease treatment. Journal of the Taiwan Institute of Chemical Engineers. 2017; 77:92–105.

10. World Alzheimer Report 2021: Journey through the diagnosis of dementia. Alzheimer's Disease International. 2021. Available from: www.alz.co.uk. (Accessed: 30 April 2023).

11. Vaz M and Silvestre S. Alzheimer's disease: Recent treatment strategies. European Journal of Pharmacology. 2020; 887:173554.

12. Alzheimer's Association. Alzheimer's disease facts and figures. Alzheimer's and Dementia. 2022; 18:700–789.

13. Alzheimer's Association. Alzheimer's disease facts and figures. Alzheimer's and Dementia. 2020; 16:391–460.

14. Mubangizi V, Maling S, Obua C and Tsai AC. Prevalence and correlates of Alzheimer's disease and related dementias in rural Uganda: Cross-sectional, population-based study. BMC Geriatrics. 2020; 20:48.

15. de Jager CA, Joska JA, Hoffman M, Borochowitz KE and Combrinck MI. Dementia in rural South Africa: A pressing need for epidemiological studies. South African Medical Journal. 2015; 105:189-190.

16. de Jager CA, Msemburi W, Pepper K and Combrinck MI. Dementia prevalence in a rural region of South Africa: A cross-sectional community study. Journal of Alzheimer's Disease. 2017; 60:1087–1096.

17. World Alzheimer report 2016: Improving healthcare for people living with dementia. Alzheimer's Disease International. 2016: Available from: www.alz.co.uk. (Accessed: 27 April 2023).

18. Meyer JC, Harirari P and Schellack N. Overview of Alzheimer's disease and its management. South African Pharmaceutical Journal.2016; 83:48-56.

19. Guerchet M, Mayston R, Lloyd-Sherlock P, Prince M, Aboderin I, Akinyemi R, Paddick S-M, Wimo A, Amoakoh-Coleman M, Uwakwe R and Ezeah P. Dementia in sub-Saharan Africa: Challenges and opportunities; [Internet].2017; 70. Available from: www.leahbeach.com. (Accessed: 25 April 2023).

20. Olayinka O, Olayinka OO, Alemu BT, Akpinar-Elci M and Grossberg GT. Toxic environmental risk factors for Alzheimer's Disease: A systematic review. Aging Medicine and Healthcare. 2019; 10:4–17.

21. Rivers-Auty J, Mather AE, Peters R, Lawrence CB and Brough D. Anti-inflammatories in Alzheimer's disease-potential therapy or spurious correlate? Brain Community. 2020; 2.

22. Cummings JL, Tong G and Ballard C. Treatment combinations for Alzheimer's disease: Current and future pharmacotherapy options. Journal of Alzheimer's Disease. 2019; 67:779–794.

23. Revadigar V, Ghalib RM, Murugaiyah V, Embaby MA, Jawad A, Mehdi SH, Hashim R and Sulaiman O. Enzyme inhibitors involved in the treatment of Alzheimer's Disease. In: Drug Design and Discovery in Alzheimer's Disease. Elsevier, United Kingdom. 2014; 142–198.

24. Bachurin SO, Bovina E and Ustyugov AA. Drugs in clinical trials for Alzheimer's Disease: The major trends. Medicinal Research Reviews. 2017; 37:1186–1225.

25. Bomasang-Layno E and Bronsther R. Diagnosis and treatment of Alzheimer's Disease: Delaware Journal of Public Health. 2021; 7:74–85.

26. dos Santos Picanco LC, Ozela PF, de Fatima de Brito Brito M, Pinheiro AA, Padilha EC, Braga FS, de Paula da Silva CHT, dos Santos CBR, Rosa JMC and da Silva Hage-Melim LI. Alzheimer's disease: A review from the pathophysiology to diagnosis, new perspectives for pharmacological treatment. Current Medicinal Chemistry. 2018; 25:3141–3159.

27. Choi SH, Kim YH, D'Avanzo C, Aronson J, Tanzi RE, Kim DY. Recapitulating amyloid β and tau pathology in human neural cell culture models - clinical implications. Neurology. 2015; 11:102.

28. Breijyeh Z and Karaman R. Comprehensive Review on Alzheimer's Disease: Causes and treatment. Molecules. 2020; 25:5789.

29. Bhushan I, Kour M, Kour G, Gupta S, Sharma S and Yadav A. Alzheimer's disease: Causes & treatment-A review. Annals of Biotechnology.2018; 1:1002.

30. Kinney JW, Bemiller SM, Murtishaw AS, Leisgang AM, Salazar AM and Lamb BT. Inflammation as a central mechanism in Alzheimer's disease. Alzheimer's & Dementia: Translational Research & Clinical Interventions. 2018; 4:575–90.

31. Li Q, He S, Chen Y, Feng F, Qu W and Sun H. Donepezil-based multi-functional cholinesterase inhibitors for treatment of Alzheimer's disease. European Journal of Medicinal Chemistry. 2018; 158:463–477.

32. De-Paula VJ, Radanovic M, Diniz BS and Forlenza O. Alzheimer's Disease. In: Harris, J. (eds) protein aggregation and fibrillogenesis in cerebral and systemic amyloid disease. Subcellular Biochemistry. Springer, Dordrecht. 2012. 62. Available from: https://doi.org/10.1007/978-94-007-5416-4_14. (Accessed: 10 June 2023).

33. Mintun MA, Lo AC, Duggan Evans C, Wessels AM, Ardayfio PA, Andersen SW, Shcherbinin S, Sparks J, Sims JR, Brys M, Apostolova LG, Salloway SP and Skovronsky DM. Donanemab in early Alzheimer's disease. New England Journal of Medicine. 2021; 384:1691–1704.

34. Tiwari S, Atluri V, Kaushik A, Yndart A and Nair M. Alzheimer's disease: Pathogenesis, diagnostics, and therapeutics. International Journal of Nanomedicine. 2019:14: 5541-5554.

35. Folch J, Petrov D, Ettcheto M, Abad S, Sánchez-López E, García ML, Olloquequi J, Beas-Zarate C, Auladell C and Camins A. Current research therapeutic strategies for Alzheimer's disease. Treatment Neural Plasticity. 2016; 2016:1–15.

36. van Oostveen WM and de Lange ECM. Imaging techniques in Alzheimer's disease: A review of applications in early diagnosis and longitudinal monitoring. International Journal of Molecular Sciences 2021; 22:2110.

37. de Oliveira AS and Machado AL. The multifunctional therapeutic approach to treatment of Alzheimer's disease: Molecular bases, pharmacology and perspectives in medicinal chemistry. American Journal of Biomedical Science & Research: 2019; 3:453–459.

38. Mendiola-Precoma J, Berumen LC, Padilla K and Garcia-Alcocer G. Therapies for prevention and treatment of Alzheimer's disease. Biomed Research International. 2016; 2016:1–17.

39. Declercq LD, Vandenberghe R, Van Laere K, Verbruggen A and Bormans G. Drug development in Alzheimer's disease: The contribution of PET and SPECT. Frontiers in Pharmacology. 2016; 7:88.

40. Kulshreshtha A and Piplani P. Current pharmacotherapy and putative disease-modifying therapy for Alzheimer's disease. Neurological Sciences. 2016; 37:1403–1435.

41. Francis PT, Parsons CG and Jones RW. Rationale for combining glutamatergic and cholinergic approaches in the symptomatic treatment of Alzheimer's disease. Expert Review of Neurotherapeutics. 2012; 12:1351–1365.

42. Liu J, Chang L, Song Y, Li H and Wu Y. The Role of NMDA Receptors in Alzheimer's Disease. Frontiers in Neuroscience. 2019;13: 43.

43. Sanabria-Castro A, Alvarado-Echeverría I and Monge-Bonilla C. Molecular pathogenesis of Alzheimer's Disease: An update. Annals of Neurosciences. 2017; 24:46–54.

44. Grossberg GT, Tong G, Burke AD and Tariot PN. Present algorithms and Future treatments for Alzheimer's Disease. Journal of Alzheimer's Disease. 2019; 67:1157–1171.

45. Danysz W and Parsons CG. Alzheimer's disease, β-amyloid, glutamate, NMDA receptors and memantine - searching for the connections. British Journal of Pharmacology 2012; 167:324–352.

46. Scheltens P, Blennow K, Breteler MMB, de Strooper B, Frisoni GB, Salloway S and Van der Flier WM. Alzheimer's disease. Lancet Seminar. 2016; 388:505–517.

47. Sun Q, Xie N, Tang B, Li R and Shen Y. Alzheimer's Disease: From genetic variants to the distinct pathological mechanisms. Frontiers in Molecular Neuroscience. 2017; 10: 319.

48. Sacuiu SF. Dementias. In: Handbook of clinical neurology (3rd ed). Neuroepidemiology. 2016: 123–151.

49. Serrano-Pozo A and Growdon JH. Is Alzheimer's Disease risk modifiable? Journal of Alzheimer's Disease. 2019; 67:795–819.

50. Cano A, Turowski P, Ettcheto M, Duskey JT, Tosi G, Sánchez-López E, García ML, Camins A, Souto EB, Ruiz A, Marquié M and Boada M. Nanomedicine-based technologies and novel biomarkers for the diagnosis and treatment of Alzheimer's disease: From current to future challenges. Journal of Nanobiotechnologica. 2021; 19:122.

51. DeTure MA and Dickson DW. The neuropathological diagnosis of Alzheimer's disease. Molecular Neurodegeneration. 2019; 14:32.

52. Drummond E and Wisniewski T. Alzheimer's disease: experimental models and reality. Acta Neuropathologica. 2017; 133:155–175.

53. Bhagya SR and Sheshadri HS. Diagnosis of Alzheimer's disease using Naive Bayesian Classifier. Neural Computational Application. 2018; 29:123–132.

54. Birks JS and Harvey RJ. Donepezil for dementia due to Alzheimer's disease. Cochrane Database of Systematic Reviews. 2018; 6:1-349.

55. Mukhopadhyay S and Banerjee D. A primer on the evolution of aducanumab: The first antibody approved for treatment of Alzheimer's disease. Journal of Alzheimer's Disease. 2021; 83:1537–1552.

56. Pais M, Martinez L, Ribeiro O, Loureiro J, Fernandez R, Valiengo L, Canineu P, Stella F, Talib L, Radanovic M and Forlenza OV. Early diagnosis and treatment of Alzheimer's disease: new definitions and challenges. Brazilian Journal of Psychiatry. 2020; 42:431–441.

57. Bortolami M, Rocco D, Messore A, di Santo R, Costi R, Madia VN, Scipione L and Pandolfi F. Acetylcholinesterase inhibitors for the treatment of Alzheimer's disease - a patent review (2016–present). Expert Opinion on Therapeutic Patents. 2021; 31:399–420.

58. Carvalho KM, Winter E and Souza Antunes AM de. Analysis of technological developments in the treatment of Alzheimer's disease through patent documents. Intelligent Information Management. 2015; 07:268–281.

59. Kumar A, Singh A, Ekavali. A review on Alzheimer's disease pathophysiology and its management: an update. Pharmacological Reports. 2015; 67:195–203.

60. Waite L. Treatment for Alzheimer's disease: has anything changed? Australian Prescriber. 2015; 38:60–63.

61. Giacobini E. Cholinesterase inhibitors: New roles and therapeutic alternatives. Pharmacological Research. 2004; 50:433–440.

62. Anand P, Singh B and Singh N. A review on coumarins as acetylcholinesterase inhibitors for Alzheimer's disease. Bioorganic & Medicinal Chemistry. 2012; 20:1175–1180.

63. MacDonald S and Caspar G. Clinical features and multidisciplinary approaches to dementia care. Journal of Multidisciplinary Healthcare. 2011; 125.

64. Das B, Dasgupta S and Ray S. Potential therapeutic roles of retinoids for prevention of neuroinflammation and neurodegeneration in Alzheimer's disease. Neural Regeneration Research. 2019; 14:1880.

65. Alvarez XA, Cacabelos R, Sampedro C, Couceiro V, Aleixandre M, Vargas M, Linares C, Granizo E, García-Fantini M, Baurecht W, Doppler E and Moessler H. Combination treatment in Alzheimer's disease: results of a randomized, controlled trial with cerebrolysin and donepezil. Current Alzheimer Research. 2011; 8:583–591.

66. Molinuevo JL, Ayton S, Batrla R, Bednar MM, Bittner T, Cummings J, Fagan AM, Hampel H, Mielke MM, Mikulskis A and O'bryant S. Current state of Alzheimer's fluid biomarkers. Acta Neuropathologica. 2018; 136:821-853.

67. Patel L and Grossberg GT. Combination therapy for Alzheimer's disease. Drugs Aging. 2011; 28:539–546.

68. Dunn B, Stein P and Cavazzoni P. Approval of Aducanumab for Alzheimer disease-The FDA's perspective. JAMA Internal Medicine. 2021; 181:1276.

69. Riederer F. Donanemab in early Alzheimer's disease. Journal fur Neurologie, Neurochirurgie und Psychiatrie. 2021; 22:142–143.

70. Yang P and Sun F. Aducanumab: The first targeted Alzheimer's therapy. Drug Discoveries Therapeutics. 2021; 15: 01061.

71. Padd IS and Parmar M. Aducanumab. In: StatPearls [Internet] Treasure Island (FL): StatPearls Publishing.2022. Available from: https://www.ncbi.nlm.nih.gov/books/NBK573062/.2022. (Accessed: 29 April 2023).

72. Corbett A. Gareth Williams G and Clive Ballard C. Drug repositioning in Alzheimer's disease. Frontiers in Bioscience, Schola. 2015; 7:432.

73. Shukla AA. High throughput screening of small molecule library: Procedure, challenges and future. Cancer Prevention & Current Research. 2016; 5:00154.

74. Feher M and Schmidt JM. Property Distributions: Property distributions: Differences between drugs, natural products, and molecules from combinatorial chemistry. Journal for Chemical Information and Computer sciences. 2003; 43:218–27.

75. Alamgir ANM. Drugs: heir natural, synthetic, and biosynthetic sources. Progress in Drug Research. 2017: 105–23.

76. Katiyar C, Kanjilal S, Gupta A and Katiyar S. Drug discovery from plant sources: An integrated approach. An International Quarterly Journal of Research in Ayurveda. 2012; 33:10.

77. Najmi A, Javed SA, Bratty M and Alhazmi HA. Modern approaches in the discovery and development of plant-based natural products and their analogues as potential therapeutic agents. Molecules. 2022; 27:349.

78. Tyagi M, Begnini F, Poongavanam V, Doak BC and Kihlberg J. Drug syntheses beyond the rule of 5. Chemistry - A European Journal. Wiley-VCH Verlag. 2020: 49–88.

79. Ulrich-Merzenich GS. Combination screening of synthetic drugs and plant derived natural products: Potential and challenges for drug development. Synergy Forum, Switzerland. Elsevier. 2014; 1:59–69.

80. Mathur S and Hoskins C. Drug development: Lessons from nature. Biomedical Report. 2017; 6:612–614.

81. Tcherniuk SO, Chesnokova O, Oleinikov I v., Potopalsky AI and Oleinikov A. Anti-malarial effect of semi-synthetic drug amitozyn. Malaria Journal. 2015; 14:1-10.

82. Rao VS and Srinivas K. Modern drug discovery process: An in silico approach. Journal of Bioinformatics and Sequence Analysis. 2011; 3:89-94.

83. Duelen R, Corvelyn M, Tortorella I, Leonardi L, Chai YC and Sampaolesi M. Medicinal biotechnology for disease modeling, clinical therapy, and drug discovery and development. In book: Introduction to Biotech Entrepreneurship: From Idea to Business. Cham: Springer International Publishing, Switzerland. 2019: 89–128.

84. Deore AB, Dhumane JR, Wagh R and Sonawane R. The sages of drug discovery and development process. Asian Journal of Pharmaceutical Research and Development. 2019; 7:62–67.

85. Prakash N and Devangi P. Drug Discovery. Journal of Antivirals & Antiretrovirals. 2010; 2:63-68.

86. Arora A, Nain P, Kumari R and Kaur J. Major causes associated with clinical trials failure and selective strategies to reduce these consequences: A review. Archives Of Pharmacy Practice. 2021; 12:45–53.

87. Yamaguchi S, Kaneko M and Narukawa M. Approval success rates of drug candidates based on target, action, modality, application, and their combinations. Clinical and Translational Science. 2021; 14:1113–1122.

88. Phatak SS, Stephan CC, Cavasotto CN. High-throughput and in silico screenings in drug discovery. Expert Opinion on Drug Discovery. 2009; 4:947–959.

89. Zang R, Li D, Tang IC, Wang J and Yang ST. Cell-based assays in high-throughput screening for drug discovery. International Journal of Biotechnology for Wellness Industries.2012; 1:31.

90. Poddar KM, Chakraborty A and Banerjee S. Neurodegeneration: Diagnosis, prevention, and therapy. In: Oxidoreductase. IntechOpen, United Kingdom. 2021. Available from: http://dx.doi.org/10.5772/intechopen.94950. (Accessed: 20 June 2023).

91. Schneider LS, Mangialasche F, Andreasen N, Feldman H, Giacobini E, Jones R, Mantua V, Mecocci P, Pani L, Winblad B and Kivipelto M. Clinical trials and late-stage drug development for Alzheimer's disease: An appraisal from 1984 to 2014. Journal of Internal Medicine. 2014; 275:251–283.

92. Gribkoff VK and Kaczmarek LK. The need for new approaches in CNS drug discovery: Why drugs have failed, and what can be done to improve outcomes. Neuropharmacology. 2017; 120:11–19.

93. Wilhelm I and Krizbai IA. In vitro models of the blood-brain barrier for the study of drug delivery to the brain. Molecular Pharmaceutics. 2014; 11:1949–1963.

94. Hingorani AD, Kuan V, Finan C, Kruger FA, Gaulton A, Chopade S, Sofat R, Macallister RJ, Overington JP, Hemingway H, Denaxas S, Prieto D and Casas JP. Improving the odds of drug development success through human genomics: modelling study. Scientific Reports. 2019; 9:18911.

95. Miao R, Xia LY, Chen HH, Huang HH and Liang Y. Improved classification of blood-brain-barrier drugs using deep learning. Scientific Reports. 2019; 9:8802.

96. Schuster D, Laggner C and Langer T. Why drugs fail - A study on side effects in new chemical entities. Current Pharmaceutical Design. 2005; 11:3545–3559.

97. Berg L, Andersson CD, Artursson E, Hörnberg A, Tunemalm AK and Linusson A. Targeting Acetylcholinesterase: Identification of chemical leads by high throughput screening, structure determination and molecular modeling. PLoS One. 2011; 6:26039.

98. Herskovits AZ, Locascio JJ, Peskind ER, Li G and Hyman BT. A luminex assay detects amyloid β oligomers in Alzheimer's disease cerebrospinal fluid. PLoS One. 2013; 8:67898.

99. McKoy AF, Chen J, Schupbach T and Hecht MH. novel inhibitor of amyloid β (aβ) peptide aggregation: From high throughput screening to efficacy in an animal model of Alzheimer disease. Journal of Biological Chemistry. 2012; 287:38992–9000.

100. Langhans SA. Three-dimensional in vitro cell culture models in drug discovery and drug repositioning. Frontiers in Pharmacology.2018; 9.

101. Cavalcante S, Kitagawa D, Rodrigues R, Cardozo M, Paula R, Correa AB and Simas A. Straightforward, economical procedures for microscale ellman's test for cholinesterase inhibition and reactivation. Química Nova. 2018. doi: 10.21577/0100-4042.20170278.

102. Huang L, Jiang Y and Chen Y. Predicting drug combination index and simulating the network-regulation dynamics by mathematical modeling of drug-targeted EGFR-ERK signaling pathway. Scientific Reports. 2017; 7:40752.

103. Gayvert KM, Aly O, Platt J, Bosenberg MW, Stern DF and Elemento O. A computational approach for identifying synergistic drug combinations. PLoS Computational Biology.2017; 13:1005308.

104. Binderup ML, Dalgaard M, Dragsted LO, Hossaini A, Ladefoged O, Lam HR, Larsen JC, Madsen C, Meyer OA, Rasmussen ES and Reffstrup TK. Combined actions and interactions of chemicals in mixtures: the toxicological effects of exposure to mixtures of industrial and environmental chemicals. National Food Institute. 2003; 12: 1- 158.

105. Walker AL, Imam SZ and Roberts RA. Drug discovery and development: Biomarkers of neurotoxicity and neurodegeneration. Experimental Biology and Medicine. 2018; 243:1037–1045.

106. Dougall IG and Unitt J. Evaluation of the biological activity of compounds: Techniques and mechanism of action studies. In The Practice of Medicinal Chemistry. Walters I (edr), Elsevier, United Kingdom. 2015; 15–43.

107. Ruiz-Garcia A, Bermejo M, Moss A and Casabo VG. Pharmacokinetics in drug discovery. Journal of Pharmaceutical Sciences. 2008; 97:654–690.

108. Aslantürk ÖS. In vitro cytotoxicity and cell viability assays: Principles, advantages, and disadvantages. In: Genotoxicity - A predictable risk to our actual world. InTech. 2018. doi: 10.5772/intechopen.71923.

109. Wu L, Yi H and Yi M. Assessment of arsenic toxicity using Allium/Vicia root tip micronucleus assays Journal of Hazardous Materials. 2010; 176:952–956.

110. Peternel L, Kotnik M, Preželj A and Urleb U. Comparison of 3 cytotoxicity screening assays and their application to the selection of novel antibacterial hits. Journal of Biomolecular Screening 2009; 14:142–150.

111. Bicker J, Alves G, Fortuna A and Falcão A. Blood–brain barrier models and their relevance for a successful development of CNS drug delivery systems: A review. European Journal of Pharmaceutics and Biopharmaceutics. 2014; 87:409–432.

112. Fong CW. Permeability of the Blood–Brain Barrier: Molecular mechanism of transport of drugs and physiologically important compounds. Journal of Membrane Biology. 2015; 248:651–669.

113. Bickel U. How to measure drug transport across the blood-brain barrier. NeuroRx®: The Journal of the American Society for Experimental NeuroTherapeutics. 2005; 2:15–26.

114. Sweeney MD, Zhao Z, Montagne A, Nelson AR, Zlokovic B. Blood-Brain Barrier: From physiology to disease and back. Physiological Reviews. 2019; 99:21–78.

115. Gawdi R, Shumway KR and Emmady PD. Physiology, Blood Brain Barrier. StatPearls. 2022. Available from: https://www.ncbi.nlm.nih.gov/books/NBK557721/. (Accessed: 07 May 2023).

116. Elfakhri KH, Duong QV, Langley C, Depaula A, Mousa YM, Lebeouf T, Cain C and Kaddoumi A. Characterization of hit compounds identified from high-throughput screening for their effect on blood-brain barrier integrity and amyloid-β Clearance: In vitro and in vivo studies. Neuroscience. 2018; 379:269–80.

117. Di L and Kerns EH. Blood-brain barrier in drug discovery optimizing brain exposure of CNS drugs and minimizing brain side effects for peripheral drugs. Hoboken, New Jersey: John Wiley & Sons Inc.: ISBN: 978-1-118-78835-6. 2015.

118. Cockerill I, Oliver JA, Xu H, Fu BM and Zhu D. Blood-brain barrier integrity and clearance of amyloid-β from the BBB. Advances in Experimental Medicine and Biology. 2018; 261–278.

119. Bagchi S, Chhibber T, Lahooti B, Verma A, Borse V and Jayant RD. In-vitro blood-brain barrier models for drug screening and permeation studies: An overview Drug Design, Development and Therapy 2019; 13:3591–3605.

120. Lipinski CA. Drug-like properties and the causes of poor solubility and poor permeability. Journal of Pharmacological and Toxicological Methods. 2000; 44:235–249.

121. Attique S, Hassan M, Usman M, Atif R, Mahboob S, Al-Ghanim K, Bilal M and Nawaz MZ. A molecular docking approach to evaluate the pharmacological properties of natural and synthetic treatment candidates for use against hypertension. International Journal of Environmental Research Public Health. 2019; 16:923.

122. Pardridge WM. Alzheimer's disease drug development and the problem of the blood-brain barrier. Alzheimer's & Dementia. 2009; 5:427–432.

123. Goodwin JT and Clark DE. In silico predictions of blood-brain barrier penetration: considerations to "keep in mind". Journal of Pharmacology and Experimental Therapeutics. 2005; 315:477–483.

124. Mensch J, Oyarzabal J, Mackie C and Augustijns P. In vivo, in vitro and in silico methods for small molecule transfer across the BBB. Journal of Pharmaceutical Sciences. 2009; 98:4429–4468.

125. Osipova ED, Komleva YK, Morgun A, Lopatina OL, Panina YA, Olovyannikova RY, Vais EF, Salmin VV and Salmina AB. Designing in vitro blood-brain barrier models reproducing alterations in brain aging. Frontiers in Aging Neuroscience.2018; 10:234.

126. Vastag M and Keseru GM. Current in vitro and in silico models of blood-brain barrier penetration: A practical view. Current Opinion in Drug Discovery & Development. 2009; 12:115–124.

127. Danon JJ, Reekie TA, Kassiou M. Challenges and opportunities in central nervous system drug discovery. Trends in Chemistry. 2019; 1:612–624.

128. Daina A, Michielin O and Zoete V. SwissADME: a free web tool to evaluate pharmacokinetics, drug-likeness and medicinal chemistry friendliness of small molecules. Scientific Reports. 2017; 7:42717.

129. Daina A and Zoete V. A BOILED-Egg to predict gastrointestinal absorption and brain penetration of small molecules. Medicinal Chemistry. 2016; 11:1117–1121.

130. Chedik L, Mias-Lucquin D, Bruyere A, Fardel O. In silico prediction for intestinal absorption and brain penetration of chemical pesticides in humans. International Journal of Environmental Research Public Health. 2017; 14:708.

131. Appelt-Menzel A, Cubukova A, Günther K, Edenhofer F, Piontek J, Krause G, Stüber T, Walles H, Neuhaus W and Metzger M. Establishment of a human blood-brain barrier co-culture model mimicking the neurovascular unit using induced pluri- and multipotent stem cells. Stem Cell Reports. 2017; 8:894–906.

132. He Y, Yao Y, Tsirka SE, Cao Y. Cell-culture models of the blood-brain barrier. Stroke 2014; 45:2514–2526.

133. Yang S, Mei S, Jin H, Zhu B, Tian Y, Huo J, Cui X, Guo A and Zhao Z. Identification of two immortalized cell lines, ECV304 and bEnd3, for in vitro permeability studies of blood-brain barrier. PLoS One. 2017; 12:0187017.

134. Thomsen MS, Humle N, Hede E, Moos T, Burkhart A and Thomsen LB. The blood-brain barrier studied in vitro across species. PLoS One. 2021; 16:0236770.

135. Felix K, Tobias S, Jan H, Nicolas S and Michael M. Measurements of transepithelial electrical resistance (TEER) are affected by junctional length in immature epithelial monolayers. Histochemistry and Cell Biology. 2021; 156:609–616.

136. Srinivasan B, Kolli AR, Esch MB, Abaci HE, Shuler ML and Hickman JJ. TEER Measurement techniques for in vitro barrier model systems. Journal of Laboratory Automation. SAGE Publications Inc. 2015; 20:107–126.

137. Srinivasan B and Kolli AR. Transepithelial/Transendothelial electrical resistance (TEER) to measure the integrity of blood-brain barrier. Neuromethods. 2019; 142:99–114.

138. Serdar BS, Erkmen T and Koçtürk S. Combinations of polyphenols disaggregate Aβ1 42 by passing through in vitro blood-brain barrier developed by endothelium, astrocyte, and differentiated SH SY5Y cells. Acta Neurobiologiae Experimentalis. 2021; 81 335-349.

139. Fujimoto T, Morofuji Y, Nakagawa S, Kovac A, Horie N, Izumo T, Niwa M,Matsuo T and Banks WA. Comparison of the rate of dedifferentiation with increasing passages among cell sources for an in vitro model of the blood–brain barrier. Journal of Neural Transmission. 2020; 127:1117-1124.

140. Cuanalo-Contreras K and Benkmann D. Towards more human and humane testing: The role of the device supplier industry. Alternatives to Laboratory Animals. 2022; 50:62-70.

141. van der Westhuizen CJ. Discovery of novel acetylcholinesterase inhibitors using an integrated computational and experimental approach. PhD thesis, University of Pretoria. 2020.

142. Ellman GL, Courtney KD, Andres V and Featherstone RM. A new and rapid colorimetric determination of acetylcholinesterase activity. Biochemical Pharmacology.1961; 7:88–95.

143. Eldeen IMS, Elgorashi EE and van Staden J. Antibacterial, anti-inflammatory, anti-cholinesterase and mutagenic effects of extracts obtained from some trees used in South African traditional medicine. Journal of Ethnopharmacology. 2005; 102:457–464.

144. Li S, Huang R, Solomon S, Liu Y, Zhao B, Santillo MF and Xia M. Identification of acetylcholinesterase inhibitors using homogenous cell-based assays in quantitative high-throughput screening platforms. Biotechnology Journal. 2017; 12:1600715.

145. Cao J, Wang M, Yu H, She Y, Cao Z, Ye J, Abd El-Aty AM, Hacımüftüoğlu A, Wang J and Lao S. An overview on the mechanisms and applications of enzyme inhibition-based methods for determination of organophosphate and carbamate pesticides. Journal of Agricultural and Food Chemistry. 2020; 68:7298–7315.

146. Li S, Li AJ, Zhao J, Santillo MF and Xia M. Acetylcholinesterase inhibition assays for high-throughput screening. In: Methods in Molecular Biology. Humana Press Inc.2022; 47–58.

147. Chou TC and Talalay P. Quantitative analysis of dose-effect relationships: the combined effects of multiple drugs or enzyme inhibitors. Advances in Enzyme Regulation.1984; 22:27–55.

148. Vichai V and Kirtikara K. Sulforhodamine B colorimetric assay for cytotoxicity screening. Natural Protocol. 2006; 1:1112–1116.

149. Mentor S and Fisher D. Exosomes form tunneling nanotubes (TUNTs) in the blood-brain barrier: a nano-anatomical perspective of barrier genesis. Frontiers in Molecular Neuroscience.2 022; 15.

150. Ali-Shtayeh MS, Jamous RM, Zaitoun SYA and Qasem IB. In-vitro screening of acetylcholinesterase inhibitory activity of extracts from Palestinian indigenous flora in relation to the treatment of Alzheimer's disease. Functional Foods in Health and Disease. 2014; 4:381-400.

151. Liu DM, Xu B and Dong C. Recent advances in colorimetric strategies for acetylcholinesterase assay and their applications. Trends in Analytical Chemistry. 2021; 142:116320.

152. Peng L, Rong Z, Wang H, Shao B, Kang L, Qi H and Chen H. A novel assay to determine acetylcholinesterase activity: The application potential for screening of drugs against Alzheimer's disease. Biomedical Chromatography. 2017; 31.

153. Bhadra S, Dalai MK, Chanda J and Mukherjee PK. Evaluation of bioactive compounds as acetylcholinesterase inhibitors from medicinal plants. Evidence-Based Validation of Herbal Medicine. 2015; 273–306.

154. Naik RS, Liu W and Saxena A. Development and validation of a simple assay for the determination of cholinesterase activity in whole blood of laboratory animals. Journal of Applied Toxicology .2013; 33:290–300.

155. Rotenberg M and Almog S. Evaluation of the decarbamylation process of cholinesterase during assay of enzyme activity. Clinica Chimica Acta. 1995; 240:107–116.

156. Kao LT and Gratzl M. Serum cholinesterase assay using a reagent-free micro pH-stat. Analytical Biochemistry. 2009; 389:93-96

157. He P, Davies J, Greenway G and Haswell SJ. Measurement of acetylcholinesterase inhibition using bienzymes immobilized monolith micro-reactor with integrated electrochemical detection. Analytica Chimica Acta. 2010; 659:914.

158. Haigh JR, Lefkowitz LJ, Capacio BR, Doctor BP and Gordon RK. Advantages of the WRAIR whole blood cholinesterase assay: comparative analysis to the micro-Ellman, Test-mate ChE, and Michel (DeltapH) assays. Chemico-Biololgical Interactions. 2008; 175:417-420.

159. Del Carlo M, Pepe A, Sergi M, Mascini M, Tarentini A and Compagnone D. Detection of coumaphos in honey using a screening method based on an electrochemical acetylcholinesterase bioassay. Talanta. 2010; 81:76-81.

160. Sun Y, Tan H and Li Y. A colorimetric assay for acetylcholinesterase activity and inhibitor screening based on the thiocholine–induced inhibition of the oxidative power of MnO2 nanosheets on 3,3′,5,5′–tetramethylbenzidine. Microchimica Acta. 2018; 185.

161. Su J, Liu H, Guo K, Chen L, Yang M and Chen Q. Research advances and detection methodologies for microbe-derived acetylcholinesterase inhibitors: A systemic review. Molecules. 2017; 22:176.

162. Järvinen P, Fallarero A, Gupta S, Mohan GC, Hatakka A and Vuorela P. Miniaturization and validation of the Ellmans reaction-based acetylcholinesterase inhibitory assay into 384-well plate format and screening of a chemical library. Combinatorial Chemistry & High Throughput Screening .2010; 13:278-284.

163. Ingkaninan K, Temkitthawon P, Chuenchom K, Yuyaem T and Thongnoi W. Screening for acetylcholinesterase inhibitory activity in plants used in Thai traditional rejuvenating and neurotonic remedies. Journal of Ethnopharmacology. 2003; 89:261–264

164. Fisher TC, Crane M and Callaghan A. An optimized microtiterplate assay to detect acetylcholinesterase activity in individual Chironomus riparius Meigen. Environmental Toxicology and Chemistry. 2000; 19:1749–1752.

165. Rienda B, Elexpe A, Tolentino-Cortez T, Gulak M, Bruzos-Cidón C, Torrecilla M, Astigarraga E and Barreda-Gómez G. Analysis of acetylcholinesterase activity in cell membrane microarrays of brain areas as a screening tool to identify tissue specific inhibitors. Analytica. 2021; 2:25-36.

166. Ffrench-Constant RH and Bonning BC. Rapid microtitre plate test distinguishes insecticide resistant acetylcholinesterase genotypes in the mosquitoes Anopheles albimanus, An. nigerrimus and Culex pipiens. Medical and Veterinary Entomology.1989; 3:9-16.

167. Jarvinen PP, Fallarero A, Gupta S, Mohan GC, Hatakka AI and Vuorela PM. Miniaturization and validation of the Ellman's reaction-based acetylcholinesterase inhibitory assay into 384-well plate format and screening of a chemical library. Combinatorial Chemistry & High Throughput Screening.2010; 13:278–284.

168. Järvinen P, Vuorela P, Hatakka A and Fallarero A. Potency determinations of acetylcholinesterase inhibitors using Ellman's reaction-based assay in screening: Effect of assay variants. Analytical Biochemistry. 2011; 408:166–168.

169. Li F, Wang ZM, Wu JJ, Wang J, Xie SS, Lan JS, Xu W, Kong LY and Wang XB. Synthesis and pharmacological evaluation of donepezil-based agents as new cholinesterase/monoamine oxidase inhibitors for the potential application against Alzheimer's disease. Journal of Enzyme Inhibition and Medical Chemistry. 2016; 31:41-53.

170. van Greunen DG, Cordier W, Nell M, van der Westhuyzen C, Steenkamp V, Panayides JL and Riley DL. Targeting Alzheimer's disease by investigating previously unexplored chemical space surrounding the cholinesterase inhibitor donepezil. European Journal of Medicinal Chemistry. 2017; 127:671-690.

171. van Greunen DG, van der Westhuizen CJ, Cordier W, Nell M, Stander A, Steenkamp V, Panayides JL and Riley DL. Novel N-benzylpiperidine carboxamide derivatives as potential cholinesterase inhibitors for the treatment of Alzheimer's disease. European Journal of Medicinal Chemistry. 2019; 179:680-693.

172. Di L and Kerns EH. Biological assay challenges from compound solubility: strategies for bioassay optimization. Drug Discovery Today. 2006; 11:446-51.

173. Kumar A and Darreh-Shori T. DMSO: A mixed-competitive inhibitor of human acetylcholinesterase. ACS Chemical Neuroscience. 2017; 8:2618–2625.

174. Gallego R, Valdés A, Sánchez-Martínez JD, Suárez-Montenegro ZJ, Ibáñez E, Cifuentes A and Herrero M. Study of the potential neuroprotective effect of Dunaliella salina extract in SH-SY5Y cell model. Analytical and Bioanalytical Chemistry. 2022; 414:5357-5371.

175. Popa-Burke I and Russell J. Compound precipitation in high-concentration DMSO solutions. Journal of Biomolecular Screening. 2014; 19:1302-1308.

176. Novales NA and Schwans JP. Comparing the effects of organic cosolvents on acetylcholinesterase and butyrylcholinesterase activity. Analytical Biochemistry. 2022; 654:114796.

177. Iversen PW, Beck B, Chen Y-F, Dere W, Devanarayan V, Eastwood BJ, Farmen MW, Iturria SJ, Montrose C and Moore RA. HTS assay validation. In: Assay Guidance Manual.2012;1–20. Available from: https://www.ncbi.nlm.nih.gov/books/NBK83783/. (Accessed; 15 May 2023).

178. Belouafa S, Habti F, Benhar S, Belafkih B, Tayane S, Hamdouch S, Bennamara A and Abourriche A. Statistical tools and approaches to validate analytical methods: methodology and practical examples. International Journal of Metrology and Quality Engineering. 2017; 8:9.

179. Eastwood BJ, Farmen MW, Iversen PW, Craft TJ, Smallwood JK, Garbison KE, Delapp NW and Smith GF. The minimum significant ratio: a statistical parameter to characterize the reproducibility of potency estimates from concentration-response assays and estimation by replicate-experiment studies. Journal of Biomolecular Screening. 2006; 11:253-261.

180. Zhang JH, Chung TDY and Oldenburg KR. A simple statistical parameter for use in evaluation and validation of high throughput screening Assays. SAGE Journal. 2016; 4:67–73.

181. Ivanov DP, Parker TL, Walker DA, Alexander C, Ashford MB, Gellert PR and Garnett MC. Multiplexing spheroid volume, resazurin and acid phosphatase viability assays for high-throughput screening of tumour spheroids and stem cell neurospheres. PloS One. 2014; 9:103817.

182. Inglese J, Johnson RL, Simeonov A, Xia M, Zheng W, Austin CP and Auld DS. High-throughput screening assays for the identification of chemical probes. Nature Chemical Biololgy. 2007; 3:466-79.

183. Chai SC, Goktug AN and Chen T. Assay validation in high throughput screening – from concept to application. Drug discovery and development - from Molecules to Medicine. 2015. Available from: http://dx.doi.org/10.5772/59765. (Accessed: 10 May 2023).

184. da Silva JI, Nicastro PC, de Oliveira PCM, Fossaluzza PC, Morais ÉP, Dias KST, da Costa R S, Castro NG, Cardoso CL and Viegas Junior C. A comparative evaluation of acetylcholinesterase inhibition by AChE-ICER and in vitro Ellman's modified method of simplified analogs 3-o-acetyl-N-benzyl-piperidine of Donepezil. Revista Virtual de Quimica. 2015; 7:2334–2346.

185. Truong B, Quiroz JP and Priefer R. Acetylcholinesterase inhibitors for Alzheimer's disease: past, present, and potential future. Medical Research Archives.2020; 8. Available from: https://esmed.org/MRA/mra/article/view/2271. (Accessed: 18 May 2023).

186. Martorana A, Giacalone V, Bonsignore R, Pace A, Gentile C, Pibiri I, Buscemi S, Lauria A and Palumbo Piccionello A. Heterocyclic scaffolds for the treatment of Alzheimer's disease. Current Pharmaceutical Design. 2016; 22:3971-3995.

187. Hiremathad A and Piemontese L. Heterocyclic compounds as key structures for the interaction with old and new targets in Alzheimer's disease therapy. Neural Regeneration Research. 2017; 12:1256–1261.

188. Gupta SM, Behera A, Jain NK, Kumar D, Tripathi A, Tripathi SM, Mujwar S, Patra J and Negi A. Indene-derived hydrazides targeting acetylcholinesterase enzyme in Alzheimer's: Design, synthesis, and biological evaluation. Pharmaceutics. 2023; 15:94.

189. Obaid RJ, Naeem N, Mughal EU, Al-Rooqi MM, Sadiq A, Jassas RS, Moussa Z and Ahmed SA. Inhibitory potential of nitrogen, oxygen and sulfur containing heterocyclic scaffolds against acetylcholinesterase and butyrylcholinesterase. RSC advances.2022; 12:19764-19855.

190. Saxena AK. The structural hybrids of acetylcholinesterase inhibitors in the treatment of Alzheimer's disease: A review. Alzheimer's & Neurodegenerative Diseases. 2019; 4:1–25.

191. Deep A, Bhatia R, Kaur R, Kumar S, Jain U, Singh H, Sandeep B, Dinesh K and Pran DK. Imidazo[1,2-a]pyridine scaffold as prospective therapeutic agents. Current Topics in Medicinal Chemistry. 2016; 17:238–250.

192. Devi N, Singh D, K. Rawal R, Bariwal J and Singh V. Medicinal attributes of Imidazo[1,2-a]pyridine derivatives: An update. Current Topics in Medicinal Chemistry. 2016; 16:2963–2994.

193. Kwong HC, Chidan Kumar CS, Mah SH, Mah YL, Chia TS, Quah CK, Lim GK and Chandraju S. Crystal correlation of heterocyclic Imidazo[1,2-a]pyridine analogues and their anticholinesterase potential evaluation. Scientific Reports. 2019; 9.

194. Sundberg RJ, Dalvie D, Cordero J and Musallam HA. Carbamate derivatives of 2-arylimidazo [1, 2-a] pyridinium salts as acetylcholinesterase inhibitors and protective agents against organophosphorus compounds. Chemical Research in Toxicology. 1993; 6:506-10.

195. Mohsen UA. Studies on imidazopyridine derivatives as acetylcholinesterase inhibitors. Clinical and Experimental Health Sciences. 2012; 2:119.

196. Gurjar AS, Darekar MN, Yeong KY and Ooi L. In silico studies, synthesis and pharmacological evaluation to explore multi-targeted approach for imidazole analogues as potential cholinesterase inhibitors with neuroprotective role for Alzheimer's disease. Bioorganic Medicinal Chemistry.2018; 26:1511-22.

197. Li H, Chen C, Xu S and Cao X. Synthesis and bioevaluation of thieno[2,3- d]pyrimidinone derivatives as potential tumor cell growth inhibitors. Journal of Chemistry. 2013. doi.org/10.1155/2013/692074.

198. Sayed MTM, Hassan RA, Halim PA and El-Ansary AK. Recent updates on thienopyrimidine derivatives as anticancer agents. Medicinal Chemistry Research. Springer.2023; 32: 659–681.

199. Abdel-Megid M, Elmahdy KM, Elkazak AM, Seada MH and Mohamed OF. Chemistry of Thienopyrimidines and their biological applications. Journal of Pharmaceutical and Applied Chemistry. 2016; 2:103–127.

200. Ali EMH, Abdel-Maksoud MS and Oh CH. Thieno[2,3-d]pyrimidine as a promising scaffold in medicinal chemistry: Recent advances. Bioorganic and Medicinal Chemistry. Elsevier Ltd; 2019; 27: 1159–1194.

201. Eissa KI, Kamel MM, Mohamed LW, Doghish AS, Alnajjar R, Al-Karmalawy AA and Kassab AE. Design, synthesis, and biological evaluation of thienopyrimidine derivatives as multifunctional agents against Alzheimer's disease. Drug Development Research. 2023; 17. Available from: https://onlinelibrary.wiley.com/doi/10.1002/ddr.22064. (Accessed: 20 June 2023).

202. González Tanarro CM and Gütschow M. Hyperbolic mixed-type inhibition of acetylcholinesterase by tetracyclic thienopyrimidines. Journal of Enzyme Inhibition and Medicinal Chemistry.2011; 26:350-358.

203. Chiriapkin AS, Kodonidi IP, Pozdnyakov DI and Glushko AA. Synthesis, in vitro and docking studies of 2-substituted 5, 6, 7, 8-tetrahydrobenzo [4, 5] thieno [2, 3-d] pyrimidine-4 (3H)-one derivatives as agents for the treatment of Alzheimer's disease. Chimica Techno Acta. 2022; 9:20229204.

204. Defert Oliver. Kinase inhibitors field of the invention. The patent cooperation treaty (PCT); Wo2007006546 A1, 2007.

205. CAS SciFindern - Chemical Compound Database | CAS [Internet]. Available from: https://www.cas.org/cas-scifindern-chemical-compound-database. (Accessed: 22 May 2023).

206. Lau WC. Novel Fyn kinase inhibitors for therapeutic applications. wo2016-us50776, Patent. 2017.

207. Ullrich AFM. EP 2 818 472 Al European patent application. EP28188472, 2014.

208. Falcenberg and Ullrich MA. 1 G protein-coupled receptor kinase 5 or GRK5 inhibiting antibodies, siRNA, microRNA, antisense oligonucleotides or small molecules for treatment of diabetes or type II diabetes mellitus. SciFinder, United States; 2015.

209. Lepailleur A, Freret T, Lemaître S, Boulouard M, Dauphin F, Hinschberger A, Dulin F, Lesnard A, Bureau R and Rault S. Dual histamine H3R/serotonin 5-HT4R ligands with antiamnesic properties: pharmacophore-based virtual screening and polypharmacology. Journal of Chemical Information and Modeling. 2014; 54:1773-84.

210. Li J, Zheng M, Shimoni O, Banks WA, Bush AI, Gamble JR and Shi B. Development of novel therapeutics targeting the blood–brain barrier: From barrier to carrier. Advanced Science. John Wiley and Sons Inc. 2021; 8.

211. Pokharel S, Gliyazova NS, Dandepally SR, Williams AL and Ibeanu GC. Neuroprotective effects of an in vitro BBB permeable phenoxythiophene sulfonamide small molecule in glutamate-induced oxidative injury. Experimental and Therapeutic Medicine. 2022; 23:1-1.

212. Mensch J, Oyarzabal J, Mackie C and Augustijns P. In vivo, in vitro and in silico methods for small molecule transfer across the BBB. Journal of Pharmaceutical Sciences. 2009; 98:4429–4468.

213. Hitchcock SA. Blood–brain barrier permeability considerations for CNS-targeted compound library design. Current Opinion in Chemical Biology. 2008; 12:318–323.

214. Lawther BK, Hons B, Fcarcsi DA, Kumar S, Frca M and Krovvidi H. Blood–brain barrier. Continuing Education in Anaesthesia Critical Care & Pain. 2011; 11:128–32.

215. Pardridge WM. Treatment of Alzheimer's disease and blood–brain barrier drug delivery. Pharmaceuticals. 2020; 13:1–25.

216. Li G, Shao K and Umeshappa CS. Recent progress in blood-brain barrier transportation research. In Gao H and Gao X (edrs). Brain Targeted Drug Delivery System. Academic Press, United States of America. 2018; 33–51.

217. Pflanzner T, Kuhlmann CR and Pietrzik CU. Blood-brain-barrier models for the investigation of transporter-and receptor-mediated amyloid-β clearance in Alzheimer's disease. Current Alzheimer Research. 2010; 7:578-590.

218. Ghosh RD, Chakraborty P, Banerjee K, Adhikary A, Sarkar A, Chatterjee M, Das T and Choudhuri SK. The molecular interaction of a copper chelate with human P-glycoprotein. Molecular and Cellular Biochemistry. 2012; 364:309-320.

219. Cecchelli R, Berezowski V, Lundquist S, Culot M, Renftel M, Dehouck MP and Fenart L. Modelling of the blood–brain barrier in drug discovery and development. Nature Reviews Drug discovery. 2007; 6:650-661.

220. Banks WA. Characteristics of compounds that cross the blood-brain barrier. BMC Neurology. 2009; 9:1-5.

221. Kabir MT, Uddin MS, Mamun AA, Jeandet P, Aleya L, Mansouri RA, Ashraf GM, Mathew B, Bin-Jumah MN and Abdel-Daim MM. Combination drug therapy for the management of Alzheimer's disease. International Journal of Molecular Sciences. 2020; 21:3272.

222. Amat-ur-Rasool H, Ahmed M, Hasnain S and Carter WG. Anti-cholinesterase combination drug therapy as a potential treatment for Alzheimer's disease. Brain Sciences. 2021; 11:184.

223. Lehár J, Krueger AS, Avery W, Heilbut AM, Johansen LM, Price ER, Rickles RJ, Short Iii GF, Staunton JE, Jin X and Lee MS. Synergistic drug combinations tend to improve therapeutically relevant selectivity. Nature Biotechnology. 2009; 27:659-66.

224. Yin N, Ma W, Pei J, Ouyang Q, Tang C, Lai L. Synergistic and antagonistic drug combinations depend on network topology. PLoS One. 2014; 9:93960.

225. Chait R, Craney A and Kishony R. Antibiotic interactions that select against resistance. Nature. 2007; 446:668-671.

226. Caesar LK and Cech NB. Synergy and antagonism in natural product extracts: when 1 + 1 does not equal 2. Natural Product Reports. 2019; 36:869–888.

227. Breitinger HG. Drug synergy-mechanisms and methods of analysis [Internet]. 2012. Available from: www.intechopen.com. (Accessed: 15 April 2023).

228. Chou TC. Theoretical basis, experimental design, and computerized simulation of synergism and antagonism in drug combination studies. Pharmacological Reviews. 2006; 58:621–681.

229. Pemovska T, Bigenzahn JW and Superti-Furga G. Recent advances in combinatorial drug screening and synergy scoring. Current Opinion in Pharmacology. 2018; 42:102–110.

230. Sun X, Vilar S and Tatonetti NP. High-throughput methods for combinatorial drug discovery. Science Translational Medicine.2013; 5:205.

231. Binderup ML, Dalgaard M, Dragsted LO, Hossaini A, Ladefoged O, Lam HR, Larsen JC, Madsen C, Meyer OA, Rasmussen ES and Reffstrup TK. Combined actions and interactions of chemicals in mixtures: the toxicological effects of exposure to mixtures of industrial and environmental chemicals. National Food Institute. 2003; 12: 1- 158.

232. Richards R, Schwartz HR, Honeywell ME, Stewart MS, Cruz-Gordillo P, Joyce AJ, Landry BD and Lee MJ. Drug antagonism and single-agent dominance result from differences in death kinetics. Nature Chemical Biology. 2020; 16:791-800.

233. Pacheco S, Pandey S, Pandey I, He M, Paing EC and PHHS U. Monotherapy vs combination therapy for the management of Alzheimer's disease.2021. Available at: https://escholarship.org/uc/item/0t34s5b8. (Accessed: 17 May 2023).

234. Lopez-Suarez L, Awabdh S, Coumoul X and Chauvet C. The SH-SY5Y human neuroblastoma cell line, a relevant in vitro cell model for investigating neurotoxicology in human: focus on organic pollutants. Neurotoxicology.2022; 10.

235. Çetinkaya A, Karabörk Ş, Çelik H and Torun İE. Evaluation of the cytotoxic efficacy of Thymoquinone and Capsaicin in the SH-SY5Y neuroblastoma cell line. International Journal of Nature and Life Sciences. 2022; 118–128.

236. Bao J, Huang B, Zou L, Chen S, Zhang C, Zhang Y, Chen M, Wan JB, Su H, Wang Y and He C. Hormetic effect of berberine attenuates the anticancer activity of chemotherapeutic agents. PloS One.2015; 10:0139298.

237. Calabrese EJ. Neuroscience and hormesis: Overview and general findings. Critical Reviews in Toxicology. 2008; 38: 249–252.

238. Martins I, Galluzzi L and Kroemer G. Hormesis, cell death and aging. Aging. 2011; 3:821.

239. Calabrese EJ. Hormetic mechanisms. Critical Reviews in Toxicology.2013; 43:580–606.

240. Mattson MP and Cheng A. Neurohormetic phytochemicals: low-dose toxins that induce adaptive neuronal stress responses. Trends in Neurosciences. 2006; 29:632–639.

241. Pallàs M, Porquet D, Vicente A and Sanfeliu C. Resveratrol: new avenues for a natural compound in neuroprotection. Current Pharmaceutical Design. 2013; 19:6726–6731.

242. Demirovic D and Rattan SIS. Curcumin induces stress response and hormetically modulates wound healing ability of human skin fibroblasts undergoing ageing in vitro. Biogerontology. 2011; 12:437–444.

243. Michaelis M, Hinsch N, Michaelis UR, Rothweiler F, Simon T, Ilhelm Doerr HW, Cinatl J and Cinatl Jr J. Chemotherapy-associated angiogenesis in neuroblastoma tumors. The American Journal of Pathology.2012; 180:1370-1377.

244. Zaremba-Czogalla M, Jaromin A, Sidoryk K, Zagórska A, Cybulski M and Gubernator J. Evaluation of the in vitro cytotoxic activity of caffeic acid derivatives and liposomal formulation against pancreatic cancer cell lines. Materials. 2020; 13:1–18.

245. Shipley MM, Mangold CA and Szpara ML. Differentiation of the SH-SY5Y human neuroblastoma cell line. Journal of Visualized Experiments. 2016; 108:53193.

246. Banks WA and Rhea EM. The blood–brain barrier, oxidative stress, and insulin resistance. Antioxidants. 2021; 10:1695.

247. Lopina OD. Enzyme Inhibitors and Activators. In: Enzyme Inhibitors and Activators. IntechOpen; 2017. doi: 10.5772/67248.

248. Tsuno N. Donepezil in the treatment of patients with Alzheimer's disease. Expert Review of Neurotherapeutics. 2009; 9:591-598.

249. Ramsay RR and Tipton KF. Assessment of enzyme inhibition: a review with examples from the development of monoamine oxidase and cholinesterase inhibitory drugs. Molecules. 2017; 2:1192.

250. Fraser DL. Evaluation of the neurotoxicity of pentachlorophenol and its active metabolites on SH-SY5Y neuroblastoma cells. 2017. Available from: https://repository.up.ac.za/handle/2263/68006. (Accessed: 12 April 2023).

251. Buker SM, Boriack-Sjodin PA and Copeland RA. Enzyme–inhibitor interactions and a simple, rapid method for determining inhibition modality. SLAS Discovery. 2019; 24:515–522.

252. Strelow J, Dewe W, Iversen PW, Brooks HB, Radding JA, McGee J and Weidner J. Mechanism of action assays for enzymes. Assay Guidance Manual.2012. Available from: https://www.ncbi.nlm.nih.gov/books/NBK92001/. (Accessed: 24 April 2023).

253. Peauger L, Azzouz R, Gembus V, Tintas ML, Sopková-de Oliveira Santos J, Bohn P, Papamicael C and Levacher V. Donepezil-based central acetylcholinesterase inhibitors by means of a "bio-oxidizable" prodrug strategy: design, synthesis, and in vitro biological evaluation. Journal of Medicinal Chemistry. 2017; 60:5909-5926.

254. Lan JS, Zhang T, Liu Y, Yang J, Xie SS, Liu J, Miao ZY and Ding Y. Design, synthesis and biological activity of novel donepezil derivatives bearing N-benzyl pyridinium moiety as potent and dual binding site acetylcholinesterase inhibitors. European Journal of Medicinal Chemistry. 2017; 133:184-196.

255. Roell KR, Reif DM and Motsinger-Reif AA. An introduction to terminology and methodology of chemical synergy-perspectives from across disciplines. Frontiers in Pharmacology. 2017; 8:158.

256. Serdar BS, Erkmen T, Ergür BU, Akan P and Koçtürk S. Which medium and ingredients provide better morphological differentiation of SH-SY5Y Cells?. MDPI-Proceedings. 2018; 2:1557.

257. Agholme L, Lindström T, Kgedal K, Marcusson J and Hallbeck M. An in vitro model for neuroscience: Differentiation of SH-SY5Y cells into cells with morphological and biochemical characteristics of mature neurons. Journal of Alzheimer's Disease. 2010; 20:1069–1082.

258. Kasteel EE, Nijmeijer SM, Darney K, Lautz LS, Dorne JL, Kramer NI and Westerink RH. Acetylcholinesterase inhibition in electric eel and human donor blood: an in vitro approach to investigate interspecies differences and human variability in toxicodynamics. Archives of Toxicology. 2020; 94:4055-4065.

259. Wiesner J, Kříž Z, Kuča K, Jun D and Koča J. Acetylcholinesterases–the structural similarities and differences. Journal of Enzyme Inhibition and Medicinal Chemistry. 2007; 22:417-424.

260. Qadri YH, Swamy AN and Rao J V. Species differences in brain acetylcholinesterase response to monocrotophos in vitro. Ecotoxicology and Environmental Safety. 1994; 28:91–98.

261. Wang C and Murphy SD. Kinetic analysis of species difference in acetylcholinesterase sensitivity to organophosphate insecticides. Toxicology and Applied Pharmacology. 1982; 66:409–419.

262. Pezzementi L, Nachon F and Chatonnet A. Evolution of Acetylcholinesterase and Butyrylcholinesterase in the Vertebrates: An atypical butyrylcholinesterase from the Medaka Oryzias latipes. PLoS One. 2011; 6:17396.

263. Onder S, Schopfer LM, Jiang W, Tacal O and Lockridge O. Butyrylcholinesterase in SH-SY5Y human neuroblastoma cells. Neurotoxicology.2022; 90:1–9.

264. Copeland RA. Determination of serum protein binding affinity of inhibitors from analysis of concentration–response plots in biochemical activity assays. Journal of Pharmaceutical Sciences.2000; 89:1000-1007.

265. Mann A and Tyndale RF. Cytochrome P450 2D6 enzyme neuroprotects against 1-methyl-4-phenylpyridinium toxicity in SH-SY5Y neuronal cells. European Journal of Neuroscience. 2010; 31:1185.

266. Lyon RC, Johnston SM, Panopoulos A, Alzeer S, McGarvie G and Ellis EM. Enzymes involved in the metabolism of gamma-hydroxybutyrate in SH-SY5Y cells: identification of an iron-dependent alcohol dehydrogenase ADHFe1. Chemico-Biological Interactions. 2009; 178:283–287.

267. Carvalho C and Moreira PI. Oxidative stress: a major player in cerebrovascular alterations associated to neurodegenerative events. Frontiers in Physiology. 2018; 9:806.

268. Lau M, Sealy B, Combes V, Morsch M and Garcia-Bennett AE. Enhanced antioxidant effects of the anti-inflammatory compound probucol when released from mesoporous silica particles. Pharmaceutics. 2022; 14:502.

269. Erickson MA, Wilson ML and Banks WA. In vitro modeling of blood-brain barrier and interface functions in neuroimmune communication. Fluids Barriers CNS. 2020; 17:1-16.

270. Helms HC, Abbott NJ, Burek M, Cecchelli R, Couraud PO, Deli MA, Förster C, Galla HJ, Romero IA, Shusta EV, Stebbins MJ, Vandenhaute E, Weksler B and Brodin B. In vitro models of the blood-brain barrier: An overview of commonly used brain endothelial cell culture models and guidelines for their use. Journal of Cerebral Blood Flow & Metabolism. 2016; 36:862-890.

271. Qosa H, Miller DS, Pasinelli P and Trotti D. Regulation of ABC efflux transporters at blood-brain barrier in health and neurological disorders. Brain Research. 2015; 1628:298-316.

272. Yuan L, van der Mei HC, Busscher HJ and Peterson BW. Two-stage interpretation of Changes in TEER of intestinal epithelial layers protected by adhering Bifidobacteria during E. coli challenges. Frontiers in Microbiology. 2020; 11:599555.

273. Mukherjee T, Squillantea E, Gillespieb M and Shao J. Transepithelial electrical resistance is not a reliable measurement of the Caco-2 monolayer integrity in Transwell. Drug Delivery. 2004; 11:11-18.

274. Fisher D, Thomas KA and Abdul-Rasool S. The synergistic and neuroprotective effects of alcohol-antioxidant treatment on blood-brain barrier endothelial cells. Alcoholism, Clinical and Experimental Research. 2020; 44:1997-2007.

275. Knox EG, Aburto MR, Clarke G, Cryan JF and O'Driscoll CM. The blood-brain barrier in aging and neurodegeneration. Molecular Psychiatry. 2022; 27:2659-2673.

276. Mursaleen L, Noble B, Somavarapu S and Zariwala MG. Micellar nanocarriers of hydroxytyrosol are protective against parkinson's related oxidative stress in an in vitro sh-sy5y co-culture system. Antioxidants. 2021; 10:887.

277. Brown RC, Morris AP and O'Neil RG. Tight junction protein expression and barrier properties of immortalized mouse brain microvessel endothelial cells. Brain Research. 2007; 1130:17–30.

278. Schreiner TG, Creangă-Murariu I, Tamba BI, Lucanu N and Popescu BO. In vitro modeling of the blood–brain barrier for the study of physiological conditions and Alzheimer's disease. Biomolecules. 2022; 12:1136.

279. Almutairi MMA, Gong C, Xu YG, Chang Y and Shi H. Factors controlling permeability of the blood-brain barrier. Cellular and Molecular Life Sciences. 2016; 73:57–77.

280. Stone NL, England TJ and O'Sullivan SE. A novel transwell blood brain barrier model using primary human cells. Frontiers in Cellular Neuroscience. 2019; 13:230.

281. Dietrich JB. Endothelial cells of the blood-brain barrier: a target for glucocorticoids and estrogens. Frontiers in Bioscience. 2004; 9:684-693.

282. Hajal C, Le Roi B, Kamm RD and Maoz BM. Biology and Models of the blood-brain barrier. Annual Review of Biomedical Engineering. 2021; 23:359–384.

283. Aday S, Cecchelli R, Hallier-Vanuxeem D, Dehouck MP and Ferreira L. Stem cell-based human blood-brain barrier models for drug discovery and delivery. Trends in Biotechnology. 2016; 34:382–393.

284. Gericke B, Römermann K, Noack A, Noack S, Kronenberg J, Blasig IE and Löscher W. A face-to-face comparison of claudin-5 transduced human brain endothelial (hCMEC/D3) cells with porcine brain endothelial cells as blood–brain barrier models for drug transport studies. Fluids and Barriers of the CNS. 2020; 17:1-6.

285. Curley SM and Cady NC. Biologically-derived nanomaterials for targeted therapeutic delivery to the brain. Science progress. 2018; 101:273-292.

286. Puris E, Fricker G and Gynther M. Targeting transporters for drug delivery to the brain: can we do better?. Pharmaceutical Research. 2022; 39:1415-1455.

287. Yan H. Stereoselective transport of drugs across the blood-brain barrier (BBB) in vivo and in vitro: Pharmacokinetic and pharmacodynamic studies of the (S)-and (R)-enantiomers of different 5-HT1A receptor agonists and antagonists (doctoral dissertation, Acta Universitatis Upsaliensis). 2002. Available from: https://www.diva-portal.org/smash/get/diva2:161536/FULLTEXT01. (Accessed: 10 June 2023).

288. Fu MB. Experimental methods and transport models for drug delivery across the blood-brain barrier. Current pharmaceutical biotechnology. 2012; 13: 1346-1359.

289. Bellettato CM and Scarpa M. Possible strategies to cross the blood–brain barrier. Italian Journal of Pediatrics. 2018; 44:127-133.

290. Keaney J and Campbell M. The dynamic blood–brain barrier. The Federation of European Biochemical Societies Journal. 2015; 282:4067-4079.

Appendix I: Research Ethics approval

UNIVERSITEIT VAN PRETORIA
UNIVERSITY OF PRETORIA
YUNIBESITHI YA PRETORIA

Faculty of Health Sciences

Institution: The Research Ethics Committee, Faculty Health Sciences, University of Pretoria complies with ICH-GCP guidelines and has US Federal wide Assurance.

- FWA 00002567, Approved dd 18 March 2022 and Expires 18 March 2027.
- IORG #: IORG0001762 OMB No. 0990-0279 Approved for use through June 30, 2025 and Expires 07/28/2026.

Faculty of Health Sciences **Research Ethics Committee**

14 September 2023

Approval Certificate
Annual Renewal

Dear Miss LM Maboko,

Ethics Reference No.: 780/2019 – Line 5
Title: Assessing the acetylcholinesterase inhibitory potential of novel pharmacophores for potential treatment of Alzheimer's disease.

The **Annual Renewal** as supported by documents received between 2023-08-21 and 2023-09-13 for your research, was approved by the Faculty of Health Sciences Research Ethics Committee on 2023-09-13 as resolved by its quorate meeting.

Please note the following about your ethics approval:

- Renewal of ethics approval is valid for 1 year, subsequent annual renewal will become due on 2024-09-14.
- Please remember to use your protocol number (780/2019) on any documents or correspondence with the Research Ethics Committee regarding your research.
- Please note that the Research Ethics Committee may ask further questions, seek additional information, require further modification, monitor the conduct of your research, or suspend or withdraw ethics approval.

Ethics approval is subject to the following:

- The ethics approval is conditional on the research being conducted as stipulated by the details of all documents submitted to the Committee. In the event that a further need arises to change who the investigators are, the methods or any other aspect, such changes must be submitted as an Amendment for approval by the Committee.

We wish you the best with your research.

Yours sincerely

On behalf of the FHS REC, Dr R Sommers
MBChB, MMed (Int), MPharmMed, PhD
Deputy Chairperson *of the Faculty of Health Sciences Research Ethics Committee, University of Pretoria*

The Faculty of Health Sciences Research Ethics Committee complies with the SA National Act 61 of 2003 as it pertains to health research and the United States Code of Federal Regulations Title 45 and 46. This committee abides by the ethical norms and principles for research, established by the Declaration of Helsinki, the South African Medical Research Council Guidelines as well as the Guidelines for Ethical Research: Principles Structures and Processes, Second Edition 2015 (Department of Health)

Research Ethics Committee
Room 4-60, Level 4, Tswelopele Building
University of Pretoria, Private Bag x323
Gezina 0031, South Africa
Tel +27 (0)12 356 3084
Email: deepeka.behari@up.ac.za
www.up.ac.za

Fakulteit Gesondheidswetenskappe
Lefapha la Disaense tša Maphelo

Appendix II: Reagents preparation

Acetylthiocholine iodide (ATCI)

Acetylthiocholine iodide was purchased from Merck/Sigma-Aldrich (St. Louis, USA) and was stored at 4°C. A fresh 2.14 mM was prepared before the start of each experiment by adding 2.9 mg to 4.5 mL mix-buffer containing 0.07% BSA.

Acetylcholinesterase (AChE)

Acetylcholinesterase from *Electrophorus electricus* (electric eel) type VI-S was purchased from Merck/Sigma-Aldrich (St. Louis, USA). A 120 U/mL stock solution was prepared by dissolving 6.6 mg AChE in 16.612 mL Tris-HCl buffer. The stock solution was aliquoted and stored until needed at -20°C.

Acetic acid

A 1% (*v/v*) solution of acetic acid was prepared by diluting 1 mL of glacial acetic acid (Merck Chemicals, SA) with distilled water to a final volume of 100 mL. The solution was stored at room temperature.

Bovine serum albumin (BSA)

Bovine serum albumin was purchased from Merck/Sigma-Aldrich (St. Louis, USA). A 2% BSA stock solution was prepared by dissolving 40 mg BSA in 20 mL mix-buffer and stored at 4°C.

Cell culture medium

Ham's F-12 nutrient mixture and Dulbecco's Modified Eagle's Medium (DMEM) were purchased from Merck/Sigma-Aldrich (St. Louis, USA), and mixed at a 1:1 ratio. The cell culture medium contained 1% antibiotics (streptomycin and penicillin G). Medium was supplemented with 10% FCS from the Scientific Group (Gauteng, SA) by adding 10 mL FCS for every 90 mL medium for SH-SY5Y neuroblastoma cells and further contained 1% non-essential antibodies and 1% sodium pyruvate for bEnd.5 cells.

Dimethyl sulfoxide (DMSO)

Undiluted DMSO was purchased from Merck Millipore (Darmstadt, Germany), and stored at room temperature. Ten times dilutions were prepared depending on the desired concentration for each assay (AChE or SRB assay). For the AChE assay, 0.5% DMSO (vehicle control) was

prepared by diluting 1 µL of 100% DMSO with 199 µL of mix-buffer. For the SRB assay, 1% vehicle control was prepared by dissolving 15 µL of 100% DMSO in 1 485 µL of DMEM.

Donepezil

Donepezil was purchased from Merck/Sigma-Aldrich (St. Louis, USA), and a 25 mM stock solution was prepared by dissolving 10 mg powder in 1.05 mL DMSO. Stock solutions were aliquoted and stored at -20°C.

5,5′-dithiobis(2-nitrobenzoic acid) (DTNB)

5,5′-dithiobis(2-nitrobenzoic acid) was purchased from Merck/Sigma-Aldrich (St. Louis, USA) and was stored at 4°C. A fresh 2.14 mM DTNB was prepared before the start of each experiment by adding 3.8 mg to 4 448 mL mix-buffer.

Galantamine

Galantamine was purchased from Merck/Sigma-Aldrich (St. Louis, USA), and a 25 mM stock solution was prepared by dissolving 10 mg powder in 1.39 mL DMSO. Stock solutions were aliquoted and stored at -20°C.

Acetylcholinesterase mix-buffer

Buffer was prepared the day before the assay setup. The mix-buffer consisted of 0.045 M Tris-HCl, 0.071 M NaCl, and 0.014 M $MgCl_2.6H_2O$ [Merck/Sigma-Aldrich (St. Louis, USA]), which was prepared by dissolving 1.77 g Tris-HCl, 1.04 g NaCl and 0.71 g $MgCl_2.6H_2O$ in 200 mL distilled water. The buffer was adjusted to pH 8 with 5 M sodium hydroxide (NaOH) and the volume was topped up with distilled water to 250 mL. The mix-buffer was stored at 4°C.

Prior to every experiment, a volume of 0.158 mL 2% BSA was added into 4.5 mL of mix-buffer (resulting in-solution concentration of 0.07%), 2.9 mg of ATCI was dissolved in 4.659 mL of mix-buffer (containing Tris-HCl, NaCl, $MgCl_2.6H_2O$ and BSA) and finally, an amount of 3.8 mg DTNB was dissolved into 4.448 mL mix-buffer (containing Tris-HCl, NaCl, $MgCl_2.6H_2O$, BSA and ATCI).

Sodium hydroxide

Sodium hydroxide was purchased from Merck/Sigma-Aldrich (St. Louis, USA). A 5 M NaOH stock was prepared by dissolving 50 g in 250 mL of distilled water.

Tris-hydrochloride (HCl) buffer

Tris-hydrochloride was purchased from Merck/Sigma-Aldrich (St. Louis, USA). A 0.05 M buffer was prepared by dissolving 3.94 g Tris-HCl in 400 mL distilled water. The buffer was adjusted to pH 8 NaOH and volume was topped up with distilled water till 500 mL was reached. The buffer was stored at 4°C.

Phosphate-buffered saline (PBS)

Phosphate-buffered saline buffer was prepared by dissolving 9.23 g of BBL™ FTA haemagglutinin powder (BD Bioscience, New Jersey, USA) in distilled water, to make a final volume of 1L. The buffer was then sterilised by autoclaving for 30 min at 120°C, and 2 bar. The buffer was then stored at 4°C.

Saponin

Saponin was purchased from Merck/Sigma-Aldrich (St. Louis, USA) and stored at room temperature. To make-up the 1% (*w/v*) positive control solution, 2 mg of the saponin powder was dissolved in 2 mL culture medium, vortexed to allow for optimum dissolution, and filter sterilised with a 0.2 µm filter.

Sulforhodamine B

Sulforhodamine B stain was purchased from Merck/Sigma-Aldrich (St. Louis, USA). A 0.057% solution was prepared by dissolving 57 mg in 100 mL 1% (*v/v*) acetic acid in distilled water and stored at 4°C.

Trichloroacetic acid (TCA)

Trichloroacetic acid was purchased from Merck Millipore (Darmstadt, Germany). A 50% (w/v) solution of TCA was prepared by dissolving 50 g of TCA crystals in distilled water, to make a final solution of 100 mL, which was stored at 4°C.

Tris-base

Tris-base powder was purchased from Merck Millipore (Darmstadt, Germany). A 10 mM solution of the tris buffer was made by dissolving 121.1 mg of tris(hydroxymethyl) aminomethane (Tris) in 100 mL distilled water. The pH of the solution was adjusted to 10.5 using NaOH, and the buffer was stored at room temperature.

TrypLE Express Enzyme

TrypLE Express enzyme was purchased as a liquid from Thermo Fisher Scientific (Massachusetts, US) and used undiluted.

Appendix III: Acetylcholinesterase inhibitory activity of the screened compounds

Table 10: Acetylcholinesterase inhibitory activity of subset **A** compounds and the associated plate barcode. Bold rows indicate compounds with ≥ 60% AChEI activity at 5 µM.

Compound no.	Plate Barcode	AChEI activity (%) ± SEM	AChEI IC_{50} (µM) ± SEM
A1	BFCP029239_2	19.39 ± 4.53	n.d
A2	BFCP029239_2	11.18 ± 2.77	n.d
A3	BFCP029239_2	12.11 ± 4.93	n.d
A4	BFCP029241_2	7.37 ± 2.48	n.d
A5	BFCP029242_2	18.74 ± 4.24	n.d
A6	BFCP029249_2	8.18 ± 3.90	n.d
A7	BFCP029255_2	12.21 ± 6.45	n.d
A8	**BFCP029264_2**	**59.87 ± 3.04**	**5.86 ± 0.01**
A9	BFCP029266_2	19.98 ± 4.47	n.d
A10	BFCP029267_2	14.77 ± 2.25	n.d
A11	BFCP029269_2	11.17 ± 3.37	n.d
A12	BFCP029272_2	6.15 ± 6.63	n.d
A13	BFCP029272_2	12.68 ± 2.90	n.d
A14	BFCP029272_2	20.50 ± 5.70	n.d
A15	BFCP029272_2	13.12 ± 3.32	n.d
A16	BFCP029273_2	5.70 ± 5.52	n.d
A17	BFCP029273_2	18.61 ± 4.02	n.d
A18	BFCP029274_2	13.37 ± 3.01	n.d
A19	BFCP029274_2	10.06 ± 2.96	n.d
A20	BFCP029274_2	4.08 ± 3.70	n.d
A21	BFCP029274_2	22.76 ± 5.30	n.d
A22	BFCP029274_2	20.90 ± 3.07	n.d
A23	BFCP029274_2	9.96 ± 2.82	n.d
A24	BFCP029274_2	12.05 ± 4.26	n.d
A25	BFCP029278_2	13.84 ± 3.08	n.d
A26	BFCP029282_2	13.79 ± 1.85	n.d
A27	BFCP029282_2	12.87 ± 1.99	n.d
A28	BFCP029282_2	6.18 ± 4.31	n.d
A29	BFCP029282_2	-10.02 ± 39.76	n.d
A30	BFCP029282_2	-37.87 ± 20.58	n.d
A31	BFCP029282_2	-42.23 ± 21.04	n.d
A32	BFCP029282_2	-6.84 ± 7.97	n.d
A33	BFCP029282_2	-5.35 ± 16.49	n.d
A34	BFCP029282_2	-13.67 ± 11.53	n.d
A35	BFCP029282_2	-23.04 ± 12.91	n.d
A36	BFCP029282_2	-20.11 ± 7.43	n.d
A37	BFCP029282_2	10.41 ± 9.42	n.d

Compound no.	Plate Barcode	AChEI activity (%) ± SEM	AChEI IC_{50} (µM) ± SEM
A38	BFCP029282_2	-7.99 ± 7.90	n.d
A39	BFCP029282_2	0.86 ± 11.40	n.d
A40	BFCP029282_2	-25.29 ± 6.41	n.d
A41	BFCP029282_2	11.33 ± 10.58	n.d
A42	BFCP029283_2	-6.06 ± 4.83	n.d
A43	BFCP029284_2	-9.94 ± 7.95	n.d
A44	BFCP029284_2	-21.86 ± 6.34	n.d
A45	BFCP029284_2	-3.42 ± 5.46	n.d
A46	BFCP029284_2	-4.42 ± 5.88	n.d
A47	BFCP029284_2	-15.00 ± 13.66	n.d
A48	BFCP029284_2	-1.80 ± 7.66	n.d
A49	BFCP029285_2	-1.37 ± 6.64	n.d
A50	BFCP029315_2	-10.48 ± 6.27	n.d
A51	**BFCP029316_2**	**66.53 ± 4.66**	**0.20 ± 0.06**
A52	BFCP029317_2	54.69 ± 14.59	n.d
A53	BFCP029321_2	-8.63 ± 12.55	n.d
A54	BFCP029342_2	-2.70 ± 8.28	n.d
A55	BFCP029346_2	-14.24 ± 7.83	n.d
A56	BFCP029346_2	-23.45 ± 8.89	n.d
A57	BFCP029346_2	38.64 ± 9.22	n.d
A58	BFCP029347_2	31.23 ± 12.83	n.d
A59	BFCP029347_2	1.74 ± 7.27	n.d
A60	BFCP029347_2	-12.97 ± 11.38	n.d
A61	BFCP029347_2	29.68 ± 9.19	n.d
A62	BFCP029347_2	26.91 ± 7.35	n.d
A63	BFCP029347_2	-2.07 ± 15.52	n.d
A64	BFCP029348_2	-22.59 ± 15.82	n.d
A65	BFCP029350_2	35.58 ± 5.27	n.d
A66	BFCP029350_2	35.54 ± 6.70	n.d
A67	BFCP029351_2	35.45 ± 15.19	n.d
A68	BFCP029351_2	-6.46 ± 8.73	n.d
A69	BFCP029351_2	38.89 ± 4.06	n.d
A70	BFCP029353_2	38.76 ± 7.07	n.d
A71	BFCP029354_2	25.67 ± 31.80	n.d
A72	BFCP029354_2	10.52 ± 18.07	n.d
A73	**BFCP029354_2**	**77.98 ± 4.12**	**3.56 ± 0.09**
A74	BFCP029354_2	38.73 ± 5.25	n.d
A75	BFCP029356_2	27.20 ± 8.96	n.d
A76	BFCP029356_2	4.30 ± 11.86	n.d
A77	BFCP029356_2	34.36 ± 4.63	n.d
A78	BFCP029356_2	29.24 ± 23.29	n.d
A79	BFCP029356_2	30.89 ± 6.83	n.d
A80	BFCP029356_2	-0.26 ± 15.81	n.d
A81	BFCP029356_2	39.23 ± 20.46	n.d

Compound no.	Plate Barcode	AChEI activity (%) ± SEM	AChEI IC_{50} (µM) ± SEM
A82	BFCP029356_2	33.21 ± 10.09	n.d
A83	BFCP029356_2	35.90 ± 7.50	n.d
A84	BFCP029356_2	28.21 ± 16.07	n.d
A85	BFCP029356_2	16.71 ± 2.48	n.d
A86	BFCP029356_2	15.20 ± 6.91	n.d
A87	BFCP029357_2	-2.16 ± 0.38	n.d
A88	BFCP029357_2	-6.07 ± 8.19	n.d
A89	BFCP029357_2	32.45 ± 4.41	n.d
A90	BFCP029357_2	19.84 ± 4.38	n.d
A91	BFCP029357_2	2.72 ± 8.94	n.d
A92	BFCP029357_2	-0.25 ± 15.24	n.d
A93	BFCP029357_2	28.98 ± 2.81	n.d
A94	BFCP029357_2	20.73 ± 7.79	n.d
A95	BFCP029358_2	8.74 ± 9.39	n.d
A96	BFCP029358_2	-1.26 ± 7.99	n.d
A97	BFCP029358_2	24.91 ± 1.12	n.d
A98	BFCP029358_2	10.51 ± 7.27	n.d
A99	BFCP029358_2	12.55 ± 8.34	n.d
A100	BFCP029358_2	-3.58 ± 4.52	n.d
A101	BFCP029359_2	28.58 ± 11.61	n.d
A102	BFCP029359_2	13.96 ± 11.75	n.d
A103	BFCP029359_2	17.04 ± 9.25	n.d
A104	BFCP029359_2	1.84 ± 4.95	n.d
A105	BFCP029359_2	38.25 ± 5.75	n.d
A106	BFCP029359_2	24.50 ± 7.17	n.d
A107	BFCP029359_2	22.35 ± 9.58	n.d
A108	BFCP029359_2	-3.37 ± 13.44	n.d
A109	BFCP029360_2	28.47 ± 2.82	n.d
A110	BFCP029361_2	14.78 ± 7.57	n.d
A111	BFCP029361_2	17.70 ± 6.99	n.d
A112	BFCP029364_2	21.41 ± 12.97	n.d
A113	BFCP029365_2	19.42 ± 3.97	n.d
A114	BFCP029365_2	12.28 ± 1.97	n.d
A115	BFCP029365_2	2.74 ± 3.39	n.d
A116	BFCP029366_2	3.62 ± 3.28	n.d
A117	BFCP029366_2	24.62 ± 4.61	n.d
A118	BFCP029366_2	4.40 ± 2.71	n.d
A119	BFCP029366_2	10.47 ± 3.09	n.d
A120	BFCP029366_2	7.48 ± 4.91	n.d
A121	BFCP029366_2	17.28 ± 2.89	n.d
A122	BFCP029366_2	6.69 ± 3.64	n.d
A123	BFCP029366_2	6.37 ± 3.26	n.d
A124	BFCP029367_2	0.91 ± 3.56	n.d
A125	BFCP029367_2	22.26 ± 5.10	n.d

Compound no.	Plate Barcode	AChEI activity (%) ± SEM	AChEI IC_{50} (µM) ± SEM
A126	BFCP029367_2	14.26 ± 3.27	n.d
A127	BFCP029367_2	6.82 ± 3.32	n.d
A128	BFCP029368_2	3.44 ± 3.54	n.d
A129	BFCP029368_2	24.32 ± 3.66	n.d
A130	BFCP029368_2	9.98 ± 2.54	n.d
A131	BFCP029368_2	0.20 ± 3.74	n.d
A132	BFCP029368_2	24.10 ± 5.42	n.d
A133	BFCP029403_2	25.79 ± 4.34	n.d
A134	BFCP029404_2	6.16 ± 2.45	n.d
A135	BFCP029406_2	42.75 ± 1.65	n.d
A136	**BFCP029407_2**	**62.33 ± 3.74**	**16.68 ± 0.04**
A137	BFCP029408_2	24.60 ± 4.26	n.d
A138	BFCP029409_2	38.07 ± 3.09	n.d
A139	BFCP029409_2	19.04 ± 3.72	n.d
A140	BFCP029409_2	27.66 ± 4.97	n.d
A141	BFCP029409_2	19.42 ± 3.43	n.d
A142	BFCP029410_2	12.28 ± 3.56	n.d
A143	BFCP029410_2	2.74 ± 3.35	n.d
A144	BFCP029410_2	3.62 ± 21.60	n.d
A145	BFCP029412_2	24.62 ± 2.34	n.d
A146	BFCP029412_2	4.40 ± 3.80	n.d
A147	BFCP029412_2	10.47 ± 19.06	n.d
A148	BFCP029413_2	7.48 ± 22.86	n.d
A149	BFCP029413_2	17.28 ± 3.13	n.d
A150	BFCP029414_2	6.69 ± 3.66	n.d
A151	BFCP029416_2	6.37 ± 14.12	n.d
A152	BFCP029421_2	0.91 ± 27.20	n.d
A153	BFCP029421_2	22.26 ± 4.34	n.d
A154	BFCP029421_2	14.26 ± 4.21	n.d
A155	BFCP029421_2	6.82 ± 10.27	n.d
A156	BFCP029425_2	3.44 ± 9.91	n.d
A157	BFCP029427_2	24.32 ± 2.97	n.d
A158	BFCP029427_2	9.98 ± 2.92	n.d
A159	BFCP029427_2	0.20 ± 22.07	n.d
A160	BFCP029427_2	24.10 ± 13.12	n.d
A161	BFCP029427_2	25.79 ± 3.06	n.d
A162	BFCP029428_2	6.16 ± 2.39	n.d
A163	BFCP029428_2	42.75 ± 18.74	n.d
A164	BFCP029428_2	62.33 ± 15.58	n.d
A165	BFCP029429_2	24.60 ± 3.80	n.d
A166	BFCP029429_2	38.07 ± 4.27	n.d
A167	BFCP029429_2	19.04 ± 3.74	n.d
A168	BFCP029430_2	27.66 ± 16.62	n.d
A169	BFCP029430_2	9.65 ± 12.23	n.d

Compound no.	Plate Barcode	AChEI activity (%) ± SEM	AChEI IC_{50} (µM) ± SEM
A170	BFCP029430_2	14.27 ± 4.47	n.d
A171	BFCP029431_2	1.00 ± 11.69	n.d
A172	BFCP029433_2	8.89 ± 10.21	n.d
A173	BFCP029435_2	19.88 ± 4.78	n.d
A174	BFCP029435_2	20.17 ± 11.01	n.d
A175	**BFCP029435_2**	**65.28 ± 8.20**	**15.37 ± 0.23**
A176	**BFCP029436_2**	**77.08 ± 6.09**	**2.78 ± 0.08**
A177	BFCP029441_2	39.61 ± 2.31	n.d
A178	BFCP029445_2	26.51 ± 4.31	n.d
A179	BFCP029445_2	12.21 ± 11.08	n.d
A180	BFCP029446_2	32.52 ± 8.98	n.d
A181	BFCP029447_2	16.05 ± 5.40	n.d
A182	BFCP029453_2	44.89 ± 2.41	n.d
A183	BFCP029455_2	18.52 ± 2.37	n.d
A184	BFCP029457_2	-5.10 ± 10.49	n.d
A185	BFCP029459_2	12.30 ± 7.61	n.d
A186	BFCP029470_2	9.82 ± 6.53	n.d
A187	BFCP029471_2	2.41 ± 8.58	n.d
A188	BFCP029471_2	-23.16 ± 10.88	n.d
A189	BFCP029477_2	16.71 ± 9.14	n.d
A190	BFCP029477_2	9.75 ± 6.83	n.d
A191	BFCP029478_2	18.45 ± 2.34	n.d
A192	BFCP029480_2	-3.53 ± 10.02	n.d
A193	BFCP029482_2	24.95 ± 2.86	n.d
A194	BFCP029482_2	7.92 ± 4.07	n.d
A195	BFCP029482_2	-2.48 ± 4.03	n.d
A196	BFCP029482_2	-3.86 ± 8.05	n.d
A197	BFCP029482_2	17.74 ± 4.09	n.d
A198	BFCP029486_2	-23.83 ± 9.98	n.d
A199	BFCP029486_2	23.25 ± 5.76	n.d
A200	BFCP029486_2	6.56 ± 4.05	n.d
A201	BFCP029241_2	1.19 ± 5.07	n.d
A202	BFCP029242_2	33.12 ± 4.90	n.d
A203	BFCP029242_2	41.59 ± 2.16	n.d
A204	BFCP029246_2	16.18 ± 3.93	n.d
A205	BFCP029246_2	9.48 ± 5.05	n.d
A206	BFCP029247_2	5.83 ± 3.02	n.d
A207	BFCP029250_2	17.90 ± 3.47	n.d
A208	BFCP029256_2	15.61 ± 4.95	n.d
A209	BFCP029256_2	6.68 ± 4.75	n.d
A210	BFCP029256_2	9.01 ± 5.16	n.d
A211	BFCP029271_2	13.04 ± 6.10	n.d
A212	BFCP029273_2	5.70 ± 5.52	n.d
A213	BFCP029273_2	18.61 ± 4.02	n.d

Compound no.	Plate Barcode	AChEI activity (%) ± SEM	AChEI IC_{50} (µM) ± SEM
A214	BFCP029274_2	13.37 ± 3.01	n.d
A215	BFCP029274_2	4.08 ± 3.70	n.d
A216	BFCP029274_2	9.96 ± 2.82	n.d
A217	BFCP029278_2	20.97 ± 4.20	n.d
A218	BFCP029278_2	11.52 ± 8.36	n.d
A219	BFCP029282_2	21.91 ± 6.62	n.d
A220	BFCP029283_2	19.50 ± 5.62	n.d
A221	BFCP029283_2	18.14 ± 6.24	n.d
A222	BFCP029283_2	7.73 ± 6.66	n.d
A223	BFCP029283_2	20.47 ± 3.10	n.d
A224	BFCP029283_2	14.82 ± 2.61	n.d
A225	BFCP029283_2	11.33 ± 3.00	n.d
A226	BFCP029283_2	6.30 ± 5.49	n.d
A227	BFCP029283_2	21.94 ± 4.63	n.d
A228	BFCP029283_2	16.98 ± 3.10	n.d
A229	BFCP029284_2	16.81 ± 2.70	n.d
A230	BFCP029284_2	16.45 ± 3.42	n.d
A231	BFCP029284_2	20.82 ± 3.18	n.d
A232	BFCP029286_2	12.35 ± 5.32	n.d
A233	BFCP029286_2	15.29 ± 2.36	n.d
A234	BFCP029286_2	12.27 ± 4.10	n.d
A235	BFCP029286_2	26.48 ± 4.98	n.d
A236	BFCP029286_2	14.32 ± 2.54	n.d
A237	BFCP029287_2	16.81 ± 3.65	n.d
A238	BFCP029287_2	16.55 ± 3.40	n.d
A239	BFCP029287_2	16.85 ± 2.89	n.d
A240	BFCP029287_2	9.93 ± 1.94	n.d
A241	BFCP029287_2	9.95 ± 1.00	n.d
A242	BFCP029287_2	10.24 ± 4.70	n.d
A243	BFCP029287_2	22.96 ± 2.56	n.d
A244	BFCP029288_2	10.22 ± 5.00	n.d
A245	BFCP029288_2	16.25 ± 2.21	n.d
A246	BFCP029288_2	18.65 ± 2.37	n.d
A247	BFCP029288_2	32.87 ± 5.96	n.d
A248	BFCP029288_2	23.64 ± 1.80	n.d
A249	BFCP029288_2	20.30 ± 1.10	n.d
A250	BFCP029288_2	7.08 ± 2.92	n.d
A251	BFCP029288_2	6.26 ± 4.53	n.d
A252	BFCP029288_2	6.30 ± 5.17	n.d
A253	BFCP029288_2	-10.81 ± 10.37	n.d
A254	BFCP029288_2	2.47 ± 3.79	n.d
A255	BFCP029288_2	11.23 ± 4.45	n.d
A256	BFCP029288_2	0.77 ± 3.71	n.d
A257	BFCP029289_2	1.23 ± 2.84	n.d

Compound no.	Plate Barcode	AChEI activity (%) ± SEM	AChEI IC_{50} (µM) ± SEM
A258	BFCP029289_2	31.18 ± 6.16	n.d
A259	BFCP029289_2	4.99 ± 3.60	n.d
A260	BFCP029289_2	5.59 ± 3.50	n.d
A261	BFCP029289_2	0.76 ± 2.63	n.d
A262	BFCP029289_2	-1.44 ± 5.53	n.d
A263	BFCP029289_2	4.90 ± 4.17	n.d
A264	BFCP029290_2	0.94 ± 2.67	n.d
A265	BFCP029290_2	-7.91 ± 4.41	n.d
A266	BFCP029290_2	-5.91 ± 7.83	n.d
A267	BFCP029291_2	35.79 ± 3.72	n.d
A268	BFCP029291_2	8.576 ± 2.48	n.d
A269	BFCP029291_2	12.60 ± 3.49	n.d
A270	BFCP029291_2	5.30 ± 5.60	n.d
A271	BFCP029291_2	20.20 ± 4.84	n.d
A272	BFCP029291_2	-0.60 ± 7.06	n.d
A273	BFCP029296_2	8.57 ± 5.57	n.d
A274	BFCP029297_2	1.32 ± 9.46	n.d
A275	BFCP029299_2	20.73 ± 2.33	n.d
A276	BFCP029300_2	3.79 ± 4.06	n.d
A277	BFCP029300_2	10.34 ± 6.59	n.d
A278	BFCP029301_2	4.96 ± 7.11	n.d
A279	BFCP029302_2	-3.63 ± 6.84	n.d
A280	BFCP029302_2	4.73 ± 4.38	n.d
A281	BFCP029303_2	5.40 ± 8.71	n.d
A282	BFCP029303_2	8.15 ± 3.46	n.d
A283	BFCP029303_2	15.29 ± 5.24	n.d
A284	BFCP029314_2	-2.09 ± 7.35	n.d
A285	BFCP029315_2	9.34 ± 4.67	n.d
A286	BFCP029316_2	8.20 ± 8.44	n.d
A287	BFCP029316_2	7.61 ± 3.48	n.d
A288	BFCP029316_2	-6.46 ± 7.67	n.d
A289	BFCP029316_2	2.91 ± 8.18	n.d
A290	BFCP029331_2	7.27 ± 6.42	n.d
A291	BFCP029332_2	7.12 ± 3.64	n.d
A292	BFCP029333_2	-5.58 ± 10.09	n.d
A293	BFCP029333_2	1.28 ± 8.81	n.d
A294	BFCP029333_2	11.68 ± 8.29	n.d
A295	BFCP029334_2	7.77 ± 5.68	n.d
A296	BFCP029337_2	1.88 ± 8.09	n.d
A297	BFCP029343_2	3.32 ± 5.84	n.d
A298	BFCP029347_2	-2.07 ± 15.52	n.d
A299	BFCP029348_2	56.27 ± 2.11	n.d
A300	BFCP029348_2	40.93 ± 4.31	n.d
A301	BFCP029348_2	-6.15 ± 2.59	n.d

Compound no.	Plate Barcode	AChEI activity (%) ± SEM	AChEI IC_{50} (µM) ± SEM
A302	BFCP029349_2	9.71 ± 5.07	n.d
A303	BFCP029351_2	13.42 ± 4.44	n.d
A304	BFCP029351_2	2.35 ± 7.17	n.d
A305	BFCP029351_2	8.19 ± 9.30	n.d
A306	BFCP029351_2	12.88 ± 8.12	n.d
A307	BFCP029351_2	7.57 ± 6.04	n.d
A308	BFCP029351_2	12.38 ± 9.15	n.d
A309	BFCP029351_2	-6.46 ± 8.73	n.d
A310	BFCP029351_2	23.84 ± 4.09	n.d
A311	BFCP029351_2	4.58 ± 6.56	n.d
A312	BFCP029351_2	6.07 ± 2.38	n.d
A313	BFCP029352_2	10.18 ± 5.33	n.d
A314	BFCP029352_2	20.78 ± 3.84	n.d
A315	BFCP029352_2	7.85 ± 3.85	n.d
A316	BFCP029352_2	14.19 ± 2.95	n.d
A317	BFCP029352_2	13.99 ± 6.09	n.d
A318	BFCP029352_2	25.00 ± 2.30	n.d
A319	BFCP029352_2	10.29 ± 2.52	n.d
A320	BFCP029353_2	9.46 ± 3.33	n.d
A321	BFCP029353_2	8.58 ± 3.26	n.d
A322	BFCP029354_2	24.56 ± 3.77	n.d
A323	BFCP029354_2	29.43 ± 2.83	n.d
A324	BFCP029354_2	5.73 ± 5.28	n.d
A325	BFCP029354_2	-15.55 ± 8.72	n.d
A326	BFCP029357_2	57.68 ± 1.60	n.d
A327	BFCP029357_2	12.26 ± 3.87	n.d
A328	BFCP029358_2	8.92 ± 3.27	n.d
A329	BFCP029359_2	-6.86 ± 7.24	n.d
A330	BFCP029359_2	26.92 ± 3.28	n.d
A331	BFCP029359_2	6.56 ± 3.59	n.d
A332	BFCP029366_2	11.16 ± 6.40	n.d
A333	BFCP029366_2	-8.12 ± 5.93	n.d
A334	BFCP029366_2	7.48 ± 4.91	n.d
A335	BFCP029366_2	26.39 ± 2.11	n.d
A336	BFCP029366_2	13.46 ± 6.97	n.d
A337	BFCP029368_2	16.61 ± 5.29	n.d
A338	BFCP029368_2	-8.95 ± 10.34	n.d
A339	BFCP029368_2	17.08 ± 4.50	n.d
A340	BFCP029368_2	12.56 ± 3.49	n.d
A341	BFCP029368_2	13.99 ± 4.65	n.d
A342	BFCP029368_2	18.24 ± 5.33	n.d
A343	BFCP029368_2	15.76 ± 4.78	n.d
A344	BFCP029368_2	12.82 ± 5.24	n.d
A345	BFCP029368_2	13.85 ± 3.32	n.d

Compound no.	Plate Barcode	AChEI activity (%) ± SEM	AChEI IC_{50} (µM) ± SEM
A346	BFCP029368_2	7.69 ± 3.68	n.d
A347	BFCP029369_2	11.92 ± 4.60	n.d
A348	BFCP029369_2	11.05 ± 2.94	n.d
A349	BFCP029369_2	12.55 ± 3.58	n.d
A350	BFCP029385_2	12.32 ± 3.27	n.d
A351	BFCP029390_2	15.66 ± 4.58	n.d
A352	BFCP029394_2	13.45 ± 2.53	n.d
A353	BFCP029395_2	10.19 ± 3.28	n.d
A354	BFCP029395_2	14.02 ± 3.59	n.d
A355	BFCP029395_2	19.04 ± 3.11	n.d
A356	BFCP029395_2	12.99 ± 5.42	n.d
A357	BFCP029395_2	12.18 ± 2.79	n.d
A358	BFCP029396_2	18.30 ± 4.44	n.d
A359	BFCP029396_2	20.93 ± 3.36	n.d
A360	BFCP029396_2	12.80 ± 4.16	n.d
A361	BFCP029401_2	13.51 ± 3.47	n.d
A362	BFCP029409_2	14.23 ± 3.59	n.d
A363	BFCP029410_2	19.28 ± 2.26	n.d
A364	BFCP029411_2	18.73 ± 4.65	n.d
A365	BFCP029418_2	19.72 ± 3.78	n.d
A366	BFCP029421_2	19.99 ± 3.53	n.d
A367	BFCP029422_2	8.85 ± 4.92	n.d
A368	BFCP029422_2	0.59 ± 2.78	n.d
A369	BFCP029422_2	-7.72 ± 5.89	n.d
A370	BFCP029423_2	3.81 ± 5.49	n.d
A371	BFCP029423_2	8.62 ± 4.45	n.d
A372	BFCP029423_2	-2.80 ± 3.56	n.d
A373	BFCP029423_2	7.45 ± 4.54	n.d
A374	BFCP029425_2	-2.12 ± 8.09	n.d
A375	BFCP029428_2	8.83 ± 2.53	n.d
A376	BFCP029428_2	8.93 ± 3.37	n.d
A377	BFCP029432_2	4.51 ± 2.85	n.d
A378	BFCP029432_2	1.85 ± 4.04	n.d
A379	BFCP029433_2	0.56 ± 9.09	n.d
A380	BFCP029440_2	18.53 ± 2.66	n.d
A381	BFCP029446_2	20.79 ± 4.62	n.d
A382	BFCP029448_2	-0.58 ± 3.83	n.d
A383	BFCP029459_2	4.47 ± 6.83	n.d
A384	BFCP029471_2	1.11 ± 4.54	n.d
A385	BFCP029471_2	6.89 ± 1.38	n.d
A386	BFCP029471_2	3.05 ± 4.38	n.d
A387	BFCP029471_2	9.71 ± 5.44	n.d
A388	BFCP029473_2	1.54 ± 3.60	n.d
A389	BFCP029475_2	-0.21 ± 3.83	n.d

Compound no.	Plate Barcode	AChEI activity (%) ± SEM	AChEI IC_{50} (µM) ± SEM
A390	BFCP029476_2	-0.62 ± 2.10	n.d
A391	BFCP029477_2	11.80 ± 8.50	n.d
A392	BFCP029477_2	9.61 ± 2.56	n.d
A393	BFCP029477_2	-0.57 ± 3.83	n.d
A394	BFCP029480_2	5.57 ± 3.66	n.d
A395	BFCP029481_2	9.36 ± 6.89	n.d
A396	BFCP029482_2	0.20 ± 4.14	n.d
A397	BFCP029482_2	10.05 ± 4.78	n.d
A398	BFCP029485_2	15.44 ± 2.61	n.d
A399	BFCP029486_2	11.92 ± 3.19	n.d
A400	BFCP029486_2	30.72 ± 2.84	n.d

AChEI: acetylcholinesterase inhibitory activity; IC_{50}: concentration causing 50% inhibitory effect; n.d: not determined; SEM: standard error of the mean.

Table 11: Acetylcholinesterase inhibitory activity of subset **B** compounds and the associated: number, compound ID, plate barcode. None of the compounds had ≥ 60% acetylcholinesterase inhibitory activity at 5 µM, hence there's no IC_{50} column.

Compound no.	Plate Barcode	AChEI activity (%) ± SEM
B1	BFCP029263_2	19.13 ± 4.85
B2	BFCP029263_2	14.59 ± 6.80
B3	BFCP029263_2	19.20 ± 4.66
B4	BFCP029264_2	20.61 ± 5.28
B5	BFCP029264_2	1.29 ± 5.82
B6	BFCP029264_2	-3.91 ± 3.79
B7	BFCP029264_2	-4.12 ± 4.62
B8	BFCP029264_2	-13.73 ± 5.34
B9	BFCP029264_2	1.84 ± 3.79
B10	BFCP029264_2	-4.44 ± 2.32
B11	BFCP029264_2	7.04 ± 4.94
B12	BFCP029264_2	-6.96 ± 3.34
B13	BFCP029264_2	5.52 ± 5.19
B14	BFCP029264_2	0.21 ± 3.76
B15	BFCP029264_2	-0.41 ± 3.64
B16	BFCP029264_2	-0.36 ± 2.97
B17	BFCP029264_2	22.37 ± 4.52
B18	BFCP029264_2	0.10 ± 2.50
B19	BFCP029264_2	-2.87 ± 3.03
B20	BFCP029264_2	-3.94 ± 3.68
B21	BFCP029264_2	30.08 ± 2.16
B22	BFCP029264_2	0.15 ± 1.92
B23	BFCP029264_2	-1.43 ± 5.19
B24	BFCP029264_2	-7.37 ± 5.22
B25	BFCP029264_2	6.35 ± 5.24
B26	BFCP029264_2	1.53 ± 2.75

Compound no.	Plate Barcode	AChEI activity (%) ± SEM
B27	BFCP029264_2	3.65 ± 4.51
B28	BFCP029264_2	1.73 ± 3.16
B29	BFCP029264_2	36.90 ± 9.82
B30	BFCP029264_2	16.10 ± 2.28
B31	BFCP029264_2	18.60 ± 4.36
B32	BFCP029264_2	7.89 ± 6.69
B33	BFCP029264_2	40.09 ± 9.70
B34	BFCP029264_2	21.99 ± 1.99
B35	BFCP029264_2	21.42 ± 5.37
B36	BFCP029264_2	27.66 ± 5.23
B37	BFCP029264_2	32.96 ± 10.79
B38	BFCP029264_2	40.19 ± 8.32
B39	BFCP029264_2	41.12 ± 1.33
B40	BFCP029264_2	12.26 ± 3.18
B41	BFCP029264_2	44.00 ± 8.40
B42	BFCP029264_2	20.12 ± 3.86
B43	BFCP029264_2	16.42 ± 2.31
B44	BFCP029264_2	16.51 ± 3.20
B45	BFCP029264_2	34.75 ± 9.88
B46	BFCP029264_2	19.02 ± 2.00
B47	BFCP029264_2	22.61 ± 1.78
B48	BFCP029264_2	7.96 ± 4.10
B49	BFCP029264_2	36.15 ± 10.38
B50	BFCP029264_2	22.47 ± 2.56
B51	BFCP029264_2	14.02 ± 1.53
B52	BFCP029264_2	14.88 ± 6.02
B53	BFCP029264_2	33.17 ± 9.16
B54	BFCP029264_2	18.32 ± 2.07
B55	BFCP029264_2	24.12 ± 3.18
B56	BFCP029264_2	14,24 ± 4.29
B57	BFCP029264_2	22.65 ± 4.38
B58	BFCP029264_2	14.01 ± 3.61
B59	BFCP029264_2	41.17 ± 6.46
B60	BFCP029264_2	8.67 ± 7.59
B61	BFCP029264_2	33.14 ± 2.59
B62	BFCP029264_2	14.57 ± 4.10
B63	BFCP029264_2	14.39 ± 3.33
B64	BFCP029264_2	2.96 ± 5.79
B65	BFCP029264_2	12.86 ± 2.59
B66	BFCP029264_2	14.73 ± 1.80
B67	BFCP029264_2	14.68 ± 2.25
B68	BFCP029264_2	15.34 ± 4.96
B69	BFCP029264_2	32.21 ± 1.98
B70	BFCP029264_2	17.28 ± 5.02

Compound no.	Plate Barcode	AChEI activity (%) ± SEM
B71	BFCP029264_2	3.10 ± 5.96
B72	BFCP029264_2	8.58 ± 6.23
B73	BFCP029264_2	11.92 ± 1.23
B74	BFCP029264_2	10.78 ± 4.15
B75	BFCP029264_2	4.49 ± 4.87
B76	BFCP029264_2	14.10 ± 5.32
B77	BFCP029264_2	21.98 ± 3.32
B78	BFCP029264_2	16.55 ± 3.44
B79	BFCP029264_2	6.94 ± 6.51
B80	BFCP029264_2	16.88 ± 2.54
B81	BFCP029264_2	19.66 ± 2.68
B82	BFCP029264_2	12.91 ± 5.15
B83	BFCP029264_2	12.99 ± 5.03
B84	BFCP029265_2	10.71 ± 7.36
B85	BFCP029265_2	17.34 ± 7.28
B86	BFCP029265_2	13.43 ± 7.99
B87	BFCP029265_2	5.74 ± 7.14
B88	BFCP029265_2	-14.26 ± 25.35
B89	BFCP029265_2	14.27 ± 11.67
B90	BFCP029265_2	2.79 ± 9.76
B91	BFCP029265_2	13.59 ± 16.57
B92	BFCP029265_2	3.79 ± 20.22
B93	BFCP029265_2	5.45 ± 11.19
B94	BFCP029265_2	3.59 ± 7.48
B95	BFCP029265_2	-3.22 ± 5.86
B96	BFCP029265_2	-8.55 ± 5.55
B97	BFCP029265_2	2.67 ± 8.98
B98	BFCP029265_2	3.07 ± 8.83
B99	BFCP029265_2	15.13 ± 7.51
B100	BFCP029265_2	5.10 ± 10.22
B101	BFCP029265_2	11.39 ± 9.37
B102	BFCP029265_2	19.39 ± 6.37
B103	BFCP029265_2	12.60 ± 6.00
B104	BFCP029265_2	-36.05 ± 17.99
B105	BFCP029265_2	-9.30 ± 11.05
B106	BFCP029265_2	9.62 ± 8.62
B107	BFCP029265_2	4.30 ± 5.00
B108	BFCP029265_2	-14.19 ± 12.42
B109	BFCP029265_2	12.28 ± 2.73
B110	BFCP029265_2	1.11 ± 4.96
B111	BFCP029265_2	7.50 ± 4.48
B112	BFCP029265_2	-1.83 ± 6.70
B113	BFCP029265_2	9.24 ± 3.13
B114	BFCP029265_2	3.11 ± 4.53

Compound no.	Plate Barcode	AChEI activity (%) ± SEM
B115	BFCP029265_2	11.42 ± 4.62
B116	BFCP029265_2	26.31 ± 3.33
B117	BFCP029265_2	8.56 ± 3.69
B118	BFCP029265_2	0.61 ± 3.11
B119	BFCP029265_2	7.41 ± 4.39
B120	BFCP029265_2	2.42 ± 3.71
B121	BFCP029265_2	13.19 ± 1.81
B122	BFCP029265_2	12.50 ± 1.94
B123	BFCP029265_2	7.64 ± 2.21
B124	BFCP029265_2	-2.13 ± 3.91
B125	BFCP029265_2	12.66 ± 1.31
B126	BFCP029265_2	8.34 ± 1.24
B127	BFCP029265_2	0.28 ± 3.48
B128	BFCP029265_2	-7.03 ± 3.47
B129	BFCP029265_2	9,48 ± 2.21
B130	BFCP029265_2	12.75 ± 3.08
B131	BFCP029265_2	4.09 ± 1.76
B132	BFCP029265_2	-0.81 ± 3.74
B133	BFCP029265_2	11.62 ± 1.52
B134	BFCP029265_2	2.30 ± 3.78
B135	BFCP029265_2	-2.59 ± 3.99
B136	BFCP029265_2	-1.95 ± 3.51
B137	BFCP029265_2	5.09 ± 3.51
B138	BFCP029265_2	9.83 ± 3.71
B139	BFCP029265_2	1.47 ± 3.75
B140	BFCP029265_2	-0.80 ± 2.11
B141	BFCP029265_2	2.47 ± 3.70
B142	BFCP029265_2	-11.02 ± 6.42
B143	BFCP029265_2	-5.55 ± 6.75
B144	BFCP029265_2	-11.72 ± 4.34
B145	BFCP029265_2	-1.26 ± 2.98
B146	BFCP029265_2	-4.30 ± 3.7
B147	BFCP029265_2	-6.22 ± 6.35
B148	BFCP029265_2	-14.76 ± 9.59
B149	BFCP029265_2	3.75 ± 4.38
B150	BFCP029265_2	19.83 ± 6.50
B151	BFCP029265_2	18.53 ± 5.40
B152	BFCP029265_2	0.01 ± 5.73
B153	BFCP029265_2	2.03 ± 2..95
B154	BFCP029265_2	1.21 ± 3.33
B155	BFCP029265_2	-4.45 ± 6.91
B156	BFCP029265_2	-6.83 ± 15.55
B157	BFCP029265_2	6.39 ± 6.70
B158	BFCP029265_2	-12.96 ± 3.75

Compound no.	Plate Barcode	AChEI activity (%) ± SEM
B159	BFCP029265_2	-11.78 ± 7.79
B160	BFCP029265_2	-10.53 ± 5.30
B161	BFCP029265_2	-18.57 ± 11.90
B162	BFCP029265_2	-6.58 ± 2.68
B163	BFCP029265_2	-8.50 ± 9.41
B164	BFCP029266_2	-8.52 ± 3.62
B165	BFCP029266_2	6.53 ± 6.38
B166	BFCP029266_2	4,21 ± 4.09
B167	BFCP029266_2	0.43 ± 9.42
B168	BFCP029266_2	-24.98 ± 13.58
B169	BFCP029266_2	-2.32 ± 6.40
B170	BFCP029266_2	1.33 ± 4.71
B171	BFCP029266_2	2.76 ± 3.29
B172	BFCP029266_2	-14.58 ± 10.83
B173	BFCP029266_2	8.86 ± 3.96
B174	BFCP029266_2	-0.66 ± 4.09
B175	BFCP029266_2	0.42 ± 4.90
B176	BFCP029266_2	-0.98 ± 5.90
B177	BFCP029266_2	7.53 ± 2.83
B178	BFCP029266_2	0.46 ± 4.34
B179	BFCP029266_2	1.23 ± 4.27
B180	BFCP029266_2	-11.35 ± 5.41
B181	BFCP029266_2	13.38 ± 2.22
B182	BFCP029266_2	0.59 ± 4.40
B183	BFCP029266_2	6.50 ± 4.90
B184	BFCP029266_2	-0.18 ± 4.16
B185	BFCP029266_2	6.01 ± 2.75
B186	BFCP029266_2	-1.62 ± 3.68
B187	BFCP029266_2	0.08 ± 2.74
B188	BFCP029266_2	-9.33 ± 6.26
B189	BFCP029266_2	0.47 ± 3.33
B190	BFCP029266_2	-3.69 ± 5.48
B191	BFCP029266_2	9.37 ± 2.79
B192	BFCP029266_2	-11.54 ± 3.43
B193	BFCP029266_2	3.55 ± 2.98
B194	BFCP029266_2	4.35 ± 11.09
B195	BFCP029266_2	-2.01 ± 22.82
B196	BFCP029266_2	-3.84 ± 18.90
B197	BFCP029266_2	21.22 ± 4.48
B198	BFCP029266_2	25.58 ± 3.78
B199	BFCP029266_2	6.94 ± 1.91
B200	BFCP029266_2	4.12 ± 6.57
B201	BFCP029266_2	8.75 ± 4.49
B202	BFCP029266_2	7.39 ± 5.20

Compound no.	Plate Barcode	AChEI activity (%) ± SEM
B203	BFCP029266_2	8,42 ± 2.15
B204	BFCP029266_2	0.89 ± 4.60
B205	BFCP029266_2	17.40 ± 2.66
B206	BFCP029266_2	10.19 ± 4.50
B207	BFCP029266_2	20.11 ± 2.10
B208	BFCP029266_2	6.26 ± 4.61
B209	BFCP029266_2	30.37 ± 3.53
B210	BFCP029266_2	12.18 ± 6.26
B211	BFCP029266_2	9.42 ± 2.23
B212	BFCP029266_2	5.57 ± 3.37
B213	BFCP029266_2	13.98 ± 0.76
B214	BFCP029266_2	7.76 ± 4.52
B215	BFCP029266_2	13.05 ± 2.75
B216	BFCP029266_2	13.43 ± 3.25
B217	BFCP029266_2	20.98 ± 2.04
B218	BFCP029266_2	9.52 ± 3.61
B219	BFCP029266_2	8.12 ± 3.05
B220	BFCP029266_2	2.46 ± 6.99
B221	BFCP029266_2	17.75 ± 1.70
B222	BFCP029266_2	4.59 ± 4.35
B223	BFCP029266_2	27.68 ± 2.48
B224	BFCP029266_2	3.06 ± 3.63
B225	BFCP029266_2	5.40 ± 1.36
B226	BFCP029266_2	0.08 ± 2.82
B227	BFCP029266_2	17.93 ± 4.96
B228	BFCP029266_2	-8.35 ± 3.57
B229	BFCP029266_2	5.67 ± 4.09
B230	BFCP029266_2	-1.97 ± 2.98
B231	BFCP029266_2	-8.37 ± 2.10
B232	BFCP029266_2	-12.19 ± 4.12
B233	BFCP029266_2	9.65 ± 2.84
B234	BFCP029266_2	-1.99 ± 2.22
B235	BFCP029266_2	-0.81 ± 3.68
B236	BFCP029266_2	-26.79 ± 1.43
B237	BFCP029266_2	8.82 ± 2.63
B238	BFCP029266_2	17.10 ± 2.23
B239	BFCP029266_2	-1.61 ± 3.84
B240	BFCP029266_2	-11,02 ± 3.49
B241	BFCP029266_2	8.54 ± 1.54
B242	BFCP029266_2	0.78 ± 2.34
B243	BFCP029267_2	-5.11 ± 3.62
B244	BFCP029267_2	-9.64 ± 3.71
B245	BFCP029267_2	10.95 ± 2.38
B246	BFCP029267_2	6.42 ± 2.08

Compound no.	Plate Barcode	AChEI activity (%) ± SEM
B247	BFCP029267_2	5.69 ± 2.80
B248	BFCP029267_2	-8.03 ± 3.37
B249	BFCP029267_2	2.23 ± 3.95
B250	BFCP029267_2	1.477 ± 5.55
B251	BFCP029267_2	-5.58 ± 5.35
B252	BFCP029267_2	-1.98 ± 3.07
B253	BFCP029267_2	1.35 ± 9.97
B254	BFCP029267_2	2.32 ± 7.06
B255	BFCP029267_2	-2.93 ± 4.24
B256	BFCP029267_2	-8.91 ± 11.51
B257	BFCP029267_2	-1.68 ± 5.34
B258	BFCP029267_2	2.79 ± 6.39
B259	BFCP029267_2	3.37 ± 8.68
B260	BFCP029267_2	-1.10 ± 4.84
B261	BFCP029267_2	8.90 ± 3.21
B262	BFCP029267_2	5.23 ± 14.45
B263	BFCP029267_2	2.23 ± 19.30
B264	BFCP029267_2	-4.44 ± 7.48
B265	BFCP029267_2	17.88 ± 7.35
B266	BFCP029267_2	9.49 ± 15.87
B267	BFCP029267_2	8.40 ± 17.90
B268	BFCP029267_2	-8.62 ± 6.24
B269	BFCP029267_2	0.07 ± 2.68
B270	BFCP029267_2	1.24 ± 9.99
B271	BFCP029267_2	-5.37 ± 22.78
B272	BFCP029267_2	-5.94 ± 2.72
B273	BFCP029267_2	11.17 ± 4.61
B274	BFCP029267_2	5.37 ± 3.94
B275	BFCP029267_2	10.49 ± 2.41
B276	BFCP029267_2	-4.60 ± 8.38
B277	BFCP029267_2	4,90 ± 3.73
B278	BFCP029267_2	0.95 ± 2.42
B279	BFCP029267_2	-3.68 ± 3.19
B280	BFCP029267_2	-6.93 ± 5.60
B281	BFCP029267_2	-3.69 ± 4.69
B282	BFCP029267_2	2.69 ± 3.96
B283	BFCP029267_2	-15.39 ± 5.93
B284	BFCP029267_2	-14.05 ± 7.06
B285	BFCP029267_2	4.87 ± 2.99
B286	BFCP029267_2	-5.66 ± 3.26
B287	BFCP029267_2	-7.66 ± 5.51
B288	BFCP029267_2	-18.90 ± 6.17
B289	BFCP029267_2	-3.33 ± 4.44
B290	BFCP029267_2	-10.56 ± 5.58

Compound no.	Plate Barcode	AChEI activity (%) ± SEM
B291	BFCP029267_2	-9.36 ± 4.57
B292	BFCP029267_2	-20.27 ± 7.54
B293	BFCP029267_2	-1.83 ± 4.73
B294	BFCP029267_2	-6.79 ± 5.51
B295	BFCP029267_2	-13.92 ± 6.00
B296	BFCP029267_2	-23.03 ± 5.12
B297	BFCP029267_2	0.96 ± 5.40
B298	BFCP029267_2	-8.22 ± 2.84
B299	BFCP029267_2	-11.06 ± 3.29
B300	BFCP029267_2	-13.05 ± 7.92
B301	BFCP029267_2	-0.05 ± 5.25
B302	BFCP029267_2	-6.36 ± 5.67
B303	BFCP029267_2	-5.39 ± 3.34
B304	BFCP029267_2	-16.06 ± 5.95
B305	BFCP029267_2	0.23 ± 8.86
B306	BFCP029267_2	-8.90 ± 21.50
B307	BFCP029267_2	-5.14 ± 8.25
B308	BFCP029267_2	-12.15 ± 6.60
B309	BFCP029267_2	12.14 ± 3.49
B310	BFCP029267_2	4.90 ± 2.25
B311	BFCP029267_2	9.04 ± 1.75
B312	BFCP029267_2	8.58 ± 6.52
B313	BFCP029267_2	3.81 ± 2.16
B314	BFCP029267_2	2,83 ± 3.30
B315	BFCP029267_2	-1.81 ± 2.48
B316	BFCP029267_2	-4.86 ± 8.30
B317	BFCP029267_2	6.94 ± 2.93
B318	BFCP029267_2	5.33 ± 3.58
B319	BFCP029267_2	0.41 ± 3.92
B320	BFCP029267_2	-1.33 ± 4.09
B321	BFCP029267_2	10.27 ± 2.65
B322	BFCP029268_2	5.51 ± 4.15
B323	BFCP029268_2	1.47 ± 2.04
B324	BFCP029268_2	5.01 ± 6.41
B325	BFCP029268_2	15.02 ± 1.88
B326	BFCP029268_2	5.39 ± 1.81
B327	BFCP029268_2	5.85 ± 4.78
B328	BFCP029268_2	8.03 ± 2.25
B329	BFCP029268_2	11.85 ± 3.77
B330	BFCP029268_2	15.70 ± 2.98
B331	BFCP029268_2	5.74 ± 4.83
B332	BFCP029268_2	3.03 ± 6.26
B333	BFCP029268_2	9.23 ± 3.69
B334	BFCP029268_2	-1.03 ± 3.46

Compound no.	Plate Barcode	AChEI activity (%) ± SEM
B335	BFCP029268_2	-1.73 ± 6.86
B336	BFCP029268_2	2.28 ± 5.48
B337	BFCP029268_2	23.06 ± 2.21
B338	BFCP029268_2	16.87 ± 1.78
B339	BFCP029268_2	17.74 ± 4.51
B340	BFCP029268_2	10.05 ± 3.50
B341	BFCP029268_2	20.95 ± 3.97
B342	BFCP029268_2	11.21 ± 4.98
B343	BFCP029268_2	15.40 ± 5.27
B344	BFCP029268_2	13.61 ± 5.43
B345	BFCP029268_2	21.55 ± 2.94
B346	BFCP029268_2	16.46 ± 3.75
B347	BFCP029268_2	17.88 ± 3.97
B348	BFCP029268_2	29.90 ± 4.48
B349	BFCP029268_2	47.66 ± 4.03
B350	BFCP029268_2	21.55 ± 3.48
B351	BFCP029268_2	23,68 ± 6.40
B352	BFCP029268_2	10.62 ± 6.16
B353	BFCP029268_2	29.40 ± 4.98
B354	BFCP029268_2	17.74 ± 3.55
B355	BFCP029268_2	16.87 ± 2.81
B356	BFCP029268_2	13.21 ± 5.72
B357	BFCP029268_2	20.90 ± 4.73
B358	BFCP029268_2	24.36 ± 2.93
B359	BFCP029268_2	18.09 ± 2.59
B360	BFCP029268_2	13.67 ± 5.00
B361	BFCP029268_2	25.66 ± 3.46
B362	BFCP029268_2	24.46 ± 3.25
B363	BFCP029268_2	28.94 ± 3.86
B364	BFCP029268_2	24.33 ± 3.71
B365	BFCP029268_2	16.01 ± 3.79
B366	BFCP029268_2	0.46 ± 3.29
B367	BFCP029268_2	3.22 ± 2.48
B368	BFCP029268_2	11.80 ± 5.88
B369	BFCP029268_2	14.46 ± 4.12
B370	BFCP029268_2	-4.74 ± 2.58
B371	BFCP029268_2	4.56 ± 3.26
B372	BFCP029268_2	6.01 ± 3.63
B373	BFCP029268_2	21.55 ± 2.99
B374	BFCP029268_2	5.90 ± 1.42
B375	BFCP029268_2	7.82 ± 2.42
B376	BFCP029268_2	-1.05 ± 2.81
B377	BFCP029268_2	12.80 ± 3.15
B378	BFCP029268_2	8.20 ± 2.96

Compound no.	Plate Barcode	AChEI activity (%) ± SEM
B379	BFCP029268_2	3.46 ± 5.34
B380	BFCP029268_2	4.14 ± 4.58
B381	BFCP029268_2	15.73 ± 3.08
B382	BFCP029268_2	2.79 ± 3.19
B383	BFCP029268_2	4.52 ± 3.53
B384	BFCP029268_2	18.90 ± 4.74
B385	BFCP029268_2	16.26 ± 3.44
B386	BFCP029268_2	1.86 ± 2.90
B387	BFCP029268_2	8,72 ± 4.07
B388	BFCP029268_2	5.12 ± 5.74
B389	BFCP029268_2	20.94 ± 4.10
B390	BFCP029268_2	5.85 ± 2.00
B391	BFCP029268_2	15.84 ± 2.95
B392	BFCP029268_2	13.77 ± 2.78
B393	BFCP029268_2	20.54 ± 10.79
B394	BFCP029268_2	13.21 ± 6.49
B395	BFCP029268_2	6.15 ± 7.35
B396	BFCP029268_2	6.60 ± 7.55
B397	BFCP029268_2	16.90 ± 12.97
B398	BFCP029268_2	13.75 ± 8.23
B399	BFCP029268_2	6.89 ± 6.90
B400	BFCP029268_2	-5.67 ± 7.59
B401	BFCP029269_2	15.67 ± 11.96
B402	BFCP029269_2	6.65 ± 7.17
B403	BFCP029269_2	5.86 ± 7.11
B404	BFCP029269_2	5.32 ± 3.55
B405	BFCP029269_2	9.716 ± 11.02
B406	BFCP029269_2	14.44 ± 5.90
B407	BFCP029269_2	0.76 ± 6.08
B408	BFCP029269_2	-2.35 ± 5.30
B409	BFCP029269_2	10.97 ± 8.51
B410	BFCP029269_2	7.66 ± 7.18
B411	BFCP029269_2	-0.92 ± 6.61
B412	BFCP029269_2	0.11 ± 7.01
B413	BFCP029269_2	13.93 ± 8.52
B414	BFCP029269_2	13.10 ± 7.91
B415	BFCP029269_2	4.45 ± 6.55
B416	BFCP029269_2	-2.92 ± 11.66
B417	BFCP029269_2	19.38 ± 6.91
B418	BFCP029269_2	19.51 ± 6.29
B419	BFCP029269_2	2.34 ± 5.41
B420	BFCP029269_2	-4.10 ± 10.68
B421	BFCP029269_2	16.67 ± 2.90
B422	BFCP029269_2	6.22 ± 2.61

Compound no.	Plate Barcode	AChEI activity (%) ± SEM
B423	BFCP029269_2	3.62 ± 4.59
B424	BFCP029269_2	-0,04 ± 5.10
B425	BFCP029269_2	7.63 ± 5.72
B426	BFCP029269_2	1.28 ± 3.27
B427	BFCP029269_2	0.76 ± 3.25
B428	BFCP029269_2	-0.60 ± 2.48
B429	BFCP029269_2	5.48 ± 5.41
B430	BFCP029269_2	-0.32 ± 2.35
B431	BFCP029269_2	-1.62 ± 2.07
B432	BFCP029269_2	-2.43 ± 3.85
B433	BFCP029269_2	6.19 ± 3.92
B434	BFCP029269_2	-1.02 ± 2.45
B435	BFCP029269_2	2.84 ± 3.46
B436	BFCP029269_2	5.88 ± 4.66
B437	BFCP029269_2	2.68 ± 7.14
B438	BFCP029269_2	2.00 ± 4.93
B439	BFCP029269_2	0.53 ± 5.29
B440	BFCP029269_2	3.97 ± 6.59
B441	BFCP029269_2	36.63 ± 5.66
B442	BFCP029269_2	10.77 ± 5.18
B443	BFCP029269_2	0.90 ± 5.38
B444	BFCP029269_2	7.96 ± 7.15
B445	BFCP029269_2	5.71 ± 3.63
B446	BFCP029269_2	2.98 ± 2.48
B447	BFCP029269_2	-0.99 ± 3.00
B448	BFCP029269_2	0.48 ± 3.28
B449	BFCP029269_2	19.88 ± 7.50
B450	BFCP029269_2	12.83 ± 4.61
B451	BFCP029269_2	20.96 ± 5.76
B452	BFCP029269_2	8.22 ± 6.85
B453	BFCP029269_2	17.37 ± 4.24
B454	BFCP029269_2	7.14 ± 2.52
B455	BFCP029269_2	-0.50 ± 5.18
B456	BFCP029269_2	3.69 ± 4.07
B457	BFCP029269_2	13.03 ± 5.88
B458	BFCP029269_2	6.06 ± 2.70
B459	BFCP029269_2	17.76 ± 3.47
B460	BFCP029269_2	4.68 ± 6.68
B461	BFCP029269_2	19.26 ± 5.44
B462	BFCP029269_2	-3.42 ± 3.56
B463	BFCP029269_2	7.19 ± 7.18
B464	BFCP029269_2	-0.85 ± 8.28
B465	BFCP029269_2	2.98 ± 5.67
B466	BFCP029269_2	10.79 ± 5.08

Compound no.	Plate Barcode	AChEI activity (%) ± SEM
B467	BFCP029269_2	14.57 ± 4.59
B468	BFCP029269_2	0.33 ± 6.23
B469	BFCP029269_2	11.46 ± 9.59
B470	BFCP029269_2	5.02 ± 5.63
B471	BFCP029269_2	2.16 ± 4.58
B472	BFCP029269_2	4.07 ± 3.23
B473	BFCP029269_2	8.17 ± 2.28
B474	BFCP029269_2	7.84 ± 1.96
B475	BFCP029269_2	7.35 ± 4.38
B476	BFCP029269_2	9.72 ± 3.01
B477	BFCP029269_2	3.32 ± 2.46
B478	BFCP029269_2	2.80 ± 3.28
B479	BFCP029269_2	-4.92 ± 2.93
B480	BFCP029270_2	-6.17 ± 7.33
B481	BFCP029270_2	2.09 ± 3.97
B482	BFCP029270_2	12.36 ± 3.49
B483	BFCP029270_2	1.57 ± 3.79
B484	BFCP029270_2	-0.90 ± 3.61
B485	BFCP029270_2	-8.46 ± 4.24
B486	BFCP029270_2	-2.08 ± 1.38
B487	BFCP029270_2	5.41 ± 2.42
B488	BFCP029270_2	-1.67 ± 4.18
B489	BFCP029270_2	5.71 ± 2.85
B490	BFCP029270_2	-8.52 ± 2.78
B491	BFCP029270_2	-3.79 ± 5.89
B492	BFCP029270_2	5.52 ± 3.34
B493	BFCP029270_2	-4.00 ± 2.90
B494	BFCP029270_2	-6.29 ± 5.06
B495	BFCP029270_2	-12.16 ± 4.52
B496	BFCP029270_2	50.87 ± 2.40
B497	BFCP029270_2	4.71 ± 4.86
B498	BFCP029270_2	-5.46 ± 3.54
B499	BFCP029270_2	-5.62 ± 2.14
B500	BFCP029270_2	8.12 ± 5.95
B501	BFCP029270_2	-6.74 ± 3.98
B502	BFCP029270_2	-6.76 ± 2.90
B503	BFCP029270_2	-16.26 ± 6.46
B504	BFCP029270_2	1.21 ± 3.06
B505	BFCP029270_2	6.60 ± 3.83
B506	BFCP029270_2	5.21 ± 2.83
B507	BFCP029270_2	19.80 ± 2.15
B508	BFCP029270_2	18.80 ± 3.72

AChE: acetylcholinesterase; SEM: standard error of the mean

Table 12: Acetylcholinesterase inhibitory activity of subset **C** compounds and the associated: number and plate barcode. Bold rows indicate compounds with ≥ 60% AChEI activity at 5 µM.

Compound no.	Plate Barcode	AChEI activity (%) ± SEM	AChEI IC_{50} (µM) ± SEM
C1	BFCP029353_2	33.49 ± 6.00	n.d
C2	BFCP029353_2	11.67 ± 4.51	n.d
C3	BFCP029353_2	22.55 ± 2.91	n.d
C4	BFCP029353_2	-2.24 ± 5.96	n.d
C5	BFCP029353_2	1.32 ± 3.64	n.d
C6	BFCP029353_2	-6.47 ± 1.54	n.d
C7	BFCP029353_2	6.34 ± 5.34	n.d
C8	BFCP029353_2	-0.91 ± 4.97	n.d
C9	BFCP029353_2	0.49 ± 2.26	n.d
C10	BFCP029353_2	-4.60 ± 2.19	n.d
C11	BFCP029353_2	34.73 ± 3.38	n.d
C12	BFCP029353_2	-0.85 ± 4.90	n.d
C13	BFCP029353_2	-6.30 ± 2.82	n.d
C14	BFCP029353_2	-4.26 ± 5.20	n.d
C15	BFCP029353_2	1.82 ± 7.25	n.d
C16	BFCP029353_2	-4.00 ± 4.20	n.d
C17	BFCP029353_2	-9.59 ± 3.65	n.d
C18	BFCP029353_2	-6.67 ± 4.53	n.d
C19	BFCP029353_2	-3.12 ± 4.78	n.d
C20	BFCP029353_2	-9.61 ± 2.06	n.d
C21	BFCP029353_2	-0.19 ± 3.82	n.d
C22	BFCP029353_2	36.93 ± 2.71	n.d
C23	BFCP029353_2	5.48 ± 5.84	n.d
C24	BFCP029353_2	-5.96 ± 2.83	n.d
C25	BFCP029353_2	-5.39 ± 3.25	n.d
C26	BFCP029353_2	-0.47 ± 5.00	n.d
C27	BFCP029353_2	1.50 ± 3.22	n.d
C28	BFCP029353_2	-6.08 ± 2.96	n.d
C29	BFCP029353_2	16.71 ± 9.24	n.d
C30	BFCP029353_2	6.80 ± 8.22	n.d
C31	BFCP029353_2	17.18 ± 6.63	n.d
C32	BFCP029353_2	58.27 ± 6.34	n.d
C33	**BFCP029353_2**	**62.77 ± 3.50**	**3.71 ± 014**
C34	BFCP029353_2	7.11 ± 8.22	n.d
C35	BFCP029353_2	14.18 ± 5.50	n.d
C36	BFCP029353_2	10.52 ± 5.70	n.d
C37	BFCP029353_2	15.15 ± 6.61	n.d
C38	BFCP029353_2	3.04 ± 6.68	n.d
C39	BFCP029353_2	7.93 ± 6.38	n.d
C40	BFCP029353_2	5.88 ± 8.21	n.d
C41	BFCP029353_2	12.54 ± 5.99	n.d

Compound no.	Plate Barcode	AChEI activity (%) ± SEM	AChEI IC_{50} (µM) ± SEM
C42	BFCP029353_2	30.62 ± 4.93	n.d
C43	**BFCP029353_2**	**72.16 ± 3.13**	**3.37 ± 0.11**
C44	BFCP029353_2	-6.41 ± 8.62	n.d
C45	BFCP029353_2	7.94 ± 6.30	n.d
C46	BFCP029353_2	-1.99 ± 7.455	n.d
C47	BFCP029353_2	3.20 ± 6.67	n.d
C48	BFCP029353_2	-1.75 ± 6.56	n.d
C49	BFCP029353_2	11.99 ± 7.03	n.d
C50	BFCP029353_2	-2.76 ± 7.19	n.d
C51	BFCP029353_2	3.11 ± 7.94	n.d
C52	BFCP029353_2	-0.36 ± 6.65	n.d
C53	**BFCP029353_2**	**63.41 ±1.89**	**3.36 ± 0.12**
C54	BFCP029353_2	3.03 ± 6.60	n.d
C55	BFCP029353_2	0.36 ± 6.19	n.d
C56	BFCP029353_2	0,11 ± 8.42	n.d
C57	BFCP029353_2	19.48 ± 5.94	n.d
C58	BFCP029353_2	7.82 ± 8.74	n.d
C59	BFCP029353_2	6.46 ± 12.19	n.d
C60	BFCP029353_2	34.46 ± 7.84	n.d
C61	BFCP029353_2	26.38 ± 3.07	n.d
C62	BFCP029353_2	23.26 ± 4.01	n.d
C63	BFCP029353_2	16.01 ± 6.61	n.d
C64	BFCP029353_2	7.23 ± 5.77	n.d
C65	BFCP029353_2	10.86 ± 7.39	n.d
C66	BFCP029353_2	16.40 ± 7.77	n.d
C67	BFCP029353_2	2.94 ± 11.29	n.d
C68	BFCP029353_2	9.67 ± 6.30	n.d
C69	BFCP029353_2	25.46 ± 5.75	n.d
C70	BFCP029353_2	29.41 ± 8.10	n.d
C71	BFCP029353_2	11.46 ± 6.63	n.d
C72	BFCP029353_2	14.54 ± 8.32	n.d
C73	BFCP029353_2	24.29 ± 6.08	n.d
C74	BFCP029353_2	10.42 ± 7.31	n.d
C75	BFCP029354_2	9.41 ± 8.49	n.d
C76	BFCP029354_2	8.44 ± 5.90	n.d
C77	BFCP029354_2	22.57 ± 3.59	n.d
C78	BFCP029354_2	19.27 ± 3.50	n.d
C79	BFCP029354_2	14.87 ± 3.53	n.d
C80	BFCP029354_2	23.72 ± 3.65	n.d
C81	BFCP029354_2	10.45 ± 5.34	n.d
C82	**BFCP029354_2**	**68.66 ± 1.86**	**7.34 ± 0.14**
C83	BFCP029354_2	6.68 ± 12.17	n.d
C84	BFCP029354_2	8.73 ± 5.47	n.d
C85	BFCP029354_2	4.36 ± 10.09	n.d

Compound no.	Plate Barcode	AChEI activity (%) ± SEM	AChEI IC_{50} (µM) ± SEM
C86	BFCP029354_2	2.08 ± 9.25	n.d
C87	BFCP029354_2	-2.94 ± 9.86	n.d
C88	BFCP029354_2	2.01 ± 10.28	n.d
C89	BFCP029354_2	47.26 ± 7.08	n.d
C90	BFCP029354_2	4.09 ± 8.26	n.d
C91	BFCP029354_2	1.09 ± 9.11	n.d
C92	BFCP029354_2	-2.35 ± 7.78	n.d
C93	BFCP029354_2	3.27 ± 8.55	n.d
C94	BFCP029354_2	-7.05 ± 7.90	n.d
C95	BFCP029354_2	-8.93 ± 8.36	n.d
C96	BFCP029354_2	2.21 ± 8.40	n.d
C97	BFCP029354_2	-12.61 ± 14.02	n.d
C98	BFCP029354_2	-3.04 ± 12.24	n.d
C99	BFCP029354_2	-13.62 ± 11.14	n.d
C100	BFCP029354_2	32.01 ± 5.54	n.d
C101	BFCP029354_2	1.95 ± 10.33	n.d
C102	BFCP029354_2	9.33 ± 10.48	n.d
C103	BFCP029354_2	3.33 ± 9.97	n.d
C104	BFCP029354_2	1.76 ± 7.60	n.d
C105	BFCP029354_2	0.56 ± 11.16	n.d
C106	BFCP029354_2	-8.07 ± 9.30	n.d
C107	BFCP029354_2	-0.53 ± 10.01	n.d
C108	BFCP029354_2	-0.77 ± 8.59	n.d
C109	BFCP029354_2	6.12 ± 13.22	n.d
C110	BFCP029354_2	7.36 ± 12.75	n.d
C111	BFCP029354_2	22.46 ± 8.72	n.d
C112	BFCP029354_2	11.56 ± 7.60	n.d
C113	BFCP029354_2	14.07 ± 5.77	n.d
C114	BFCP029354_2	16.64 ± 1.92	n.d
C115	BFCP029354_2	8.81 ± 2.89	n.d
C116	BFCP029354_2	3.16 ± 4.68	n.d
C117	BFCP029354_2	6.08 ± 2.50	n.d
C118	BFCP029354_2	26.95 ± 2.98	n.d
C119	BFCP029354_2	7.92 ± 1.36	n.d
C120	BFCP029354_2	18.07 ± 0.79	n.d
C121	BFCP029354_2	6.53 ± 2.14	n.d
C122	BFCP029354_2	8.97 ± 3.33	n.d
C123	BFCP029354_2	10.23 ± 1.84	n.d
C124	BFCP029354_2	2.67 ± 3.37	n.d
C125	BFCP029354_2	6.75 ± 4.57	n.d
C126	BFCP029354_2	10.69 ± 3.68	n.d
C127	BFCP029354_2	3.53 ± 3.24	n.d
C128	BFCP029354_2	25.78 ± 2.83	n.d
C129	**BFCP029354_2**	**65.03 ± 1.75**	**12.52 ± 0.12**

Compound no.	Plate Barcode	AChEI activity (%) ± SEM	AChEI IC_{50} (µM) ± SEM
C130	BFCP029354_2	7.49 ± 4.55	n.d
C131	BFCP029354_2	17.00 ± 2.04	n.d
C132	BFCP029354_2	6.30 ± 4.01	n.d
C133	BFCP029354_2	6.73 ± 3.82	n.d
C134	BFCP029354_2	5.74 ± 2.82	n.d
C135	BFCP029354_2	5.94 ± 2.72	n.d
C136	BFCP029354_2	7.33 ± 2.03	n.d
C137	BFCP029354_2	4.58 ± 3.92	n.d
C138	BFCP029354_2	3.51 ± 2.38	n.d
C139	BFCP029354_2	-0.54 ± 2.14	n.d
C140	BFCP029354_2	13.70 ± 4.20	n.d
C141	BFCP029354_2	17.07 ± 7.64	n.d
C142	BFCP029354_2	-4.70 ± 7.56	n.d
C143	BFCP029354_2	-13.70 ± 8.57	n.d
C144	BFCP029354_2	0.90 ± 10.55	n.d
C145	BFCP029354_2	16.04 ± 13.72	n.d
C146	BFCP029354_2	2.43 ± 3.58	n.d
C147	BFCP029354_2	-14.87 ± 10.82	n.d
C148	BFCP029354_2	-27.07 ± 16.23	n.d
C149	BFCP029354_2	10.32 ± 1.03	n.d
C150	BFCP029354_2	-8.08 ± 5.50	n.d
C151	BFCP029354_2	9.70 ± 9.85	n.d
C152	BFCP029354_2	-27.10 ± 11.93	n.d
C153	BFCP029354_2	0.37 ± 5.75	n.d
C154	BFCP029354_2	-28.48 ± 14.92	n.d
C155	BFCP029355_2	-22.79 ± 11.13	n.d
C156	BFCP029355_2	-30.45 ± 15.44	n.d
C157	BFCP029355_2	-3.44 ± 10.14	n.d
C158	BFCP029355_2	-24.61 ± 13.24	n.d
C159	BFCP029355_2	-26.81 ± 15.33	n.d
C160	BFCP029355_2	-41.14 ± 20.50	n.d
C161	BFCP029355_2	-25.02 ± 12.88	n.d
C162	BFCP029355_2	-25.65 ± 13.39	n.d
C163	BFCP029355_2	-60.54 ± 14.30	n.d
C164	BFCP029355_2	-38.66 ± 17.29	n.d
C165	BFCP029355_2	-5.31 ± 14.10	n.d
C166	BFCP029355_2	20,59 ± 11.09	n.d
C167	BFCP029355_2	-35.46 ± 22.82	n.d
C168	BFCP029355_2	-48.43 ± 18.90	n.d
C169	BFCP029355_2	9.99 ± 4.48	n.d
C170	BFCP029355_2	8.75 ± 3.78	n.d
C171	BFCP029355_2	8.98 ± 1.91	n.d
C172	BFCP029355_2	19.13 ± 6.57	n.d
C173	BFCP029355_2	14.22 ± 4.49	n.d

Compound no.	Plate Barcode	AChEI activity (%) ± SEM	AChEI IC_{50} (µM) ± SEM
C174	BFCP029355_2	18.20 ± 5.20	n.d
C175	BFCP029355_2	55.27 ± 2.15	n.d
C176	BFCP029355_2	-0.11 ± 4.60	n.d
C177	BFCP029355_2	23.68 ± 2.66	n.d
C178	BFCP029355_2	8.96 ± 4.50	n.d
C179	BFCP029355_2	9.98 ± 2.10	n.d
C180	BFCP029355_2	6.44 ± 4.61	n.d
C181	BFCP029355_2	7.20 ± 3.53	n.d
C182	BFCP029355_2	-0.89 ± 6.26	n.d
C183	BFCP029355_2	24.28 ± 2.23	n.d
C184	BFCP029355_2	21.45 ± 3.37	n.d
C185	BFCP029355_2	56.94 ± 0.76	n.d
C186	BFCP029355_2	12.68 ± 4.52	n.d
C187	BFCP029355_2	2.47 ± 2.75	n.d
C188	BFCP029355_2	4.89 ± 3.25	n.d
C189	**BFCP029355_2**	**69.00 ± 2.04**	**4.49 ± 0.08**
C190	BFCP029355_2	8.85 ± 3.61	n.d
C191	BFCP029355_2	0.55 ± 3.05	n.d
C192	BFCP029355_2	10.67 ± 6.99	n.d
C193	BFCP029355_2	33.20 ± 1.70	n.d
C194	BFCP029355_2	-1.54 ± 4.35	n.d
C195	BFCP029355_2	6.31 ± 2.48	n.d
C196	BFCP029355_2	23.10 ± 3.63	n.d
C197	BFCP029355_2	17.55 ± 1.36	n.d
C198	BFCP029355_2	16.01 ± 2.82	n.d
C199	BFCP029355_2	17.32 ± 4.96	n.d
C200	BFCP029355_2	27.31 ± 3.57	n.d
C201	BFCP029355_2	25.53 ± 4.09	n.d
C202	BFCP029355_2	13.87 ± 2.98	n.d
C203	BFCP029355_2	15.17 ± 2.10	n.d
C204	BFCP029355_2	19.72 ± 4.12	n.d
C205	BFCP029355_2	22.19 ± 2.84	n.d
C206	BFCP029355_2	17.30 ± 2.22	n.d
C207	BFCP029355_2	16.70 ± 3.68	n.d
C208	BFCP029355_2	15.29 ± 1.43	n.d
C209	BFCP029355_2	27.71 ± 2.63	n.d
C210	BFCP029355_2	15.94 ± 2.23	n.d
C211	BFCP029355_2	13.19 ± 3.84	n.d
C212	BFCP029355_2	10.29 ± 3.49	n.d
C213	BFCP029355_2	20.64 ± 1.54	n.d
C214	BFCP029355_2	24.14 ± 2.34	n.d
C215	BFCP029355_2	11.16 ± 3.62	n.d
C216	BFCP029355_2	1.98 ± 3.71	n.d
C217	BFCP029355_2	24.16 ± 2.38	n.d

Compound no.	Plate Barcode	AChEI activity (%) ± SEM	AChEI IC_{50} (µM) ± SEM
C218	BFCP029355_2	15.53 ± 2.08	n.d
C219	BFCP029355_2	20.14 ± 2.80	n.d
C220	BFCP029355_2	13.96 ± 3.37	n.d
C221	BFCP029355_2	11.79 ± 3.95	n.d
C222	BFCP029355_2	0.77 ± 5.55	n.d
C223	BFCP029355_2	16.32 ± 5.35	n.d
C224	BFCP029355_2	19.18 ± 3.07	n.d
C225	BFCP029355_2	11.22 ± 9.97	n.d
C226	BFCP029355_2	-0.03 ± 7.06	n.d
C227	BFCP029355_2	10.93 ± 4.24	n.d
C228	BFCP029355_2	-17.30 ± 11.51	n.d
C229	BFCP029355_2	8.54 ± 5.34	n.d
C230	BFCP029355_2	0.42 ± 6.39	n.d
C231	BFCP029355_2	-3.84 ± 8.68	n.d
C232	BFCP029355_2	-6.93 ± 4.84	n.d
C233	BFCP029355_2	21.58 ± 3.21	n.d
C234	BFCP029355_2	-12.27 ± 14.45	n.d
C235	BFCP029356_2	-26.47 ± 19.30	n.d
C236	BFCP029356_2	2.61 ± 7.48	n.d
C237	BFCP029356_2	25.66 ± 7.35	n.d
C238	BFCP029356_2	-14.37 ± 15.87	n.d
C239	BFCP029356_2	-22.72 ± 17.90	n.d
C240	BFCP029356_2	9.46 ± 6.24	n.d
C241	BFCP029356_2	18.12 ± 2.68	n.d
C242	BFCP029356_2	-6.84 ± 9.99	n.d
C243	BFCP029356_2	-33.52 ± 22.78	n.d
C244	BFCP029356_2	12.26 ± 2.72	n.d
C245	BFCP029356_2	15.86 ± 4.16	n.d
C246	BFCP029356_2	9.48 ± 3.91	n.d
C247	BFCP029356_2	9.24 ± 2.41	n.d
C248	BFCP029356_2	-1.34 ± 8.38	n.d
C249	BFCP029356_2	4.94 ± 3.73	n.d
C250	BFCP029356_2	7.20 ± 2.42	n.d
C251	BFCP029356_2	10.75 ± 3.19	n.d
C252	BFCP029356_2	-1.93 ± 5.60	n.d
C253	BFCP029356_2	24.58 ± 4.69	n.d
C254	BFCP029356_2	25.41 ± 3.96	n.d
C255	BFCP029356_2	20.60 ± 5.93	n.d
C256	BFCP029356_2	12.36 ± 7.06	n.d
C257	BFCP029356_2	42.38 ± 2.99	n.d
C258	BFCP029356_2	24.66 ± 3.26	n.d
C259	BFCP029356_2	25.93 ± 5.51	n.d
C260	BFCP029356_2	19.65 ± 6.17	n.d
C261	BFCP029356_2	31.14 ± 4.44	n.d

Compound no.	Plate Barcode	AChEI activity (%) ± SEM	AChEI IC_{50} (µM) ± SEM
C262	BFCP029356_2	27.01 ± 5.58	n.d
C263	BFCP029356_2	26.66 ± 4.57	n.d
C264	BFCP029356_2	14.80 ± 7.54	n.d
C265	BFCP029356_2	25.61 ± 4.73	n.d
C266	BFCP029356_2	21.91 ± 5.51	n.d
C267	BFCP029356_2	16.85 ± 6.00	n.d
C268	BFCP029356_2	13.85 ± 5.12	n.d
C269	BFCP029356_2	20.23 ± 5.40	n.d
C270	BFCP029356_2	33.96 ± 2.84	n.d
C271	BFCP029356_2	22.49 ±3.29	n.d
C272	BFCP029356_2	17.27 ± 7.92	n.d
C273	BFCP029356_2	24.33 ± 5.25	n.d
C274	BFCP029356_2	19.04 ± 5.67	n.d
C275	BFCP029356_2	18,60 ± 3.34	n.d
C276	BFCP029356_2	13.97 ± 5.95	n.d
C277	BFCP029356_2	19.49 ± 8.86	n.d
C278	BFCP029356_2	17.39 ± 21.50	n.d
C279	BFCP029356_2	8.95 ± 8.25	n.d
C280	BFCP029356_2	11.90 ± 6.60	n.d
C281	BFCP029356_2	16.23 ± 3.49	n.d
C282	BFCP029356_2	14.41 ± 2.25	n.d
C283	BFCP029356_2	9.13 ± 1.75	n.d
C284	BFCP029356_2	8.35 ± 6.52	n.d
C285	BFCP029356_2	9.76 ± 2.16	n.d
C286	BFCP029356_2	8.99 ± 3.30	n.d
C287	BFCP029356_2	3.62 ± 2.48	n.d
C288	BFCP029356_2	11.22 ± 8.30	n.d
C289	BFCP029356_2	18.77 ± 2.93	n.d
C290	BFCP029356_2	7.99 ± 3.58	n.d
C291	BFCP029356_2	7.80 ± 3.92	n.d
C292	BFCP029356_2	14.14 ± 4.09	n.d
C293	BFCP029356_2	10.78 ± 2.65	n.d
C294	BFCP029356_2	7.56 ± 4.15	n.d
C295	BFCP029356_2	11.42 ± 2.04	n.d
C296	BFCP029356_2	20.96 ± 6.41	n.d
C297	BFCP029356_2	10.15 ± 1.88	n.d
C298	BFCP029356_2	15.21 ± 1.81	n.d
C299	BFCP029356_2	3.36 ± 4.78	n.d
C300	BFCP029356_2	17.14 ± 2.25	n.d
C301	BFCP029356_2	6.95 ± 3.77	n.d
C302	BFCP029356_2	5.33 ± 2.98	n.d
C303	BFCP029356_2	3.12 ± 4.83	n.d
C304	BFCP029356_2	5.58 ± 6.26	n.d
C305	BFCP029356_2	10.13 ± 3.69	n.d

Compound no.	Plate Barcode	AChEI activity (%) ± SEM	AChEI IC_{50} (µM) ± SEM
C306	BFCP029356_2	10.65 ± 3.46	n.d
C307	BFCP029356_2	6.73 ± 6.86	n.d
C308	BFCP029356_2	8.38 ± 5.48	n.d
C309	BFCP029356_2	12.27 ± 2.21	n.d
C310	BFCP029356_2	10.13 ± 1.78	n.d
C311	BFCP029356_2	-4.55 ± 4.51	n.d
C312	BFCP029356_2	1,78 ± 3.50	n.d
C313	BFCP029356_2	16.60 ± 3.97	n.d
C314	BFCP029357_2	2.57 ± 4.98	n.d
C315	BFCP029357_2	4.57 ± 5.27	n.d
C316	BFCP029357_2	-11.93 ± 5.27	n.d
C317	BFCP029357_2	8.10 ± 5.43	n.d
C318	BFCP029357_2	1.84 ± 2.94	n.d
C319	BFCP029357_2	10.59 ± 3.75	n.d
C320	BFCP029357_2	-0.65 ± 3.97	n.d
C321	BFCP029357_2	6.84 ± 4.48	n.d
C322	BFCP029357_2	18.65 ± 4.03	n.d
C323	BFCP029357_2	2.63 ± 3.48	n.d
C324	BFCP029357_2	13.66 ± 6.40	n.d
C325	BFCP029357_2	14.93 ± 6.16	n.d
C326	BFCP029357_2	6.73 ± 4.98	n.d
C327	BFCP029357_2	4.91 ± 3.55	n.d
C328	BFCP029357_2	17.37 ± 2.81	n.d
C329	BFCP029357_2	16.82 ± 5.72	n.d
C330	BFCP029357_2	17.22 ± 4.73	n.d
C331	BFCP029357_2	15.82 ± 2.93	n.d
C332	BFCP029357_2	20.40 ± 2.59	n.d
C333	BFCP029357_2	17.68 ± 5.00	n.d
C334	BFCP029357_2	10.17 ± 3.46	n.d
C335	BFCP029357_2	16.47 ± 3.25	n.d
C336	BFCP029357_2	20.33 ± 3.86	n.d
C337	BFCP029357_2	9.75 ± 3.79	n.d
C338	BFCP029357_2	20.72 ± 3.29	n.d
C339	BFCP029357_2	13.50 ± 2.48	n.d
C340	BFCP029357_2	-2.92 ± 5.88	n.d
C341	BFCP029357_2	8.53 ± 4.12	n.d
C342	BFCP029357_2	6.25 ± 2.58	n.d
C343	BFCP029357_2	8.76 ± 3.26	n.d
C344	BFCP029357_2	2.57 ± 3.63	n.d
C345	BFCP029357_2	24.68 ± 2.99	n.d
C346	BFCP029357_2	12.03 ± 1.42	n.d
C347	BFCP029357_2	1.75 ± 2.42	n.d
C348	BFCP029357_2	13.98 ± 2.81	n.d
C349	BFCP029357_2	41,27 ± 3.15	n.d

Compound no.	Plate Barcode	AChEI activity (%) ± SEM	AChEI IC_{50} (µM) ± SEM
C350	BFCP029357_2	2.63 ± 2.97	n.d
C351	BFCP029357_2	3.65 ± 5.34	n.d
C352	BFCP029357_2	2.52 ± 4.58	n.d
C353	BFCP029357_2	8.35 ± 3.05	n.d
C354	BFCP029357_2	15.50 ± 3.19	n.d
C355	BFCP029357_2	13.37 ± 3.53	n.d
C356	BFCP029357_2	0.83 ± 4.74	n.d
C357	BFCP029357_2	12.67 ± 3.44	n.d
C358	BFCP029357_2	35.06 ± 2.90	n.d
C359	BFCP029357_2	12.19 ± 4.07	n.d
C360	BFCP029357_2	1.84 ± 5.74	n.d
C361	BFCP029357_2	11.55 ± 4.10	n.d
C362	BFCP029357_2	9.22 ± 2.00	n.d
C363	BFCP029357_2	11.71 ± 2.95	n.d
C364	BFCP029357_2	22.42 ± 2.78	n.d
C365	BFCP029357_2	10.11 ± 10.79	n.d
C366	BFCP029357_2	0.65 ± 6.49	n.d
C367	BFCP029357_2	26.39 ± 7.35	n.d
C368	BFCP029357_2	6.85 ± 7.55	n.d
C369	BFCP029357_2	1.49 ± 12.97	n.d
C370	BFCP029357_2	8.13 ± 8.23	n.d
C371	BFCP029357_2	4.44 ± 6.90	n.d
C372	BFCP029357_2	2.32 ± 7.59	n.d
C373	BFCP029357_2	4.91 ± 11.96	n.d
C374	BFCP029357_2	7.24 ± 7.17	n.d
C375	BFCP029357_2	19.47 ± 7.11	n.d
C376	BFCP029357_2	18.40 ± 3.55	n.d
C377	BFCP029357_2	9.59 ± 11.02	n.d
C378	BFCP029357_2	5.16 ± 5.90	n.d
C379	BFCP029357_2	6.46 ± 6.09	n.d
C380	BFCP029357_2	-0.50 ± 5.30	n.d
C381	BFCP029357_2	5.43 ± 8.51	n.d
C382	BFCP029357_2	2.23 ± 7.18	n.d
C383	BFCP029357_2	9.63 ± 6.61	n.d
C384	BFCP029357_2	-0.67 ± 7.01	n.d
C385	BFCP029357_2	7.23 ± 8.52	n.d
C386	BFCP029357_2	0.06 ± 7.91	n.d
C387	BFCP029357_2	20.37 ± 6.55	n.d
C388	BFCP029357_2	9.48 ± 11.66	n.d
C389	BFCP029357_2	8.82 ± 6.91	n.d
C390	BFCP029357_2	-3.53 ± 6.29	n.d
C391	BFCP029357_2	7.09 ± 5.41	n.d
C392	BFCP029357_2	-10.98 ± 10.68	n.d
C393	BFCP029357_2	8.99 ± 2.90	n.d

Compound no.	Plate Barcode	AChEI activity (%) ± SEM	AChEI IC_{50} (µM) ± SEM
C394	BFCP029358_2	24.58 ± 2.61	n.d
C395	BFCP029358_2	7.27 ± 4.59	n.d
C396	BFCP029358_2	7.61 ± 5.10	n.d
C397	BFCP029358_2	3.41 ± 5.72	n.d
C398	BFCP029358_2	11.47 ± 3.27	n.d
C399	BFCP029358_2	9.29 ± 3.45	n.d
C400	BFCP029358_2	2.26 ± 2.48	n.d
C401	BFCP029358_2	2.08 ± 5.41	n.d
C402	BFCP029358_2	6.88 ± 2.35	n.d
C403	BFCP029358_2	9.94 ± 2.07	n.d
C404	BFCP029358_2	3.45 ± 3.85	n.d
C405	BFCP029358_2	7.74 ± 3.92	n.d
C406	BFCP029358_2	10.01 ± 2.45	n.d
C407	BFCP029358_2	6.77 ± 3.46	n.d
C408	BFCP029358_2	3.86 ± 4.66	n.d
C409	BFCP029358_2	12.94 ± 7.14	n.d
C410	BFCP029358_2	9.47 ± 4.93	n.d
C411	BFCP029358_2	12.40 ± 5.29	n.d
C412	BFCP029358_2	14.18 ± 6.56	n.d
C413	BFCP029358_2	25.38 ± 5.66	n.d
C414	BFCP029358_2	21.48 ± 5.18	n.d
C415	BFCP029358_2	21.45 ± 5.38	n.d
C416	BFCP029358_2	21.02 ± 7.15	n.d
C417	BFCP029358_2	8.744 ± 3.63	n.d
C418	BFCP029358_2	17.11 ± 2.48	n.d
C419	BFCP029358_2	10.42 ± 3.00	n.d
C420	BFCP029358_2	15.01 ± 3.28	n.d
C421	BFCP029358_2	-6.57 ± 7.50	n.d
C422	BFCP029358_2	3.32 ± 4.61	n.d
C423	BFCP029358_2	-11.47 ± 5.76	n.d
C424	BFCP029358_2	-11.73 ± 6.85	n.d
C425	BFCP029358_2	-7.19 ± 4.24	n.d
C426	BFCP029358_2	-0.75 ± 2.52	n.d
C427	BFCP029358_2	-1.32 ± 5.18	n.d
C428	BFCP029358_2	-1.55 ± 4.07	n.d
C429	BFCP029358_2	3.00 ± 5.88	n.d
C430	BFCP029358_2	17.06 ± 2.70	n.d
C431	BFCP029358_2	0.85 ± 3.47	n.d
C432	BFCP029358_2	-0.60 ± 6.68	n.d
C433	BFCP029358_2	-4.88 ± 5.44	n.d
C434	BFCP029358_2	0.35 ± 3.56	n.d
C435	BFCP029358_2	-13.95 ± 7.18	n.d
C436	BFCP029358_2	-16.00 ± 8.28	n.d
C437	BFCP029358_2	-5.24 ± 5.67	n.d

Compound no.	Plate Barcode	AChEI activity (%) ± SEM	AChEI IC_{50} (µM) ± SEM
C438	BFCP029358_2	-6.17 ± 5.08	n.d
C439	BFCP029358_2	-6.58 ± 4.59	n.d
C440	BFCP029358_2	-18.62 ± 6.23	n.d
C441	BFCP029358_2	-5.90 ± 9.59	n.d
C442	BFCP029358_2	10.54 ± 5.63	n.d
C443	BFCP029358_2	12.14 ± 4.58	n.d
C444	BFCP029358_2	4.83 ± 3.23	n.d
C445	BFCP029358_2	-25.88 ± 7.49	n.d
C446	BFCP029358_2	-12.77 ± 3.30	n.d
C447	BFCP029358_2	-2.57 ± 3.35	n.d
C448	BFCP029358_2	-11.40 ± 3.29	n.d
C449	BFCP029358_2	17.61 ± 2.93	n.d
C450	BFCP029358_2	10.68 ± 1.95	n.d
C451	BFCP029358_2	10.07 ± 2.13	n.d
C452	BFCP029358_2	13.55 ± 6.29	n.d
C453	BFCP029358_2	7.26 ± 4.20	n.d
C454	BFCP029358_2	6.99 ± 3.40	n.d
C455	BFCP029358_2	-0.26 ± 4.37	n.d
C456	BFCP029358_2	7.35 ± 4.74	n.d
C457	BFCP029358_2	10.61 ± 2.33	n.d
C458	BFCP029358_2	10.96 ± 3.17	n.d
C459	BFCP029358_2	0.62 ± 3.80	n.d
C460	BFCP029358_2	5.81 ± 2.28	n.d
C461	BFCP029358_2	13.30 ± 2.62	n.d
C462	BFCP029358_2	14.85 ± 1.74	n.d
C463	BFCP029358_2	18.31 ± 1.17	n.d
C464	BFCP029358_2	-3.46 ± 2.86	n.d
C465	BFCP029358_2	6.03 ± 4.47	n.d
C466	BFCP029358_2	7.02 ± 1.97	n.d
C467	BFCP029358_2	0.94 ± 5.28	n.d
C468	BFCP029358_2	-5.41 ± 6.54	n.d
C469	BFCP029358_2	16.59 ± 3.27	n.d
C470	BFCP029358_2	8.28 ± 5.61	n.d
C471	BFCP029358_2	3.15 ± 4.26	n.d
C472	BFCP029358_2	14.08 ± 7.07	n.d
C473	BFCP029358_2	12.52 ± 3.42	n.d
C474	BFCP029359_2	11.86 ± 4.59	n.d
C475	BFCP029359_2	2.54 ± 2.47	n.d
C476	BFCP029359_2	1.88 ± 4.95	n.d
C477	BFCP029359_2	4.06 ± 5.05	n.d
C478	BFCP029359_2	-4.26 ± 4.31	n.d
C479	BFCP029359_2	-2.81 ± 6.10	n.d
C480	BFCP029359_2	-5.64 ± 3.90	n.d
C481	BFCP029359_2	7.09 ± 3.20	n.d

Compound no.	Plate Barcode	AChEI activity (%) ± SEM	AChEI IC_{50} (µM) ± SEM
C482	BFCP029359_2	4.28 ± 4.13	n.d
C483	BFCP029359_2	0.74 ± 3.51	n.d
C484	BFCP029359_2	-20.29 ± 6.49	n.d
C485	BFCP029359_2	6.46 ± 4.45	n.d
C486	BFCP029359_2	-3.62 ± 5.83	n.d
C487	BFCP029359_2	-3.04 ± 3.77	n.d
C488	BFCP029359_2	-17.62 ± 9.40	n.d
C489	BFCP029359_2	-1.08 ± 5.59	n.d
C490	BFCP029359_2	6.62 ± 11.49	n.d
C491	BFCP029359_2	-5.73 ± 4.98	n.d
C492	BFCP029359_2	-9.07 ± 3.43	n.d
C493	BFCP029359_2	-4.10 ± 4.07	n.d
C494	BFCP029359_2	-7.58 ± 7.16	n.d
C495	BFCP029359_2	-13.24 ± 7.41	n.d
C496	BFCP029359_2	-16.81 ± 9.10	n.d
C497	BFCP029359_2	8.00 ± 4.45	n.d
C498	BFCP029359_2	5.92 ± 4.80	n.d
C499	BFCP029359_2	-2.26 ± 3.52	n.d
C500	BFCP029359_2	-14.79 ± 10.77	n.d
C501	BFCP029359_2	4.01 ± 4.20	n.d
C502	BFCP029359_2	-2.58 ± 4.60	n.d
C503	BFCP029359_2	-2.16 ± 5.25	n.d
C504	BFCP029359_2	-4.55 ± 6.93	n.d
C505	BFCP029359_2	14.07 ± 5.54	n.d
C506	BFCP029359_2	11.18 ± 2.38	n.d
C507	BFCP029359_2	3.95 ± 5.14	n.d
C508	BFCP029359_2	1.11 ± 6.18	n.d
C509	BFCP029359_2	14.44 ± 1.61	n.d
C510	BFCP029359_2	7.71 ± 7.06	n.d
C511	BFCP029359_2	4.86 ± 2.91	n.d
C512	BFCP029359_2	4.39 ± 4.50	n.d
C513	BFCP029359_2	15.73 ± 2.24	n.d
C514	BFCP029359_2	5.26 ± 4.07	n.d
C515	BFCP029359_2	7.20 ± 2.70	n.d
C516	BFCP029359_2	-1.43 ± 5.55	n.d
C517	BFCP029359_2	13.53 ± 2.20	n.d
C518	BFCP029359_2	7.27 ± 2.27	n.d
C519	BFCP029359_2	6.36 ± 3.08	n.d
C520	BFCP029359_2	13.15 ± 3.08	n.d
C521	BFCP029359_2	13.05 ± 3.93	n.d
C522	BFCP029359_2	8.10 ± 3.11	n.d
C523	BFCP029359_2	7.78 ± 1.45	n.d
C524	BFCP029359_2	0.19 ± 4.04	n.d
C525	BFCP029359_2	19.13 ± 7.24	n.d

Compound no.	Plate Barcode	AChEI activity (%) ± SEM	AChEI IC_{50} (µM) ± SEM
C526	BFCP029359_2	28.44 ± 9.78	n.d
C527	BFCP029359_2	30.92 ± 6.31	n.d
C528	BFCP029359_2	22.45 ± 7.19	n.d
C529	BFCP029359_2	15.74 ± 2.16	n.d
C530	BFCP029359_2	5.07 ± 4.58	n.d
C531	BFCP029359_2	11.05 ± 3.37	n.d
C532	BFCP029359_2	4.71 ± 3.95	n.d
C533	BFCP029359_2	20.24 ± 6.69	n.d
C534	BFCP029359_2	15.27 ± 8.65	n.d
C535	BFCP029359_2	18.96 ± 8.03	n.d
C536	BFCP029359_2	-4.70 ± 11.97	n.d
C537	BFCP029359_2	26.86 ± 7.90	n.d
C538	BFCP029359_2	12.45 ± 10.70	n.d
C539	BFCP029359_2	6.10 ± 11.97	n.d
C540	BFCP029359_2	-3.46 ± 10.11	n.d
C541	BFCP029359_2	26.96 ± 8.58	n.d
C542	BFCP029359_2	12.88 ± 8.94	n.d
C543	BFCP029359_2	17.32 ± 11.50	n.d
C544	BFCP029359_2	-2.60 ± 10.88	n.d
C545	BFCP029359_2	13.98 ± 9.54	n.d

AChE: acetylcholinesterase; IC_{50}: concentration causing 50% inhibitory effect; n.d: not determined; SEM: standard error of the mean

Appendix IV: Chromatograms of screened compounds indicating that no degradation took place

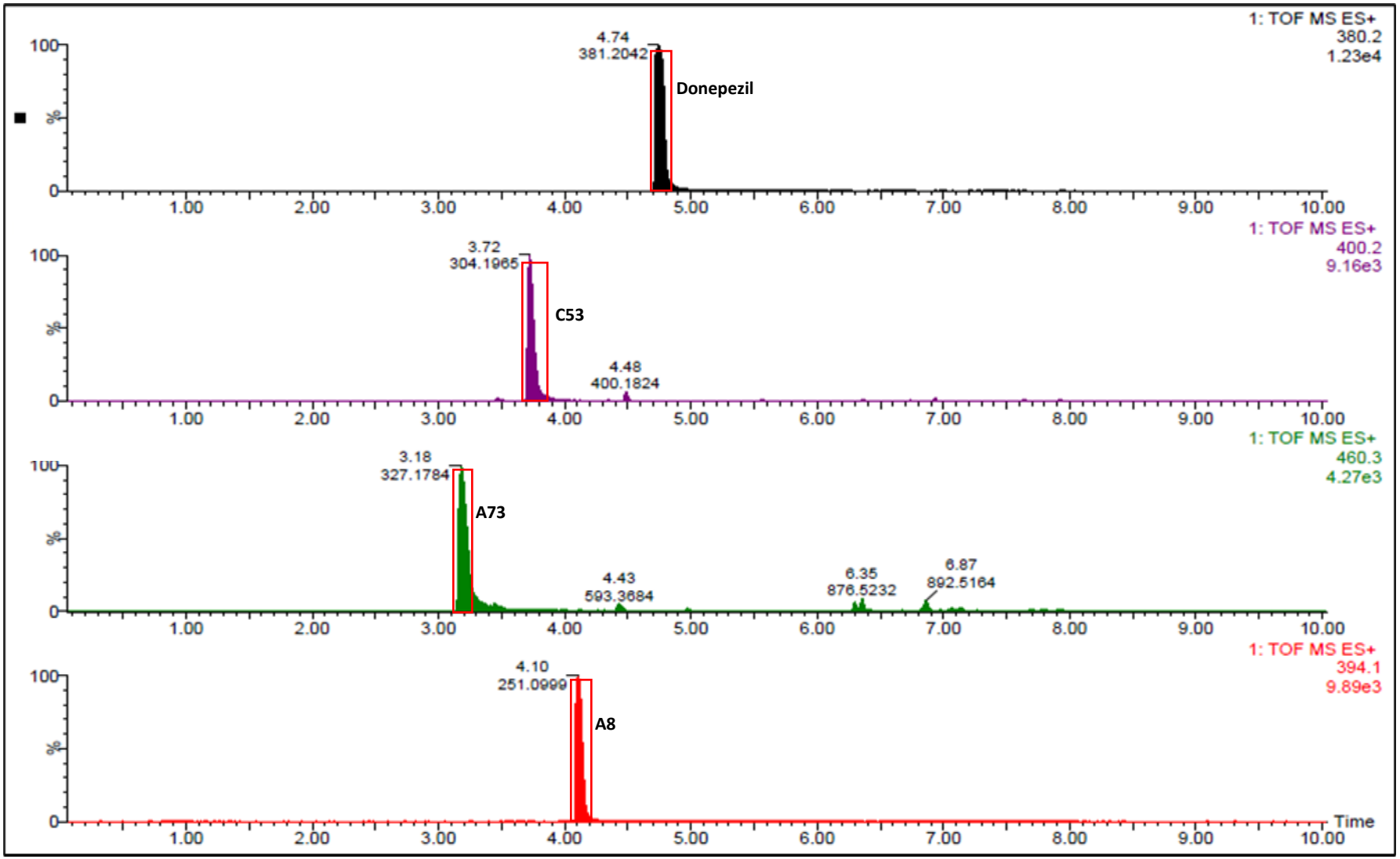

Figure 28: The positive electrospray ionisation chromatograms for donepezil, **A8**, **A73**, and **C53**.

Appendix V: Chromatograms of the apical and basal medium indicating that compounds penetrated the blood-brain barrier

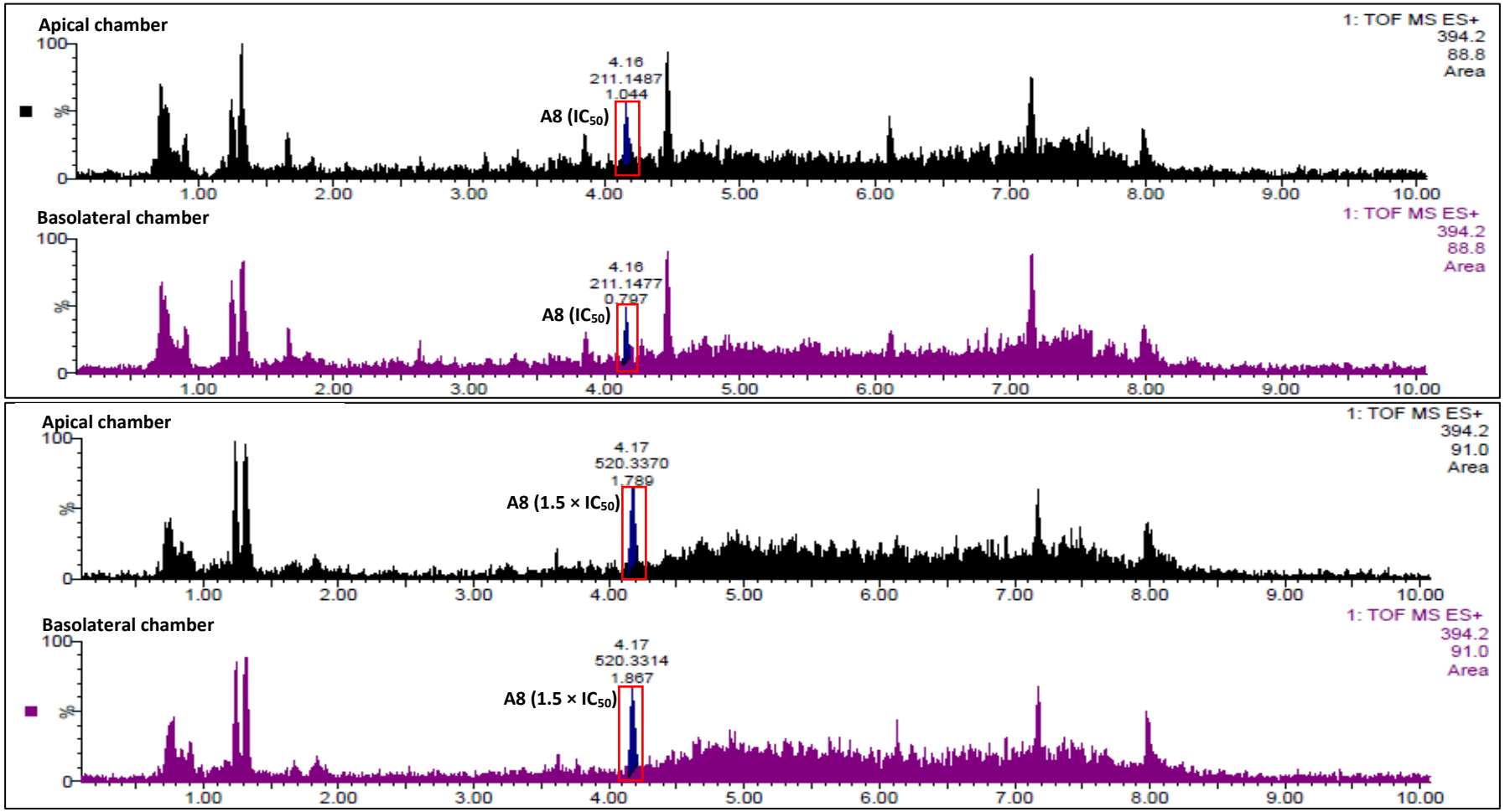

Figure 29: The positive electrospray ionisation chromatograms for **A8** at half maximal inhibitory concentration and 1.5 × half maximal inhibitory concentration.

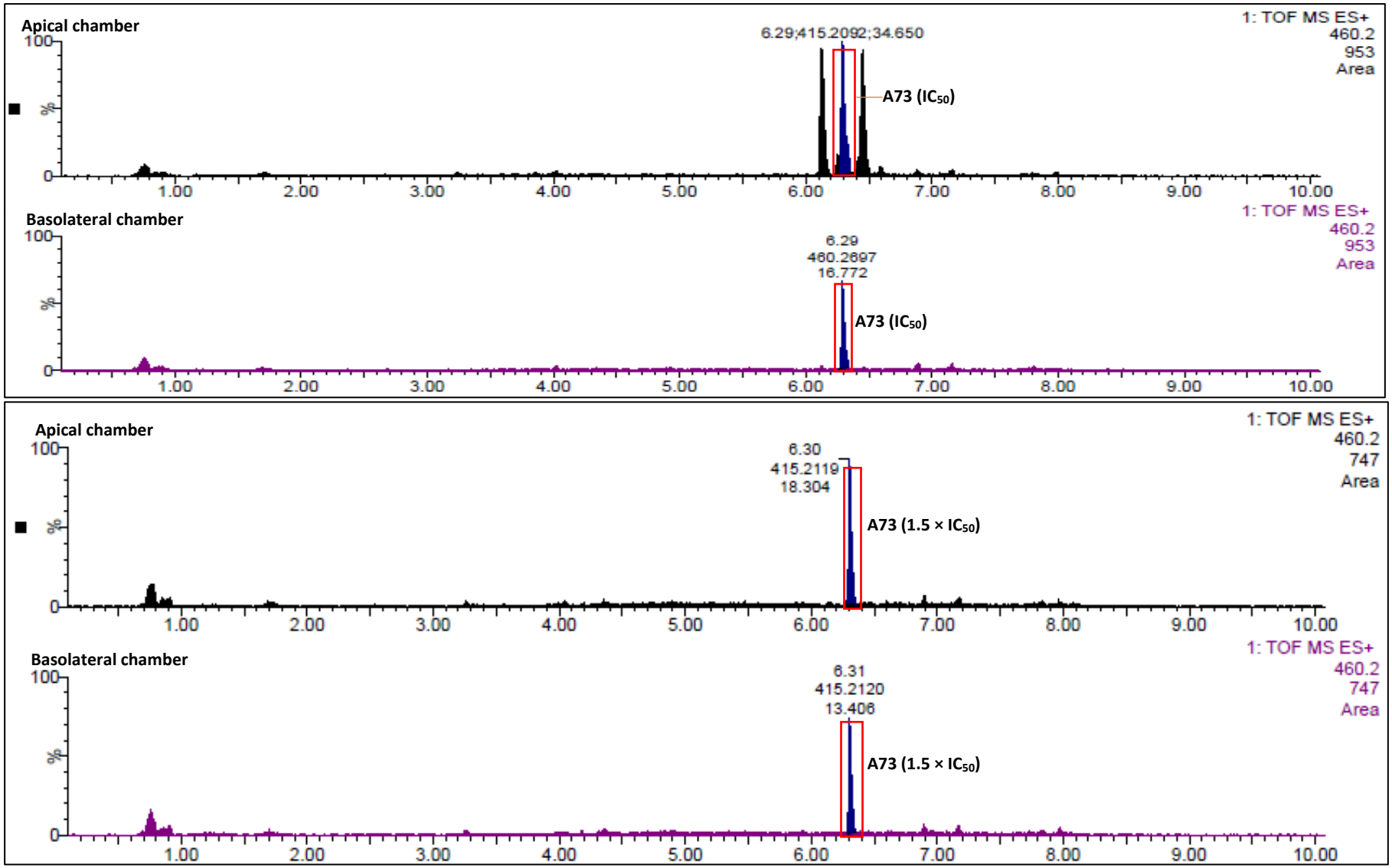

Figure 30: The positive electrospray ionisation chromatograms for **A73** at half maximal inhibitory concentration and 1.5 × half maximal inhibitory concentration.

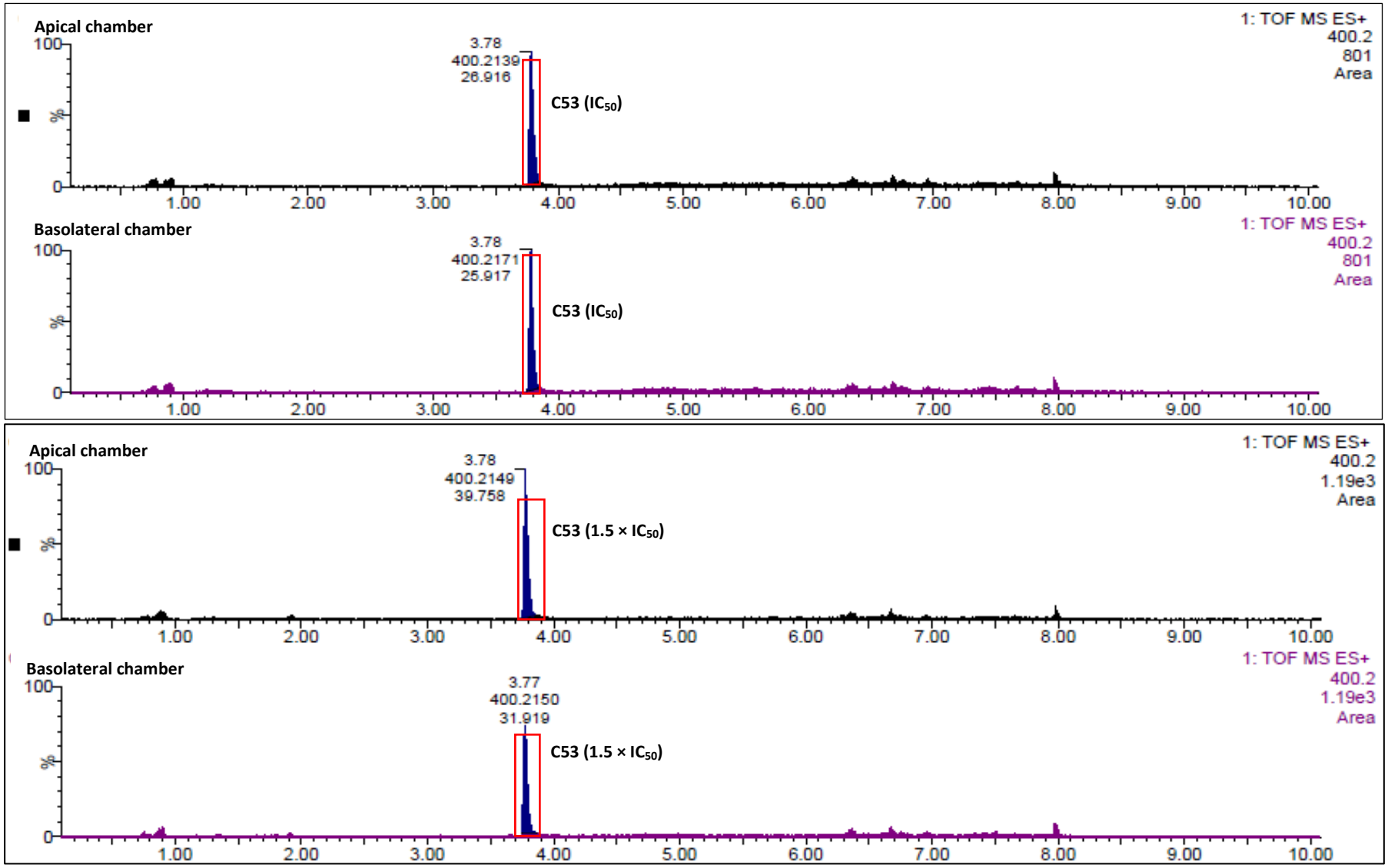

Figure 31: The positive electrospray ionisation chromatograms for **C53** at half maximal inhibitory concentration and 1.5 × half maximal inhibitory concentration.

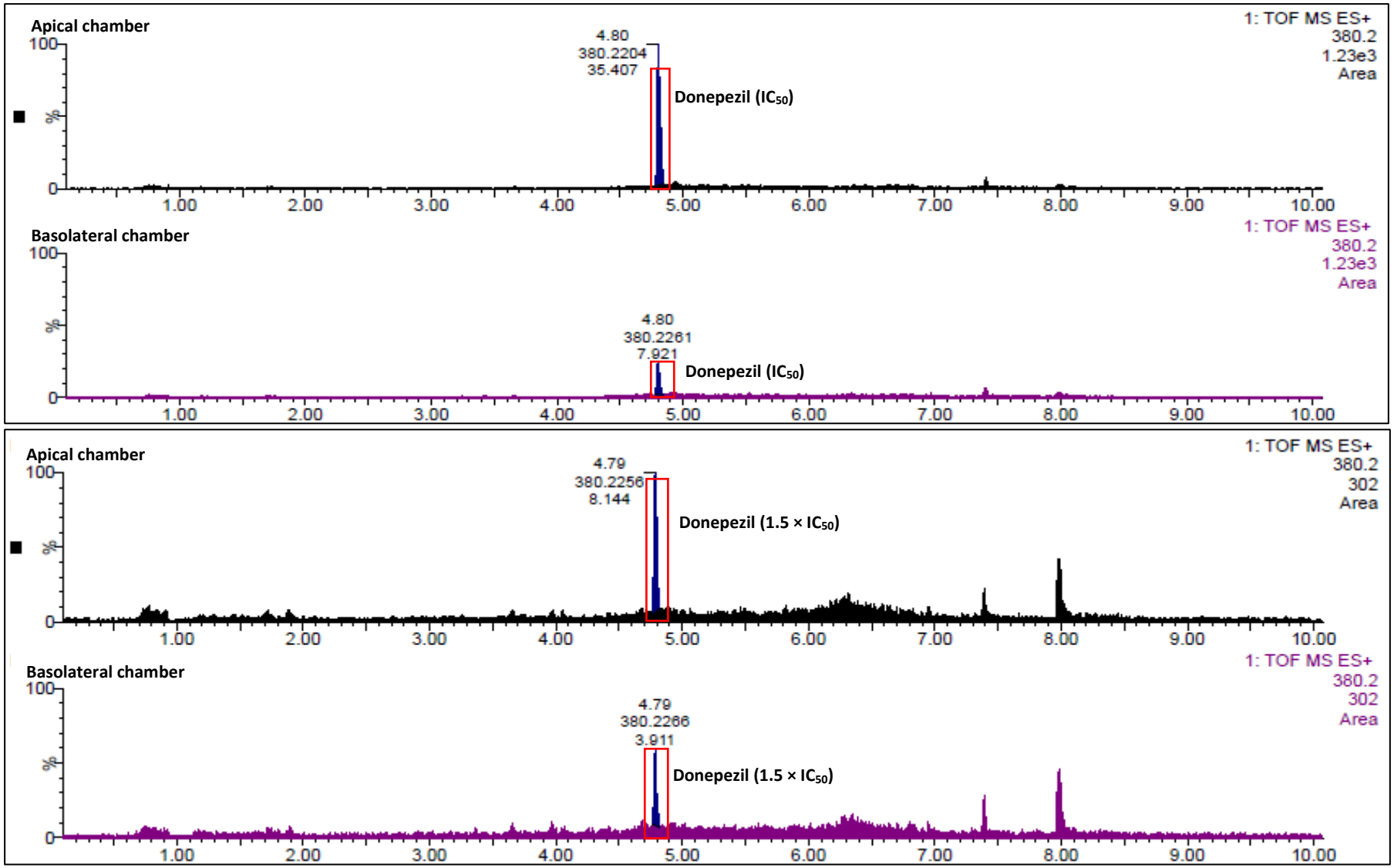

Figure 32: The positive electrospray ionisation chromatograms for donepezil at half maximal inhibitory concentration and 1.5 × half maximal inhibitory concentration.